



# Durham E-Theses

---

## *Composite models of weak gauge bosons*

Speirs, Neil Alexander

### How to cite:

---

Speirs, Neil Alexander (1985) *Composite models of weak gauge bosons*, Durham theses, Durham University. Available at Durham E-Theses Online: <http://etheses.dur.ac.uk/6817/>

### Use policy

---

The full-text may be used and/or reproduced, and given to third parties in any format or medium, without prior permission or charge, for personal research or study, educational, or not-for-profit purposes provided that:

- a full bibliographic reference is made to the original source
- a [link](#) is made to the metadata record in Durham E-Theses
- the full-text is not changed in any way

The full-text must not be sold in any format or medium without the formal permission of the copyright holders.

Please consult the [full Durham E-Theses policy](#) for further details.

COMPOSITE MODELS OF WEAK GAUGE BOSONS

COMPOSITE MODELS OF WEAK GAUGE BOSONS

THESIS SUBMITTED TO  
THE UNIVERSITY OF DURHAM

BY

NEIL ALEXANDER SPEIRS, B.Sc. (NEWCASTLE)  
FOR THE DEGREE OF DOCTOR OF PHILOSOPHY

The copyright of this thesis rests with the author.  
No quotation from it should be published without  
his prior written consent and information derived  
from it should be acknowledged.

DEPARTMENT OF PHYSICS  
DURHAM UNIVERSITY

JUNE 1985



16.OCT.1985

## CONTENTS

	Page
Chapter 1 The Standard Model	1
1.1 Introduction	1
1.2 Gauge Theories	1
1.3 Spontaneous Symmetry Breaking and the Standard Model	6
Chapter 2 Composite Models	13
2.1 General Remarks	13
2.2 Quark and Lepton Masses and Chiral Symmetry	17
2.3 Experimental Bounds on Compositeness	21
2.4 Models with Fermionic and Bosonic Constituents	24
2.5 Models with Fermionic Constituents Only	28
Chapter 3 The Internal Structure of Weak Bosons	32
3.1 Introduction	32
3.2 Vector Dominance and its Applications	33
3.3 Universality of the Weak Current	39
3.4 Effective Lagrangians and W-Dominance	41
3.5 The Effective Lagrangian from Feynman Diagrams	45
3.6 The Size of the Weinberg Angle	50
3.7 The Z Wavefunction	51
3.8 Conclusions	52

Chapter 4	A Spectrum of Composite States	54
4.1	Introduction	54
4.2	The Masses of Composite Weak Bosons	54
4.3	Excited States	61
4.4	Decay Widths of New States	68
4.5	Coloured Bosons	69
4.6	Summary	72
Chapter 5	The Width of the Z in Composite Models	74
5.1	Introduction	74
5.2	Standard Model Z Decays	74
5.3	Anomalous Decays into Gauge Bosons	78
5.4	Experimental Results	92
5.5	Effective Interactions	94
5.6	Hypergluon Decays	101
5.7	Summary	108
Chapter 6	Conclusions	113
	References	116

## ACKNOWLEDGEMENTS

I am extremely grateful to Peter Collins for his generous advice, support and many helpful ideas given throughout the period of this research. I should also like to thank him for reading the manuscript.

In addition I thank the staff and research students of the particle physics group at Durham - Peter Collins, Alan Martin, Mike Pennington, Fred Gault, Chris Maxwell, Stuart Grayson, Tim Spiller, James Webb, Anthony Worrall, King Lun Au, Martin Carter, Tony Peacock, John Michopoulos, Simon Webb and particularly my room-mates Anthony Allan and Nigel Glover for providing such a friendly and stimulating environment in which to work. I am also grateful to Jonathan Helliwell for the loan of drawing materials.

I thank the SERC for providing financial support.

This thesis is dedicated to my family.

## COMPOSITE MODELS OF WEAK GAUGE BOSONS

Neil Alexander Speirs

### ABSTRACT

Composite models of quarks, leptons and weak bosons are reviewed. It is shown that they can reproduce the low energy results of the Standard Weinberg-Salam Model of electroweak interactions. The consequences of assuming composite W and Z bosons are examined and many new particles are predicted, including excited W and Z states and their pseudoscalar partners. Estimates of the masses and decay widths of these particles are given. It is also shown that coloured weak bosons may exist in the energy range 100-200 GeV.

The decays of a composite Z boson are studied in detail using both a potential model and an effective Lagrangian approach. It is found that the width is likely to be significantly different from that of the elementary Z of the Standard Model. In particular there are additional contributions to the decays  $Z \rightarrow q\bar{q}g$  and  $Z \rightarrow ggg$  which are likely to affect the total Z width by an appreciable amount. The decay of the Z into hypercoloured particles is also examined and it is found that the width is likely to exceed greatly the current experimental bound.

It is concluded that the W and Z bosons are likely to be elementary particles because if they were composite their decay widths would be much greater than is found experimentally, unless of course their internal dynamics are quite unlike the model which has been employed.

## CHAPTER 1 THE STANDARD MODEL

### 1.1 Introduction

It has been discovered that all the interactions so far observed in nature can be explained by four fundamental forces. These are the strong and weak nuclear forces, electromagnetism and gravity. These forces act between quarks and leptons which are currently believed to be the fundamental building blocks of matter. In Table 1.1 a list of elementary particles together with some of their quantum numbers is given. In this chapter the main results of the successful "Standard Model" of these interactions are described as a prelude to the introduction of composite models in chapter 2.

### 1.2 Gauge Theories

Recent developments in particle physics have revealed the relevance of gauge invariance in describing the electromagnetic, strong and weak interactions. Gauge theories have become important for two reasons. The first is that gauge theories are renormalizable - that is to say the divergences which occur in higher order calculations can all be removed in a well defined way. The second reason is the great success of one particular gauge theory, namely Quantum Electrodynamics (QED) [1.1]. The QED prediction for the anomalous magnetic moment of the muon is in agreement with the experimental result to within 1 part in  $10^5$ .

QED describes the electromagnetic interaction of spin 1/2 fermions with a spin 1 photon. The Lagrangian for QED is given by



Table 1.1

Elementary particles and some of their Quantum Numbers

	Spin	Baryon Number B	Lepton Number L	Charge Q
Quarks				
d (down)	1/2	1/3	0	-1/3
u (up)	1/2	1/3	0	+2/3
s (strange)	1/2	1/3	0	-1/3
c (charm)	1/2	1/3	0	+2/3
b (bottom)	1/2	1/3	0	-1/3
t (top)	1/2	1/3	0	+2/3
Leptons				
e (electron)	1/2	0	1	-1
$\nu_e$ (electron neutrino)	1/2	0	1	0
$\mu$ (muon)	1/2	0	1	-1
$\nu_\mu$ (muon neutrino)	1/2	0	1	0
$\tau$ (tau)	1/2	0	1	-1
$\nu_\tau$ (tau neutrino)	1/2	0	1	0
Gauge bosons				
$\gamma$ (photon)	1	0	0	0
$W^\pm, Z$ (weak bosons)	1	0	0	$\pm 1, 0$
$g_i$ ( $i=1, \dots, 8$ gluons)	1	0	0	0

$$L = \bar{\psi} (i\gamma^\mu \partial_\mu - m) \psi + e\bar{\psi}\gamma^\mu A_\mu \psi - 1/4 F_{\mu\nu} F^{\mu\nu} \quad (1.1)$$

where  $\psi$  is the fermion field,  $A_\mu$  is the photon field and  $F_{\mu\nu}$  is the electromagnetic field strength tensor defined by

$$F_{\mu\nu} = \partial_\mu A_\nu - \partial_\nu A_\mu \quad (1.2)$$

The Lagrangian (1.1) is invariant under global (position independent) phase transformations

$$\psi \rightarrow \exp(-i\alpha) \psi \quad (1.3)$$

However, it is not essential to require that  $\alpha$  be fixed uniquely at all points of space and time. In fact the Lagrangian (1.1) is invariant under local (position dependent) transformations

$$\psi \rightarrow \exp(-i\alpha(x)) \psi \quad (1.4)$$

where  $\alpha$  now depends on position provided that  $A_\mu$  transforms as

$$A_\mu \rightarrow A_\mu + (1/e) \partial_\mu \alpha(x) \quad (1.5)$$

which is the usual gauge transformation for the electromagnetic vector potential.

Requiring local gauge invariance has the consequence of restricting the coupling of the photon to fermions to be of the above minimal form i.e. the second term in (1.1) with no form factors or derivative terms. In addition, local gauge invariance forbids the inclusion of a mass term for the photon of the type  $m^2 A_\mu A^\mu$ . The impressive success of QED suggests that this gauge invariance is an important property of the theory so it is natural to attempt to describe the strong and weak interactions in this way too.

In QED, one is dealing with the simple gauge symmetry of an Abelian U(1) group (1.4) with constant generators. Quantum Chromodynamics (QCD) is the theory of the strong interaction [1.2, 1.3] and is described by an SU(3) group called "colour". The quarks lie in the fundamental triplet representation of this group. There are eight group generators  $T^a$  ( $a=1,8$ ) which lie in the adjoint representation and can be expressed as traceless 3 x 3 matrices. The  $T^a$  form a Lie algebra

$$[T^a, T^b] = if^{ab}_c T^c \quad (1.6)$$

where the  $f_{abc}$  are the structure constants of the algebra.

The basic Lagrangian of QCD is

$$L = \bar{q} (i\gamma^\mu \partial_\mu - m) q - g (\bar{q} \gamma^\mu T_a q) G^a_\mu - 1/4 G^a_{\mu\nu} G_a^{\mu\nu} \quad (1.7)$$

where  $q$  is a quark field of mass  $m$ ,  $G^a_\mu$  ( $a=1,8$ ) is an octet of massless vector gauge bosons called gluons,  $G^a_{\mu\nu}$  is the gluon field strength tensor and  $g$  is the strong coupling constant. Since SU(3) is a non-abelian group, the gauge transformations are more complicated. The QCD Lagrangian (1.7) is invariant under the infinitesimal gauge transformations

$$\begin{aligned} q &\rightarrow (1 + i\alpha_a(x) T^a) q \\ G^a_\mu &\rightarrow G^a_\mu - (1/g) \partial_\mu \alpha^a - f^{ab}_c \alpha_b G^c_\mu \end{aligned} \quad (1.8)$$

if the field strength tensor is given by

$$G^a_{\mu\nu} = \partial_\mu G^a_\nu - \partial_\nu G^a_\mu - g f^a_{bc} G^b_\mu G^c_\nu \quad (1.9)$$

It can be seen from (1.9) that the gluon kinetic energy term  $G^a_{\mu\nu} G_a^{\mu\nu}$

contains triple and quartic gluon interactions. This self coupling is a consequence of the non-abelian nature of the gauge group and shows that QCD is very different from the Abelian QED.

The strong coupling  $g$  depends upon momentum in a well defined way. The coupling "constant"  $\alpha_S = g^2/4\pi$  is said to "run". At two different momentum scales  $Q^2$  and  $\mu^2$  one finds

$$\alpha_S(Q^2) = \frac{\alpha_S(\mu^2)}{1 + (\beta_0/4\pi) \alpha_S(\mu^2) \ln(Q^2/\mu^2)} \quad (1.10)$$

where  $\beta_0 = 11 - 2/3 N_F$  and  $N_F$  is the number of fermions.

In the analogous formula for QED one has

$$\alpha(Q^2) = \frac{\alpha(\mu^2)}{1 - (\alpha(\mu^2)/3\pi) \log(Q^2/\mu^2)} \quad (1.11)$$

Superficially the formulae (1.10) and (1.11) appear very similar. However, the signs in the denominators are important since for QCD if  $N_F < 16$  then  $\beta_0 > 0$  and  $\alpha_S(Q^2) < \alpha_S(\mu^2)$  for  $Q^2 > \mu^2$ . This property of QCD is known as asymptotic freedom since  $\alpha_S(Q^2) \rightarrow 0$  as  $Q^2 \rightarrow \infty$  and enables sensible perturbative calculations to be performed at high  $Q^2$ . However, (1.11) gives  $\alpha(Q^2) > \alpha(\mu^2)$  for  $Q^2 > \mu^2$ . Notice that in QED  $\alpha$  does not diverge until  $Q^2 \approx 10^{56} \text{ (GeV)}^2$  which is not something to worry about since one expects quantum gravity effects to modify the theory long before these energies are attained. One can also re-express  $\alpha_S$  in terms of a momentum scale for the colour force

$$\alpha_S(Q^2) = \frac{4\pi}{\beta_0 \log(Q^2/\Lambda_C^2)} \quad (1.12)$$

where  $\Lambda_C^2 = \mu^2 \exp(-4\pi/\alpha_S\beta_0)$  is found to be [1.4, 1.5] in the range 200-400 MeV. Like QED, QCD has been successfully confronted by experiment though not to the same sort of accuracy.

It was hoped that weak interactions could also be described by a gauge theory. However, in the case of the weak force, the postulated vector bosons have to be massive because of the short range of the interaction, yet gauge invariance forbids an explicit mass term of the form  $m_\mu^2 A^\mu$ . Hence if weak interactions are to be described by a gauge theory, a more subtle method of introducing the vector boson mass must be found.

### 1.3 Spontaneous Symmetry Breaking and the Standard Model

The existence of massive vector bosons indicates that if weak interactions have a gauge symmetry, then it must be broken. The symmetry breaking could be described simply by adding non-gauge invariant pieces such as a mass term to the Lagrangian. Unfortunately, this destroys some of the favourable features of the original gauge theory, notably its unitarity and renormalizability. Alternatively, the gauge symmetry can be broken by the method of "spontaneous symmetry breaking" which gives masses to the vector bosons but maintains the important properties of the theory. The idea is to construct a theory with a Lagrangian which is exactly symmetric with respect to the group transformations but which gives rise to a non-invariant ground state. The non-invariance of the ground state (or vacuum) leads to a well defined pattern of symmetry breaking effects.

Glashow initially [1.6] and later Weinberg [1.7] and Salam [1.8]

proposed that an SU(2) x U(1) gauge group could describe both the weak interaction and QED. This theory which uses the Higgs spontaneous symmetry breakdown mechanism [1.9] was subsequently shown by t'Hooft [1.10] to be renormalizable.

The Lagrangian of the Weinberg-Salam SU(2) x U(1) gauge theory with four vector bosons coupled to an SU(2) doublet of complex scalar fields is

$$L = (D_\mu \varphi)^\dagger (D^\mu \varphi) - V(\varphi^\dagger \varphi) - 1/4 W_{\mu\nu}^a W_a^{\mu\nu} - 1/4 B_{\mu\nu} B^{\mu\nu} \quad (1.13)$$

where  $W_{\mu\nu}^a$  ( $a=1,3$ ) is the field strength tensor for the SU(2) gauge fields  $W_\mu^a$  and  $B_{\mu\nu}$  is the tensor for the U(1) group. The "covariant derivative" of the scalar field  $\varphi$  is defined by

$$D_\mu \varphi = (\partial_\mu + ig\tau_a/2 W_\mu^a + ig' 1/2 B_\mu) \varphi \quad (1.14)$$

where  $\tau^a$  are the three Pauli matrices. The coupling constants  $g$  and  $g'$  correspond to the SU(2) and U(1) groups respectively. The scalar potential  $V(\varphi^\dagger \varphi)$  is taken to be

$$V(\varphi^\dagger \varphi) = \mu^2 \varphi^\dagger \varphi + \lambda (\varphi^\dagger \varphi)^2 \quad (1.15)$$

where  $\lambda > 0$  so that  $V$  is bounded below. If  $\mu^2 > 0$  then  $V$  has a minimum at  $\varphi^\dagger \varphi = 0$  and the ground state is invariant under the gauge group. However, if  $\mu^2 < 0$  then  $V$  has a minimum when  $\varphi^\dagger \varphi = v^2/2$  where  $v^2 = -\mu^2/\lambda$ . When the particle content of the theory is computed with this vacuum, it is found that three of the scalars have become the longitudinal components of the gauge bosons which have acquired masses. One writes

$$\varphi(x) = \frac{1}{\sqrt{2}} \begin{bmatrix} 0 \\ v + h(x) \end{bmatrix} \quad (1.16)$$

such that  $\varphi_{\text{vacuum}} = v/\sqrt{2}$  as above. Then the covariant derivative in (1.13) gives

$$\begin{aligned} (D_\mu \varphi)^\dagger (D^\mu \varphi) &= 1/2 (\partial_\mu h)(\partial^\mu h) + 1/2 (gv/2)^2 (W_\mu^1 W_1^\mu + W_\mu^2 W_2^\mu) \quad (1.17) \\ &+ 1/2 (v/2)^2 [(gW_\mu^3 - g'B_\mu)(gW_3^\mu - g'B^\mu)] + \text{higher order terms} \end{aligned}$$

Now define

$$\begin{aligned} W_\mu^\pm &= (1/\sqrt{2}) (W_\mu^1 \mp iW_\mu^2) \\ Z_\mu &= \cos\theta_W W_\mu^3 - \sin\theta_W B_\mu \\ A_\mu &= \sin\theta_W W_\mu^3 + \cos\theta_W B_\mu \end{aligned} \quad (1.18)$$

where  $\tan\theta_W = g'/g$ . Equation (1.17) now yields

$$\begin{aligned} (D_\mu \varphi)^\dagger (D^\mu \varphi) &= 1/2 (\partial_\mu h)(\partial^\mu h) + M_W^2 (W_\mu^+ W_\mu^- + W_\mu^- W_\mu^+) + M_Z^2 (Z_\mu Z_\mu) \quad (1.19) \\ &+ \text{higher order terms} \end{aligned}$$

By comparing (1.17) and (1.19) it can be seen that three of the gauge bosons have acquired mass whilst the fourth is massless.

$$M_{W^\pm} = gv/2 \quad M_Z = M_W/\cos\theta_W \quad (1.20)$$

Associating the massless boson  $A_\mu$  with the photon gives the relations

$$e = g \sin\theta_W = g' \cos\theta_W \quad (1.21)$$

The existence of the massless gauge boson indicates the preservation of an unbroken U(1) symmetry as required by QED.

Fermions are introduced into the Standard Model in left-handed weak doublets and right-handed singlets of the SU(2) weak isospin

group. For example with leptons  $\nu_e$  and  $e$  one has

$$\begin{pmatrix} \nu_{eL} \\ e_L \end{pmatrix} ; e_R$$

where  $e_L \equiv 1/2 (1 - \gamma_5)e$ ,  $e_R \equiv 1/2 (1 + \gamma_5)e$  are left and right handed components respectively at momenta  $\gg m_e$ . For this reason the SU(2) group is often labelled with a subscript L. The fermions also have a U(1) weak hypercharge quantum number Y and after symmetry breaking the combination

$$Q = 1/2 (\tau^3 + Y) \quad (1.22)$$

remains unbroken where  $\tau^3/2$  is the diagonal generator of the SU(2) group. Q is identified with the electric charge - the quantum number of the unbroken electromagnetic U(1).

The SU(2) x U(1)<sub>Y</sub> Lagrangian for quark and lepton interactions with the gauge bosons is

$$L = \bar{L}\gamma^\mu (i\partial_\mu - g\tau_a/2 W_\mu^a - g'Y/2 B_\mu)L + \bar{R}\gamma^\mu (i\partial_\mu - g'Y/2 B_\mu)R \quad (1.23)$$

where L denotes a left handed fermion (quark or lepton) doublet and R denotes a right handed fermion singlet. The charged weak current is of the form

$$J_+^\mu = \bar{\nu}_e \gamma^\mu 1/2(1 - \gamma_5)e \quad (1.24)$$

The corresponding neutral weak current is of the form

$$\begin{aligned} J_\mu^{NC} &\equiv J_\mu^3 - \sin^2\theta_W J_\mu^{EM} \\ &= 1/2 \bar{\nu}_L \gamma_\mu \nu_L - 1/2 \bar{e}_L \gamma_\mu e_L - \sin^2\theta_W (\bar{e}_L \gamma_\mu e_L + \bar{e}_R \gamma_\mu e_R) \end{aligned} \quad (1.25)$$

From the vector-axial structure of the charged weak current, one obtains

$$G_F/\sqrt{2} = g^2/8M_W^2 \quad (1.26)$$

where  $G_F$  is the Fermi weak coupling constant which is the effective coupling of a pointlike (low energy) four-Fermi interaction. Using (1.21), (1.26) and  $\alpha = e^2/4\pi$  one obtains

$$M_W = \left[ \frac{\pi\alpha}{\sqrt{2}G_F} \right]^{1/2} \frac{1}{\sin\theta_W} = \frac{37.3}{\sin\theta_W} \text{ GeV} \quad (1.27)$$

and consequently

$$M_Z = \frac{M_W}{\cos\theta_W} = \frac{74.6}{\sin 2\theta_W} \text{ GeV} \quad (1.28)$$

Measurements of  $\sin^2\theta_W$  give a world average [1.11]

$$\sin^2\theta_W = 0.218 \pm 0.010 \quad (1.29)$$

which leads to  $M_W = 80$  GeV and  $M_Z = 90$  GeV. Radiative corrections [1.12] increase these estimates to give

$$M_W = 82 \pm 2.4 \text{ GeV} \quad M_Z = 93 \pm 1.6 \text{ GeV} \quad (1.30)$$

These vector bosons have been discovered at the CERN  $p\bar{p}$  collider [1.13, 1.14] with the latest values for the masses given by [1.15]

$$M_W = 81.5 \pm 1.0 \pm 1.5 \text{ GeV} \quad (1.31)$$

$$M_Z = 92.4 \pm 1.1 \pm 1.4 \text{ GeV}$$

which are in excellent agreement with theoretical predictions. The

parameter  $\rho$  which specifies the relative strengths of the neutral and charged weak interactions is given by

$$\rho = \frac{M_W^2}{M_Z^2 \cos^2 \theta_W} \quad (1.32)$$

and has been measured experimentally [1.16, 1.17, 1.18] to have the value

$$\rho = 1.02 \pm 0.02 \quad (1.33)$$

In the Lagrangian (1.23), a fermion mass term was excluded by gauge invariance because the left and right-handed fermions transform differently under  $SU(2)_L$ . One attractive feature of the Weinberg-Salam Model is that the Higgs doublet which generates the masses of the weak bosons is also sufficient to give masses to the quarks and leptons. This is achieved by introducing into the Lagrangian, Higgs-fermion couplings of the form

$$L = -G_e [(\bar{\nu}_e, \bar{e})_L \varphi(x) e_R + \bar{e}_R \varphi^\dagger(x) \begin{pmatrix} \nu_e \\ e \end{pmatrix}_L] \quad (1.34)$$

where  $\varphi(x)$  is given by (1.16). After spontaneous symmetry breaking one obtains

$$L = \frac{-G_e v}{\sqrt{2}} (\bar{e}_L e_R + \bar{e}_R e_L) - \frac{G_e}{\sqrt{2}} (\bar{e}_L e_R + \bar{e}_R e_L) h \quad (1.35)$$

If  $G_e$  is chosen such that  $m_e = G_e v/\sqrt{2}$  then

$$L = -m_e \bar{e}e - (m_e/v) \bar{e}eh \quad (1.36)$$

so that an electron mass term has arisen. The additional Higgs-fermion coupling must be very small since  $v = 246$  GeV but since  $G_e$  is arbitrary, the mass of the electron is not predicted. Since all fermion masses are generated in this way, each mass stems from a free coupling parameter in the theory. Notice that because of the form of the Higgs doublet with the upper component being zero there is no mass term for the neutrino. When one generates the quark masses the upper member of the doublet gains its mass from a new Higgs field

$$\varphi_C = -i\tau_2\varphi^* \quad (1.37)$$

which transforms in the same way as  $\varphi$  under SU(2).

In conclusion, the Standard Model of weak interactions based on an SU(3) x SU(2) x U(1) gauge theory is in impressive agreement with low energy experiments. Nevertheless this theory does have some theoretical difficulties and much arbitrariness. These problems and a possible solution are discussed in the following chapter.

## CHAPTER 2 COMPOSITE MODELS

### 2.1 General Remarks

The Standard Model described in Chapter 1 has been remarkably successful in its explanation of low energy experimental results. However, there are several questions which the Standard Model does not and cannot answer. There is a proliferation of parameters which is theoretically unsatisfactory. The quark and lepton masses are proportional to the coupling constant between fermions and Higgs scalars and cannot be calculated a priori. In addition, there is no convincing explanation for the different orders of magnitude of the masses in different generations. The number of generations is undetermined by the theory and there is no indication why left-handed particles should be placed in SU(2) doublets and right-handed particles in SU(2) singlets. The quantisation of electric charge in units of  $1/3 e$  is mysterious if one believes that the Standard Model is the fundamental theory.

The Higgs sector which generates the masses of all particles including the W and Z bosons is often viewed as being the least appealing feature of the Standard Model. There is no experimental evidence to support the case for a fundamental Higgs scalar and such a particle could have a mass anywhere between 10 GeV and 1 TeV.

One final complaint is perhaps the most important. The previous problems are all either unanswered questions or a matter of aesthetics. However, the "naturalness" problem does not fall into either of these categories. This problem occurs because elementary scalar particles acquire enormous masses due to heavy fermion loops,

(see Figure 2.1), unless the parameters of the theory are very finely tuned.

Attempts to extend the Standard Model in order to answer some of these questions include Left-Right Symmetric Models [2.1], Grand Unified Theories [2.2], Technicolour [2.3], Supersymmetry [2.4] and Compositeness [2.5]. For example, one way to solve the naturalness problem is to invoke supersymmetry. This theory has a symmetry between bosons and fermions so that every fermion has a supersymmetric bosonic partner and vice versa. The contribution to the loop diagrams from a fermion and its superpartner will be proportional to the mass difference between them and so need not be large.

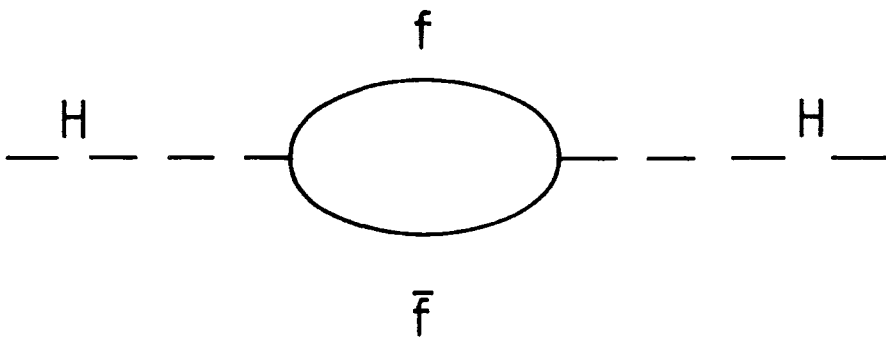
In composite models, the "naturalness" problem can be solved either by supposing that  $W$ 's and  $Z$ 's are composite and have masses generated by their bound state dynamics, whereupon elementary Higgs scalars need not occur, or alternatively by observing that the Higgs boson may itself be a composite object made of fermion-antifermion constituents.

The aims of composite models are as follows.

- a). To explain the charge and colour pattern of the fermions within each generation. This property will follow from the quantum numbers of the constituents.
- b). The quark and lepton masses and also the Kobayashi-Maskawa mixing angles [2.6] should be calculable dynamical parameters of the theory. The pattern of the masses among and between generations should follow from the dynamics of the bound states.
- c). To solve the "naturalness" problem.

It is usually supposed that quarks and leptons are bound states

Figure 2.1



Contributions to the Higgs mass from heavy fermion loops.

of several constituents which can either be fermions alone or both fermions and bosons. Examples of such models are given in Sections 2.4 and 2.5. The constituents must be bound together by a very strong and presumably confining force. This new force is commonly called "hypercolour" and is usually supposed to be a non-abelian confining gauged force like colour. The constituents carry a new hypercolour quantum number but composite particles are hypercolour singlets. The size of the composite bound state quarks and leptons will be determined by the hypercolour confinement scale  $\Lambda_H$ . The present experimental limits (see Section 2.3) indicate  $1/\Lambda_H \ll 10^{-18} \text{ m}$  i.e.  $\Lambda_H \gg 100 \text{ GeV}$ . The hypercolour binding is usually considered to be analogous to the confining colour force in QCD. Of course this is not the only way to bind the quark and lepton constituents. Indeed it is not absolutely certain that the laws of ordinary quantum mechanics hold true at such small distances. However, it will be assumed throughout that such drastic modifications are not needed, even deep inside quarks and leptons.

If quarks and leptons are composite, one may ask whether any of the gauge bosons might also be composite. Photons and gluons are massless which is a consequence of their interactions being exactly gauge invariant. If they were composite, one would expect terms  $O(1/\Lambda_H)$  to induce a small mass in the corresponding boson. No such mass is observed for the photon and a gluon mass would result in the breakdown of confinement. This leads one to conclude that photons and gluons are probably elementary.

However, the situation with the massive W and Z particles is quite different. In the Standard Model the weak interaction symmetry

is spontaneously broken by the Higgs mechanism which results in the gauge bosons acquiring a mass. Alternatively, it could be that the weak interaction is merely a residual effect and the SU(2) symmetry is only global. The weak bosons would be composite objects and play a roll analogous to that of the  $\rho$ ,  $\omega$  mesons in QCD. If this is the case, one expects  $\Lambda_H$  to be of the order of 100 GeV which is the energy scale of the Fermi coupling constant.

## 2.2 Quark and Lepton Masses and Chiral Symmetry

A theoretical difficulty of compositeness is that the masses of the quarks and leptons are all very much smaller than the hypercolour confinement scale  $\Lambda_H$ . This is contrary to the natural view that bound states should have masses of the order of the scale of the binding force. For example in QCD the masses of the lightest hadrons are of the order of a few hundred MeV and the colour confinement scale  $\Lambda_C$  is about 200 - 400 MeV.

Two mechanisms which use symmetry arguments have been suggested to explain the near masslessness of composite fermions. The first scheme requires the introduction of spontaneously broken supersymmetry. Supersymmetry operators transform bosons into fermions and the charges which generate the transformations carry fermionic quantum numbers. Hence spontaneously breaking supersymmetry will produce massless Goldstone fermions. All the quarks and leptons may then be interpreted as being massless Goldstone fermions which acquire masses through breaking of the supersymmetry.

The second mechanism for producing nearly massless composite fermions does not require supersymmetry but uses chiral symmetry.

Chiral symmetry is the separate conservation of left and right handed gauge invariance and is broken by a mass term in a Lagrangian of the form

$$m\psi^\dagger\psi = m ( \psi_L^\dagger \psi_R + \psi_R^\dagger \psi_L ) \quad (2.1)$$

where  $\psi_L = 1/2 (1 - \gamma_5) \psi$  and  $\psi_R = 1/2 (1 + \gamma_5) \psi$ . Hence one can force a set of composite fermions to be massless by imposing the following two conditions on the underlying interactions.

- 1). The interaction must have a chiral symmetry which prevents mixing of left and right handed composite fermions.
- 2). The interactions do not cause the chiral symmetry to be spontaneously broken.

The first condition is satisfied if the hypercolour interactions are gauge invariant and so is not a strong constraint. However, the second condition which requires that the chiral symmetry is not broken spontaneously is non trivial and may impose strong constraints on the hypercolour interactions.

The most straightforward way to obtain chiral symmetry for composite states is to impose it at the constituent level. However, this does not guarantee an unbroken symmetry for the composite quarks and leptons. For example in QCD with almost massless quarks, chiral symmetry is broken spontaneously leaving massive fermions (the nucleons) and light pions which are the almost massless Goldstone bosons. Clearly the dynamics of the hypercolour force must differ considerably from QCD in this respect.

It has been found by t'Hooft [2.7] that to have an unbroken global chiral symmetry imposes non trivial constraints on the

underlying theory. The t'Hooft consistency conditions are based upon the fact that theories possessing global chiral symmetries have Green's functions with anomalous divergences which could break the symmetry. The anomaly [2.8, 2.9] arises because of the short distance behaviour of triangle graphs with fermion loops (see Figure 2.2). Defining the three point function

$$(2\pi)^4 \delta^4(\sum q_i) \Gamma_{\alpha\beta\gamma}(q_1, q_2, q_3) = \int \prod_i d^4 x_i e^{i q_i x_i} \langle 0 | T(J_\alpha(x_1) J_\beta(x_2) J_\gamma(x_3)) | 0 \rangle \quad (2.2)$$

where  $J_\mu$  is a global symmetry current then it follows that

$$q_3^\gamma \Gamma_{\alpha\beta\gamma}(q_1, q_2, q_3) = A_J \epsilon_{\alpha\beta\gamma\tau} q_1^\alpha q_2^\tau \quad (2.3)$$

where  $A_J$  is a constant determined by the representation of the fermions to which  $J_\mu$  couples (see Figure 2.2). Writing  $J_\mu$  in terms of left and right handed components of the fermions in the theory one obtains

$$A_J = (1/8\pi^2) \sum_i \text{Tr} \{ (\lambda_R^i)^3 - (\lambda_L^i)^3 \} \quad (2.4)$$

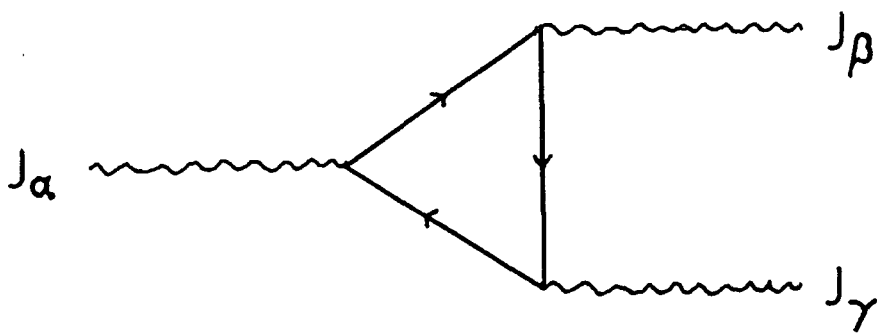
The t'Hooft condition which must necessarily be satisfied if chirality is not to be spontaneously broken is that for all currents  $J_\mu$

$$(A_J)_{\text{bound states}} = (A_J)_{\text{preons}} \quad (2.5)$$

where  $A_J$  in the preon theory is computed for all possible global symmetry currents and  $(A_J)_{\text{bound states}}$  is calculated only in terms of the massless excitations which are supposed to result from the binding.

Some insight into the condition may be obtained [2.10, 2.11] by

Figure 2.2



The anomaly from the triangle graph between three global currents  $J_\mu$  connected by a fermion loop.

considering the form of  $\Gamma$  at  $q_1^2 = q_2^2 = q_3^2 = q^2$ . At this point  $\Gamma$  contains terms with an  $A_J/q^2$  singularity which must be reproduced when calculating  $\Gamma$  in terms of bound states of the theory. The singularities must be a consequence of massless particles in the bound state spectrum. If there is spontaneous breakdown of the symmetry associated with  $J_\mu$  then  $A_J$  is related to the coupling of the resulting Goldstone boson to the two remaining currents. This is the case in QCD where one uses the anomaly to compute the rate for  $\pi^0 \rightarrow 2\gamma$ . However, if the symmetry associated with  $J_\mu$  remains unbroken, then there must be massless fermionic bound states which contribute to the singularity with the same residue  $A_J$  as in the preon case. This is precisely the condition given by (2.5). There are three possibilities:

- 1). Chiral symmetry is completely broken.
- 2). Chiral symmetry remains unbroken so composite massless fermions may be present.
- 3). Chiral symmetry is partially broken. This allows both massless fermions and scalars to be formed.

Unfortunately the constraint discussed above is only strong for case 2 and so a particular model cannot be discarded solely because it fails to satisfy the t'Hooft anomaly condition.

### 2.3 Experimental Bounds on Compositeness

One can extract information about the compositeness of quarks and leptons from low energy data by consideration of precisely measured parameters, rare processes, anomalous processes and also by looking for new particles. The effective Lagrangian of quarks and leptons

must reproduce the Standard Model except for terms  $O(1/\Lambda_H)$ . The anomalous magnetic moment of the electron has been measured very accurately by experiment and has been calculated to high precision in QED. One has [2.12, 2.13]

$$(g - 2)_{\text{expt}} = (g - 2)_{\text{QED}} + \Delta g_e \quad (2.6)$$

and  $\Delta g_e < 5 \times 10^{-10}$ . One expects

$$\Delta g_e \sim A \frac{m_e}{\Lambda_H} + B \left( \frac{m_e}{\Lambda_H} \right)^2 \quad (2.7)$$

where A and B are constants. However, if it is chiral symmetry which causes the electron to be almost massless, then  $A = 0$  [2.14, 2.15] and the first correction is of order  $(m_e/\Lambda_H)^2$ . If  $B \approx 1$  then one obtains the bound  $\Lambda_H > 22 \text{ GeV}$ . A similar calculation for the muon [2.12, 2.13] using  $\Delta g_\mu < 3 \times 10^{-8}$  yields  $\Lambda_H > 580 \text{ GeV}$ .

If quarks and leptons are composite, a sign of this at low energies ( $\ll \Lambda_H$ ) is an effective four fermi interaction [2.16]

$$L = 4\pi C \bar{f}_1 \bar{f}_2 f_3 f_4 \quad (2.8)$$

This effective Lagrangian describes rare processes such as  $\mu \rightarrow \bar{e}e$ ,  $K_L \rightarrow \mu^+ e^-$ ,  $K^+ \rightarrow \pi^+ \mu^+ e^-$  and  $\mu N \rightarrow eN$ . Experimental limits give bounds on  $\Lambda_H > 100 \text{ TeV}$  if  $C=1$  [2.17]. However, without knowledge of the hypercolour dynamics, no quantitative value of C can be given. It may be that the small overlap of the fermion wavefunctions causes C to be very small and removes the above constraint on  $\Lambda_H$ .

Proton decay will be a consequence of compositeness if quarks and leptons are composed of the same constituents. Processes such as

$uu \rightarrow \bar{d}e^+$  will result in the proton lifetime

$$\tau \sim (\Lambda_H^4/m_p^5) \quad (2.9)$$

The experimental limit on the proton lifetime from the decay  $p \rightarrow e^+\pi^0$  is  $\tau/\text{Br}(p \rightarrow e^+\pi^0) > 10^{32}$  years [2.18] and so one requires either  $\Lambda_H \gtrsim 10^{15}$  GeV and  $C \sim 1$  or that  $C$  is very small or zero.

Anomalous contact interactions such as  $e^+e^- \rightarrow e^+e^-$ ,  $\mu^+\mu^-$ ,  $q\bar{q}$  etc. should have values of  $C$  of order 1 if the interactions do not involve a change of flavour. Experimental data from  $e^+e^-$  annihilation at PETRA produces the bound  $\Lambda_H \gtrsim 500$  GeV [2.19].

Perhaps the most convincing way to demonstrate compositeness is to find new particles which do not fit the Standard Model. If the weak bosons are composite, in addition to the quarks and leptons, one expects new scalar bosons and possibly also coloured partners for the  $W$ 's and  $Z$ 's. The properties of such particles are discussed in chapter 4. In addition to these particles one might observe excited states of quarks and leptons. The current bounds on excited electrons and muons comes from the  $e^+e^-$  annihilation experiments PETRA and PEP [2.20] and are

$$\frac{a^2 + b^2}{m_\mu^{2*}} < (330 \text{ GeV})^{-2}, \quad \frac{a^2 + b^2}{m_e^{2*}} < (58 \text{ GeV})^{-2} \quad (2.10)$$

where  $a$  and  $b$  are the coupling strengths in the gauge invariant  $l^*l\gamma$  vertex

$$L_{ll^* \gamma} = \frac{e}{2m_l^*} \bar{l}^* \sigma^{\mu\nu} (a + b\gamma_5) l F_{\mu\nu} \quad (2.11)$$

Recently, excited leptons were used as an explanation for the large

number of  $l^+l^-\gamma$  events observed during the 1983/84 run of the CERN  $p\bar{p}$  collider [2.21, 2.22]. In this run, three out of thirteen  $Z$  decays into leptons also emitted a hard photon and the decay  $Z \rightarrow l^*l \rightarrow ll\gamma$  was proposed as a possible mechanism for an excited lepton [2.23, 2.24]. However, the latest run of the collider has failed to find any  $ll\gamma$  events [2.25, 2.26] and the ratio  $(Z \rightarrow ll\gamma)/(Z \rightarrow ll)$  is of the order of a few percent in accordance with the prediction of the Standard Model for the bremsstrahlung rate. Hence there are no experimental signs of excited leptons. Signatures for the decay of excited quarks (starks) have been discussed by De Rujula et al. [2.27] but again there are no experimental signs of these particles.

In summary, there is currently no experimental evidence for compositeness but bounds on the scale of an underlying force are somewhat uncertain and not particularly strong. It is difficult to say more than that  $\Lambda_H > 100$  GeV. The remainder of this chapter is spent discussing some of the simple composite models which have been proposed. These fall broadly into two classes: models with fermionic and bosonic constituents are described in section 2.4 and models with fermionic constituents only in section 2.5. It should be emphasised that none of these models is very convincing and they are not serious candidates for a final theory.

#### 2.4 Models with Fermionic and Bosonic Constituents

In models where quarks and leptons are comprised of a fermion and a boson, these constituents can be combined in a straightforward way. If the hypercolour group is  $SU(N_H)$  then the fermion can transform as an  $N$  and the boson as an  $\bar{N}$  or vice versa. Hypercolour singlet quarks

and leptons can then always be made since  $N \times \bar{N} = 1 + (N^2 - 1)$ . Hence the number of hypercolours is undetermined in these models and the underlying symmetry group is taken to be  $SU(N_H) \times SU(3)_C \times U(1)_{EM}$ .

The most simple assignment of quantum numbers to give one family of fermions is that used in the haplon (from the Greek "haplos" meaning simple) model [2.28] i.e.

	Spin	Charge	Colour	Hypercolour
$\alpha$	1/2	1/2	1	N
$\beta$	1/2	-1/2	1	N
x	0	1/6	3	$\bar{N}$
y	0	-1/2	1	$\bar{N}$

where  $\alpha, \beta$  are Dirac spinors carrying  $SU(2)$  quantum numbers and the scalars x, y carry colour and lepton number. The first generation of hypercolour singlet quarks and leptons are composed of haplons bound in the following way:

$$\begin{aligned} \nu_e &= (\alpha\gamma)_1 & u &= (\alpha x)_3 \\ e^- &= (\beta\gamma)_1 & d &= (\beta x)_3 \end{aligned}$$

In this scheme, the fermions do not carry colour. However it is easy to re-assign the quantum numbers so that most or all of the constituents are colour triplets i.e.

	Spin	Charge	Colour	Hypercolour
$\alpha$	1/2	1/2	3	N
$\beta$	1/2	-1/2	3	N
x	0	1/6	1	$\bar{N}$
y	0	-1/2	$\bar{3}$	$\bar{N}$

or

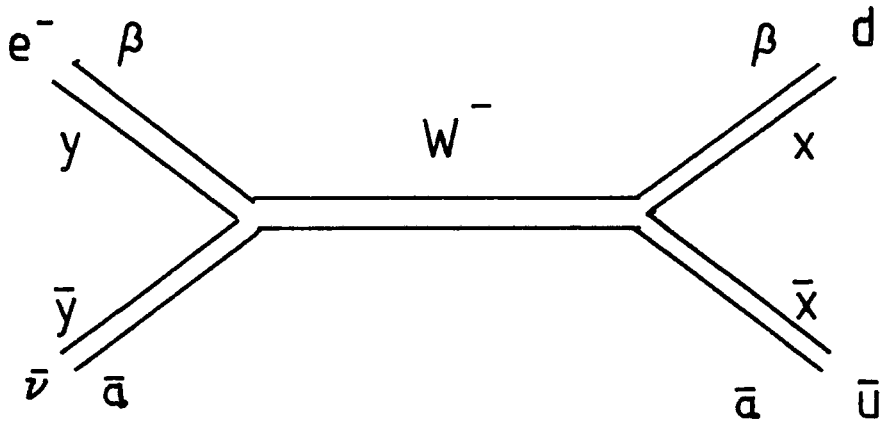
	Spin	Charge	Colour	Hypercolour
$\alpha$	1/2	1/2	$\bar{3}$	N
$\beta$	1/2	-1/2	$\bar{3}$	N
x	0	1/6	$\bar{3}$	$\bar{N}$
y	0	-1/2	3	$\bar{N}$

Additional generations can be constructed by giving the scalars x and y a generation index, or they may be interpreted as radially excited bound states of the first family.

The above class of models is particularly convenient for a composite description of the weak bosons. Weak interactions can be visualised as proceeding through diagrams of the type shown in Figure 2.3. Since the QHD Lagrangian is invariant under the interchange of  $\alpha$  and  $\beta$ , one can identify weak isospin with the SU(2) subgroup contained within the U(2) symmetry. The  $W^{\pm}$  and  $W^3$  are the bound states  $\alpha\bar{\beta}$ ,  $\bar{\alpha}\beta$  and  $1/\sqrt{2}(\alpha\bar{\alpha} - \beta\bar{\beta})$ . The  $W^3$  mixes with the photon to produce a Z (see chapter 3). One can also construct an SU(2) isosinglet particle given by  $W^0 = 1/\sqrt{2}(\alpha\bar{\alpha} + \beta\bar{\beta})$  but this has not been observed by experiment and so presumably must be much heavier than the W and Z. This particle is discussed in more detail in subsequent chapters. It should be emphasised that in this scheme, weak interactions are not described by a gauge theory but only by an effective theory. The masses of the weak bosons are not generated by spontaneous symmetry breaking thus removing the need for Higgs scalars.

One problem in the haplon model, and indeed in many other composite models, is the parity violation in weak interactions. If the hypercolour gauge group is SU( $N_H$ ) then one would expect parity to

Figure 2.3



The weak interaction  $e^- \bar{\nu} \rightarrow W^- \rightarrow \bar{u} d$  in the Haplion model.

be conserved. Its violation may be related in some way which is not yet understood to the fact that the fermions are much lighter than the hypercolour scale  $\Lambda_H$ . Alternatively it may be that only left handed fermions bind in the above fashion and right handed objects are either elementary or are constructed in a different manner.

Other composite models with a fermion and a boson as the fundamental constituents have much the same general form as the haplon model described above but with different specific details [2.29, 2.30, 2.31, 2.32]. The haplon model is very convenient to use when discussing composite weak bosons since the structure of the weak force is particularly simple in this scheme. For this reason and for the sake of definiteness, the haplon model will commonly be used as an example model in subsequent chapters.

### 2.5 Models with Fermionic Constituents Only

In these models quarks and leptons are made of three constituent fermions bound by a hypercolour force. The hypercolour gauge group must be  $SU(3)$  since  $N \times N \times N$  will form a hypercolour singlet only for the value  $N = 3$ . Hence the full underlying symmetry is given by  $SU(3)_H \times SU(3)_C \times U(1)_{EM}$ . In the rishon (= primary in Hebrew) model [2.33], all quarks and leptons in a generation can be built from just two fermionic constituents.

	Spin	Charge	Colour	Hypercolour
T	1/2	1/3	3	3
V	1/2	0	$\bar{3}$	3

The first generation of quarks and leptons are built from these

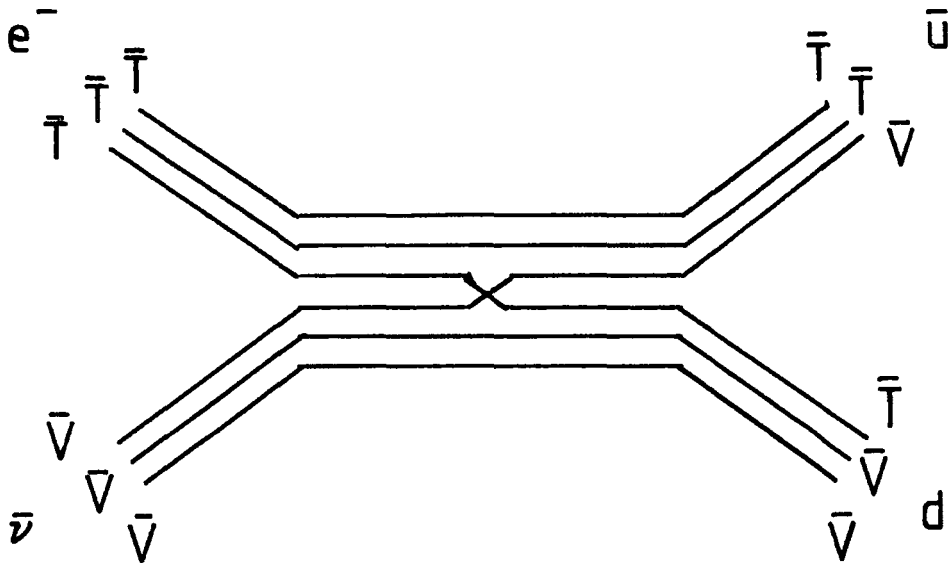
constituents in the following way

$e^+$	TTT	$\bar{\nu}_e$	$\bar{V}\bar{V}\bar{V}$
u	TTV	d	$\bar{V}\bar{V}\bar{T}$
$\bar{d}$	TVV	$\bar{u}$	$\bar{V}\bar{T}\bar{T}$
$\nu_e$	VVV	$e^-$	$\bar{T}\bar{T}\bar{T}$

In this scheme, the weak interactions are residual hypercolour forces operating at short distances between bound state objects. The force is analogous to the residual colour force acting between two colourless hadrons. The weak bosons can be thought of as bound states of six rishons - for example  $W_L^+ = T_L T_L T_R V_R V_R V_L$ . An example of weak boson exchange in the rishon model is shown in Figure 2.4. It can be seen that weak boson exchange is much more complicated than in the haplon model of the previous section. However, this is equivalent to  $W_L^+ = (e_L^+ \nu_e)$ ,  $(u_L \bar{d}_L)$ , etc., and as the force binding the preons into quarks and leptons is very strong, the W may be effectively a fermion-antifermion bound state just as it is in the haplon model.

An entirely different composite model with three fermionic constituents factorises the colour, flavour and generation number [2.34, 2.35, 2.36, 2.37]. In the Standard Model one can distinguish three types of symmetry - the weak interaction gauge symmetry  $SU(2)_{\text{Weak}}$ , the colour gauge symmetry  $SU(3)_C$  and a symmetry between generations  $SU(N)_F$ . Thus for three generations one has the symmetry  $SU(2)_W \times SU(3)_C \times SU(3)_F$ . It is possible to build a model where each constituent carries one of the above symmetries. The  $SU(2)_W$  constituents are called "weakons", the  $SU(3)_C$  constituents "chromons" and the  $SU(3)_F$  constituents "familons". The quarks and leptons of the first generation are given by

Figure 2.4



The weak interaction  $e^- \bar{\nu} \rightarrow W^- \rightarrow \bar{u} d$  in the Rishon model.

$$\begin{aligned} \nu_e &= (W_u, C_0, F_1) & u_r &= (W_u, C_i, F_1) \\ e^- &= (W_d, C_0, F_1) & d_r &= (W_d, C_i, F_1) \end{aligned}$$

where  $i$  runs over the colours red, green and blue. Notice that because leptons are colourless, a leptonic chromon  $C_0$  must be introduced. The weak bosons are fermion-antifermion ( $W\bar{W}$ ) bound states in this model. Notice that in all the schemes discussed, the weak bosons can be considered to be made from a fermion-antifermion pair so that the haplon model [2.28] serves as a general example of composite weak interactions.

The models which factorise colour, flavour and generation number have many problems - for example, one has no knowledge of the binding between the constituents or whether photons and gluons are bound states. Models of this type cannot be ruled out but they are far from satisfactory at present and shall not be considered further.

## CHAPTER 3 THE INTERNAL STRUCTURE OF WEAK BOSONS

### 3.1 Introduction

In the past, short range forces have been found to be a consequence of the substructure of the interacting particles. For example, molecular and Van-der-Waals forces are residual electromagnetic forces arising from the polarisation of the electronic substructure of neutral atoms. Similarly the short range nuclear force has turned out to be a remnant of the underlying colour force between the hadrons' constituents (the quarks). The colour neutral hadrons are polarised and the nuclear force is the observed result. The only short distance interaction which is not known to be due to a residual force between constituents is the weak interaction. In this case the force is mediated via elementary gauge bosons (W's and Z's) which acquire mass by the Higgs spontaneous symmetry breakdown mechanism discussed in chapter 1. Because the gauge bosons are massive, the force only operates at short distances  $\sim \hbar/M_W c$ .

Since the W's and Z's have the masses and decays predicted by the Weinberg-Salam  $SU(2) \times U(1)$  theory they are generally supposed to be elementary structureless, particles. Nevertheless it is possible that  $SU(2) \times U(1)$  is merely an effective theory which describes only the low energy properties of some more fundamental hypercolour theory. In chapter 2 it was noted that several composite models of quarks and leptons also contained composite weak bosons. If the radii of quarks and leptons are related to the Fermi scale of  $(300 \text{ GeV})^{-1} \approx 10^{-17} \text{ cm}$ ,

it is natural to assume that W bosons will have a similar size. If one believes that the weak force is a residual interaction of a hitherto undetected force, then the short range nature of the weak interaction would arise because quarks and leptons are hypercolour singlets but with radii of about  $(1 \text{ TeV})^{-1}$ . This interpretation of weak interactions changes the status of the W and Z. They become merely the lowest lying  $J^{PC} = 1^{--}$  bound states of the quark and lepton constituents and hypergluons are the new fundamental gauge bosons. The  $SU(2) \times U(1)$  electroweak theory is only an effective theory which works at distances greater than the hypercolour confinement scale  $\hbar/\Lambda_H c$ .

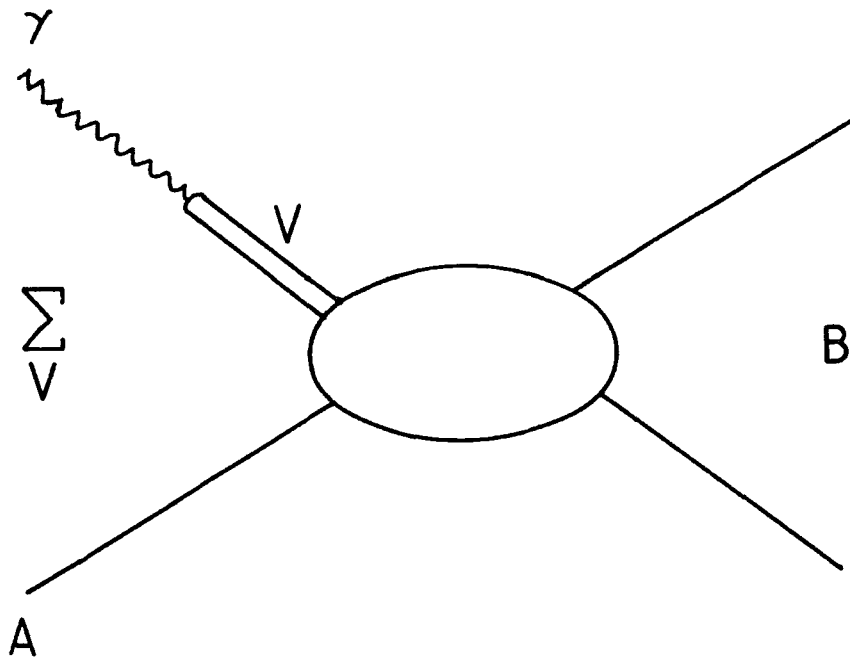
When one describes the weak interactions as an effective theory, it seems natural to look for parallels with the strong nuclear force and attempt to apply the ideas used in QCD. One such idea which will be used extensively is the application of "vector dominance" [3.1, 3.2] in weak interactions.

### 3.2 Vector Dominance and its Applications

In QCD, an interesting and useful feature of photon-hadron interactions is that they are very much like hadron-hadron interactions. This is because of vector dominance of electromagnetic interactions, the photon-hadron coupling proceeding through the vector mesons  $V \equiv \rho, \omega, \phi$  etc. (see Figure 3.1). The amplitude for the process  $\gamma A \rightarrow B$  can thus be written in the form

$$T_{\gamma A \rightarrow B}(Q^2, s, t, \dots) = \frac{1}{V} \left[ \frac{e}{f_V} \right] \frac{m_V^2}{m_V^2 + Q^2} T_{VA \rightarrow B}(s, t, \dots) \quad (3.1)$$

Figure 3.1



Vector dominance of the process  $\gamma A \rightarrow B$ . The photon interacts via the lightest vector mesons  $\rho, \omega, \phi$  etc.

where  $T_{VA \rightarrow B}$  are the on-shell vector meson scattering amplitudes and the coupling constants  $f_V^{-1}$  can be measured in the annihilation process of Figure 3.2.

The cross section for the processes of Figure 3.2 into a final state F, neglecting interference between vector mesons, is given by

$$\sigma(e^+e^- \rightarrow F) = 4\pi\alpha \frac{\left(\frac{e}{f_V}\right)^2 \left(\frac{m_V^2}{s}\right)^2}{\left(s - m_V^2\right)^2 + m_V^2 \Gamma_t^2} \frac{m_V \Gamma_t^V B_F^V}{\Gamma_t^V} \quad (3.2)$$

where  $\Gamma_t^V$  is the total width and  $B_F^V$  is the branching fraction to the final state F. In the narrow width approximation one obtains

$$\sigma(e^+e^- \rightarrow F) = 4\pi\alpha \frac{\left(\frac{e}{f_V}\right)^2}{V} \delta(s - m_V^2) B_F^V \quad (3.3)$$

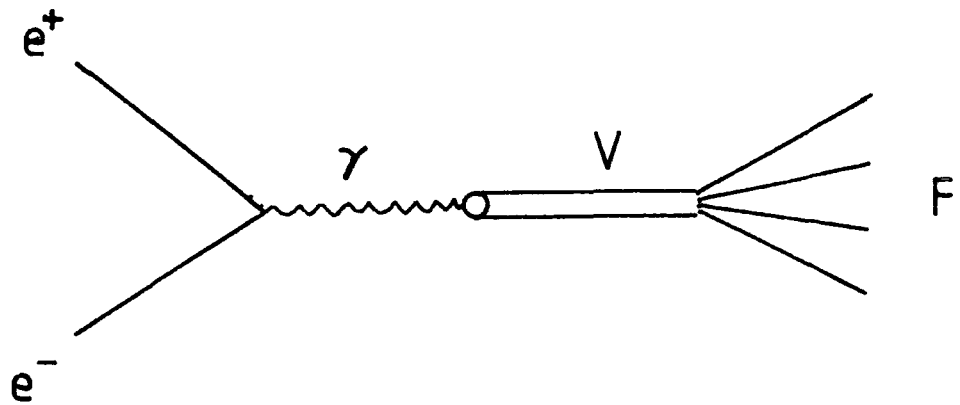
so that, given  $B_F^V$ , measuring  $\sigma$  enables  $f_V$  to be deduced. The decay width into lepton pairs can then be computed using

$$\Gamma(V \rightarrow e^+e^-) = \frac{m_V \alpha}{3} \left(\frac{e}{f_V}\right)^2 \quad (3.4)$$

The results obtained for the lowest lying vector meson ( $\rho$ ) are  $f_\rho = 4.91 \pm 0.20$  and hence  $\Gamma_\rho = 7.1 \pm 0.5$  keV [3.3]. This decay constant is often expressed in terms of the dimensional quantity  $F_V \equiv m_V/f_V$  whereupon  $F_\rho = 0.16 \pm 0.01$  GeV.

One can attempt to describe the weak interactions in the same way. Composite W's and Z's are the lowest mass vector bosons and play the same role as the  $\rho$  mesons of QCD. Concentrating attention on the haplon model [2.28] of section 2.4, the weak interaction is carried by the two fields  $\alpha$  and  $\beta$ . These fields form a global SU(2) isovector

Figure 3.2



Vector dominance in  $e^+e^-$  annihilation. The photon-meson couplings  $f_V^{-1}$  can be deduced by measuring the cross-section  $\sigma(e^+e^- \rightarrow F)$ .

triplet

$$\begin{bmatrix} W^+ \\ W^3 \\ W^- \end{bmatrix} = \begin{bmatrix} \alpha\bar{\beta} \\ 1/\sqrt{2} (\alpha\bar{\alpha} - \beta\bar{\beta}) \\ \bar{\alpha}\beta \end{bmatrix} \quad (3.5)$$

Before mixing,  $M(W^+) = M(W^-) = M(W^3)$  as there is exact isospin symmetry but since the Z particle has a larger mass than the W, one requires that the  $W^3$  boson and the photon must mix [3.4, 3.5, 3.6] somewhat in analogy with  $\rho - \gamma$  mixing in QCD (see Figure 3.3). The strength of the  $W^3 - \gamma$  transition  $\lambda_W$  is directly related to the electroweak parameter  $\sin^2\theta_W$  by [3.6]

$$\sin^2\theta_W = (e/g) \lambda_W \quad (3.6)$$

where  $g$  is the W-fermion coupling constant, which is related to the Fermi coupling by  $G_F = \sqrt{2}g^2/8M_W^2$  so that

$$M_W = 2^{-5/4} G_F^{-1/2} g = 123g \text{ GeV} \quad (3.7)$$

and from [3.6]

$$M_Z^2 = M_W^2 / (1 - \lambda_W^2) \quad (3.8)$$

$\lambda_W$  is determined by the W decay constant  $F_W$  which is defined by analogy with the  $\rho^0$  decay constant  $F_\rho$  above by

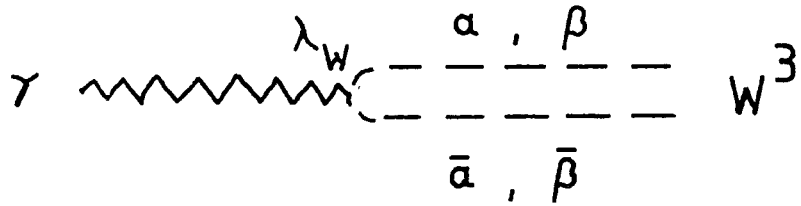
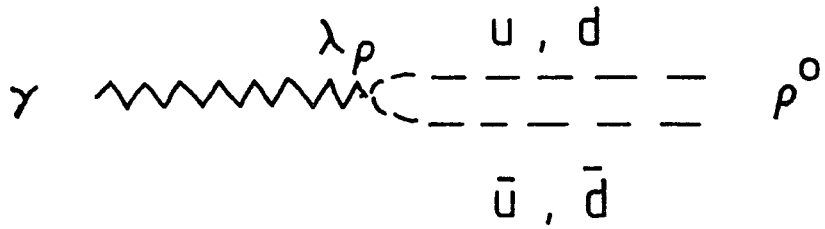
$$\lambda_W = \frac{eF_W}{M_W} = \frac{e}{f_W} \quad (3.9)$$

Hence

$$\langle 0 | j_\mu^{(3)} | W^3 \rangle = \langle 0 | 1/2 (\bar{\alpha}\gamma_\mu\alpha - \bar{\beta}\gamma_\mu\beta) | W^3 \rangle = \epsilon_\mu M_W F_W = \epsilon_\mu M_W^2 / f_W \quad (3.10)$$

If one constructs a non-relativistic bound state model of the

Figure 3.3



Photon - bound state mixing. In QCD the degree of mixing is given by  $\lambda_\rho^2 = 1/260$ . In composite models  $W^3$ - $\gamma$  mixing causes the Z to be heavier than the W.  $\lambda_W^2 \approx \sin^2 \theta_W \approx 0.218$ .

weak bosons the decay constant  $F_W$  can be expressed approximately in terms of its wave function. One has [3.7]

$$|W^3\rangle = \frac{1}{\sqrt{2}} \frac{1}{\sqrt{N_H}} \frac{1}{\sqrt{N_C}} \sum_i \sum_j (\bar{\alpha}_{ij} \alpha_{ij} - \bar{\beta}_{ij} \beta_{ij}) \varphi(x) \quad (3.11)$$

where  $i, j$  are hypercolour and colour labels respectively and  $\varphi(x)$  is the co-ordinate space wavefunction describing the haplons in a  $W$  boson. Combining equations (3.10) and (3.11) gives

$$\langle 0 | j_\mu^3 | W^3 \rangle = \epsilon_\mu (2N_C N_H M_W)^{1/2} \varphi(0) = \epsilon_\mu M_W F_W \quad (3.12)$$

so that with (3.6), (3.9) and (3.12)

$$\sin^2 \theta_W = (e^2/g) \sqrt{N_C} \sqrt{N_H} (2/M_W^3)^{1/2} \varphi(0) \quad (3.13)$$

This important result relating  $\sin^2 \theta_W$  to the bound state wavefunction at the origin will be used extensively in chapters 4 and 5.

In the rest of this chapter, it will be demonstrated that composite weak bosons, in conjunction with other quite natural assumptions, can reproduce the low energy behaviour of the Standard Model weak current.

### 3.3 Universality of the Weak Current

Several aspects of bound state models can be derived from a local current algebra of weak currents [3.8]. The weak isospin charges  $F_i^W$  ( $i=1,2,3$ ) obey the algebra

$$[ F_i^W, F_j^W ] = i \epsilon_{ijk} F_k^W \quad (3.14)$$

Suppose that these charges can be written as integrals over charge densities  $F_{0i}^W(x)$  i.e.

$$F_i^W(x^0) = \int F_{0i}^W(x) d^3x \quad (3.15)$$

and suppose in addition that these local charge densities obey at equal times the local current algebra

$$[ F_{0i}^W(x), F_{0j}^W(y) ]_{x^0=y^0} = i\epsilon_{ijk} F_{0k}^W \delta^{(3)}(\vec{x} - \vec{y}) \quad (3.16)$$

This algebra need not be satisfied if quarks and leptons are not pointlike. However, it is satisfied in the haplon model where currents are bilinear in  $\alpha$  and  $\beta$ . Consider now the matrix elements of the left-handed weak neutral current  $F_{\mu 3}^L(x)$  between left handed quark and lepton states. Weak isospin algebra requires a universal normalization at  $t=0$  i.e.  $F_e(0) = F_\mu(0) = F_\nu(0) = 1$  etc. where  $t$  is the momentum transfer. Suppose that one uses the W-dominance approximation where weak boson exchange is dominated by the lowest lying W pole. One has

$$F_f(t) = \frac{M_W^2}{f_W} \frac{f_W^{ff}}{M_W^2 - t} \quad (3.17)$$

where  $f_W^{ff}$  is the W-fermion coupling constant and  $f$  is one of the fermions  $e^-$ ,  $\nu_e$ ,  $\mu^-$ ,  $\nu_\mu$  etc. Using  $F_f(0) = 1$ , one finds

$$g \equiv f_W^{ff} = f_W \quad (3.18)$$

so that the W bosons couple with the same strength to all quarks and leptons. Hence the universality of weak interactions results from W-dominance of the weak current.

### 3.4 Effective Lagrangians and W-Dominance

In order to see how composite models reproduce the low energy features of the Standard Model [3.4, 3.5, 3.6], such as the structure of the weak neutral current and the Weinberg mass relations (1.27) and (1.28), consider first of all a model without electromagnetism. The lowest mass vector bosons form an isovector triplet ( $W^+$ ,  $W^-$ ,  $W^3$ ) coupled to the left-handed weak isospin current. Neglecting higher mass excitations, one has the effective Lagrangian

$$L = -1/4 W_{\mu\nu} W^{\mu\nu} + 1/2 m_1^2 W_\mu W^\mu - g_1 W_\mu J_\mu^L \quad (3.19)$$

where  $m_1 \equiv M_{W^\pm}$ ,  $J_\mu^L = \bar{L}\gamma_\mu \tau/2 L = 1/2 (\bar{\nu}_L \gamma_\mu \nu_L - \bar{e}_L \gamma_\mu e_L)$  and  $W_\mu$  is the isotriplet vector boson field.

Now switch on electromagnetism and consider photon interactions with composite quarks and leptons. It has been shown in section 3.2 how, in QCD, photon-hadron interactions proceed via the lowest mass vector bosons -  $\rho, \omega, \phi$  etc. One can repeat this vector dominance for the hypercolour force and suppose the photon-quark (lepton) interactions proceed via the lowest lying vector mesons of QHD in what has come to be called "W-dominance" [3.9]. In the neutral current sector, the isovector  $W^3$  and the lowest lying isoscalar boson dominate. In the Lagrangian formalism one has

$$L = \lambda_1 [ -1/4 (F_{\mu\nu} W^{3\mu\nu} + W_{\mu\nu}^3 F^{\mu\nu}) - g_1 A_\mu J_1^\mu ] \quad (3.20)$$

where  $\lambda_1$  is the  $W^3$ -photon mixing and  $J_1^\mu = J_\mu^{L3}$ .

In addition to the above terms, one must cater for  $SU(2)_L$

isoscalar bosons which couple to the isodoublet fermions via an isoscalar current and also for right-handed bosons. None of these currents has yet been observed and it is convenient to describe their effective interactions by a single heavy neutral isoscalar boson Y of mass  $m_2 \gg m_1$ . This introduces an additional term into the neutral current Lagrangian

$$\begin{aligned}
 L = & - 1/4 W_{\mu\nu}^0 W^{0\mu\nu} + 1/2 m_2^2 W_\mu^0 W^{0\mu} - g_2 W_\mu^0 J_2^\mu \\
 & + \lambda_2 [ - 1/4 (F_{\mu\nu} W^{0\mu\nu} + W_{\mu\nu}^0 F^{\mu\nu}) - g_2 A_\mu J_2^\mu ]
 \end{aligned} \tag{3.21}$$

Combining (3.19)-(3.21) and adding an electromagnetic self interaction kinetic energy term, one has for the neutral current

$$\begin{aligned}
 L = & - 1/4 F_{\mu\nu} F^{\mu\nu} - 1/4 W_{\mu\nu}^3 W^{3\mu\nu} + 1/2 m_1^2 W_\mu^3 W^{3\mu} - g_1 W_\mu^3 J_1^\mu \\
 & + \lambda_1 [ - 1/4 (F_{\mu\nu} W^{3\mu\nu} + W_{\mu\nu}^3 F^{\mu\nu}) - g_1 A_\mu J_1^\mu ] \\
 & - 1/4 W_{\mu\nu}^0 W^{0\mu\nu} + 1/2 m_2^2 W_\mu^0 W^{0\mu} - g_2 W_\mu^0 J_2^\mu \\
 & + \lambda_2 [ - 1/4 (F_{\mu\nu} W^{0\mu\nu} + W_{\mu\nu}^0 F^{\mu\nu}) - g_2 A_\mu J_2^\mu ]
 \end{aligned} \tag{3.22}$$

In order to find the physical masses and couplings arising from this Lagrangian, one uses the propagator matrix formalism [3.10, 3.11, 3.12] to diagonalize equation (3.22). Following [3.9] one obtains

$$- 2 L_{\text{eff}} = \frac{1}{q^2} (\lambda_1 g_1 J_1 + \lambda_2 g_2 J_2)^2 \quad (3.23)$$

$$+ \frac{1}{q^2 - M_1^2} \frac{1}{b_1^2} \left[ \lambda_1 g_1 \frac{m_1^2}{m_1^2 - M_1^2} J_1 + \lambda_2 g_2 \frac{m_2^2}{m_2^2 - M_1^2} J_2 \right]^2$$

$$+ \frac{1}{q^2 - M_2^2} \frac{1}{b_2^2} \left[ \lambda_1 g_1 \frac{m_1^2}{m_1^2 - M_2^2} J_1 + \lambda_2 g_2 \frac{m_2^2}{m_2^2 - M_2^2} J_2 \right]^2$$

with

$$\Delta = 1 - \lambda_1^2 - \lambda_2^2$$

$$b_i = \left[ \Delta + \lambda_1^2 \frac{m_1^4}{(m_1^2 - M_i^2)^2} + \lambda_2^2 \frac{m_2^4}{(m_2^2 - M_i^2)^2} \right]^{1/2}$$

The mass eigenvalues are

$$M_\gamma = 0$$

$$M_Z^2 \equiv M_1^2 = (1/2\Delta) [ m_1^2(1 - \lambda_2^2) + m_2^2(1 - \lambda_1^2) - \Gamma ] \quad (3.24)$$

$$M_Y^2 \equiv M_2^2 = (1/2\Delta) [ m_1^2(1 - \lambda_2^2) + m_2^2(1 - \lambda_1^2) + \Gamma ]$$

where

$$\Gamma \equiv [ m_1^4(1 - \lambda_2^2)^2 + m_2^4(1 - \lambda_1^2)^2 - 2m_1^2 m_2^2 (\Delta - \lambda_1^2 \lambda_2^2) ]^{1/2}$$

Clearly the first term in (3.23) corresponds to photon interactions and so one must insist that

$$\lambda_1 g_1 = \lambda_2 g_2 = e \quad (3.25)$$

If one identifies the electromagnetic current  $J^{\text{EM}} = J_1 + J_2 = J^3 + J^Y$

and supposes that  $\lambda_i < 1$  and  $m_1^2 \ll m_2^2$  then

$$\begin{aligned}
 2 L_{\text{eff}} = & -\frac{e^2}{q^2} J_{\text{EM}}^2 + \frac{1}{q^2 - M_1^2} F_1^2 (J^3 - \sin^2 \theta_1 J_{\text{EM}})^2 \\
 & + \frac{1}{q^2 - M_2^2} F_2^2 (J^Y + \sinh^2 \theta_2 J_{\text{EM}})^2
 \end{aligned} \tag{3.26}$$

where

$$M_2^2 = M_1^2 = m_1^2 / (1 - \lambda_1^2) + O(\lambda^4) \tag{3.27}$$

$$M_Y^2 = M_2^2 = m_2^2 / (1 - \lambda_2^2) + O(\lambda^4)$$

$$F_1^2 = g_1^2 / (1 - \lambda_1^2) + O(\lambda^4, m_1^2/m_2^2) \tag{3.28}$$

$$F_2^2 = g_2^2 / (1 + \lambda_2^2) + O(\lambda^4, m_1^2/m_2^2)$$

$$\sin^2 \theta_1 = \lambda_1^2 + O(\lambda^6, m_1^2/m_2^2) \tag{3.29}$$

$$\sinh^2 \theta_2 = \lambda_2^2 (1 + \lambda_1^2) m_1^2/m_2^2 + O(\lambda^6, m_1^4/m_2^4)$$

i.e.

$$2 L_{\text{eff}} = \frac{e^2}{q^2} J_{\text{EM}}^2 + \frac{g_1^2}{1 - \lambda_1^2} \frac{1}{(q^2 + m_1^2 / (1 - \lambda_1^2))} (J^3 - \lambda_1^2 J_{\text{EM}})^2 \tag{3.30}$$

+ higher order terms

$$\rightarrow \frac{e^2}{q^2} J_{\text{EM}}^2 + \frac{g_1^2}{m_1^2} \left[ (J^3 - \lambda_1^2 J_{\text{EM}})^2 + O(\lambda^6, m_1^2/m_2^2) \right] \tag{3.31}$$

as  $q^2 \rightarrow 0$ .

Hence the low energy neutral current behaviour of the Standard Model has been reproduced by equation (3.31) to leading order in  $\lambda^2$

and  $m_1^2/m_2^2$  if one associates the Weinberg angle  $\theta_W$  with  $\theta_1$  in (3.29). Note that equation (3.27) becomes the Weinberg mass relation (1.28) in lowest order in  $\lambda^2$  and  $(m_1/m_2)^2$ , and will reproduce the Standard Model if  $m_1 \ll m_2$ .

One can also obtain these results by the more intuitive approach of summing Feynman diagrams which will be described in the next section.

### 3.5 The Effective Lagrangian from Feynman Diagrams

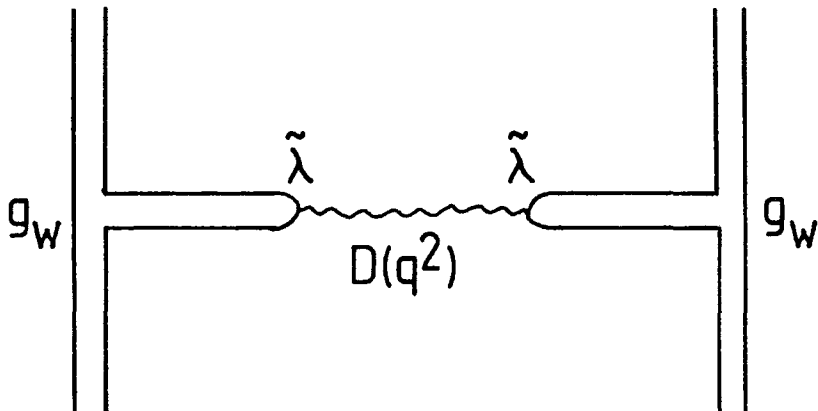
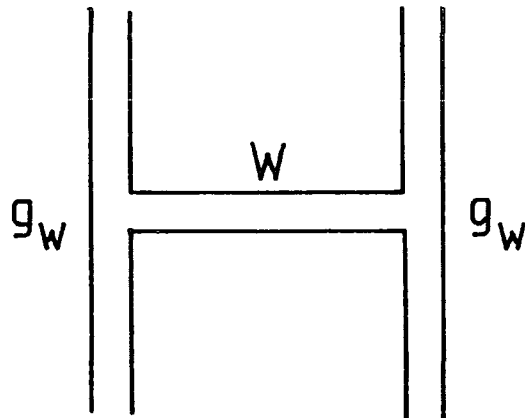
The Feynman diagrams for the electromagnetic and weak neutral current are given in Figure 3.4. The full Lagrangian for these interactions is then [3.13]

$$\begin{aligned}
 -2 L_{\text{eff}} = & \sum_i \frac{g_{W_i}}{q^2 - m_{W_i}^2} j^{(3)2} + \sum_i \frac{g_{Y_i}}{q^2 - m_{Y_i}^2} j^{(Y)2} \\
 & + D(q^2) \left[ \sum_i g_{W_i} \tilde{\chi}_{W_i} \frac{m_{W_i}^2}{q^2 - m_{W_i}^2} j^{(3)} + \sum_i g_{Y_i} \tilde{\chi}_{Y_i} \frac{m_{Y_i}^2}{q^2 - m_{Y_i}^2} j^{(Y)} \right] \quad (3.32)
 \end{aligned}$$

where  $g_{W_i}$  are the  $W_i$ -fermion couplings and  $\tilde{\chi}_{W_i}$  the non-renormalized  $W_i$ -photon couplings, and similarly for  $Y_i$ .  $D(q^2)$  denotes the photon propagator and represents the diagrams of Figure 3.5. Summing the contributions from these diagrams yields

$$\begin{aligned}
 D(q^2) = & \frac{1}{q^2} + \frac{1}{q^2} \sum_i \left[ \tilde{\chi}_{i,m_i^2} \frac{1}{q^2 - m_i^2} \tilde{\chi}_{i,m_i^2} + \tilde{\chi}_{i,m_i^2} \right] \frac{1}{q^2} \\
 & + \frac{1}{q^2} \sum_i [ \quad ] \frac{1}{q^2} \sum_j [ \quad ] \frac{1}{q^2} + \text{higher order terms} \quad (3.33)
 \end{aligned}$$

Figure 3.4



The weak neutral current between composite quarks and leptons.  $D(q^2)$  is the photon propagator.



$$= \frac{1}{q^2} \left[ 1 - \sum_i \frac{\tilde{\chi}_i^2 m_i^2}{q^2 - m_i^2} \right]^{-1} \quad (3.34)$$

where the index  $i$  runs over all  $W$ 's and  $Y$ 's. Introducing renormalized couplings  $\lambda_i^2 = \tilde{\chi}_i^2 (1 + \sum_j \tilde{\chi}_j^2)^{-1}$ , the neutral mass eigenvalue equation is obtained by setting the denominator of (3.34) equal to zero i.e.

$$q^2 = 0 \quad \text{or} \quad 1 + \sum_i \lambda_i^2 \left[ \frac{m_i^2}{q^2} - 1 \right]^{-1} = 0 \quad (3.35)$$

One obtains for (3.32) as  $q^2 \rightarrow 0$

$$2 L_{\text{eff}}(q^2 \rightarrow 0) = - (e^2/q^2) J_{\text{EM}}^2 + G_W [ (J^3 - S_W^2 J_{\text{EM}})^2 + C_W J_{\text{EM}}^2 ] \\ + G_Y [ (J^Y - S_Y^2 J_{\text{EM}})^2 + C_Y J_{\text{EM}}^2 ] \quad (3.36)$$

where  $J^{\text{EM}} = J^3 + J^Y$  so that

$$\sum_i \lambda_{Wi} g_{Wi} = \sum_i \lambda_{Yi} g_{Yi} = e \quad (3.37)$$

and

$$G_W \equiv \sum_i g_{Wi}^2 / m_{Wi}^2 \\ S_W^2 \equiv (e/G_W) \sum_i g_{Wi} \lambda_{Wi} / m_{Wi}^2 \\ C_W \equiv (e^2/G_W) \sum_i \lambda_{Wi}^2 / m_{Wi}^2 - S_W^4 \quad (3.38)$$

and similarly for  $G_Y$ ,  $S_Y$  and  $C_Y$ .

Equation (3.36) can now be expressed in terms of Standard Model

parameters. One has, using the charged current normalisation

$$G_W = 8G_F/\sqrt{2}$$

$$2L_{\text{eff}}(q^2 \rightarrow 0) = -(e^2/q^2)J_{\text{EM}}^2 + \rho \ 8G_F/\sqrt{2} [(J^3 - \sin^2\theta_W J^{\text{EM}})^2 + C_{\text{EM}}^2] \quad (3.39)$$

where

$$\rho \equiv 1 + \sqrt{2}G_Y/8G_F = 1 + G_Y/G_W$$

$$\sin^2\theta_W \equiv (1/\rho) [ S_W^2 + (\rho - 1)(1 - S_Y^2) ] \quad (3.40)$$

$$\rho.C \equiv C_W + (\rho - 1) C_Y + [(\rho - 1)/\rho] (1 - S_W^2 - S_Y^2)^2$$

If one uses W-dominance in the above equations and considers the contribution from only one massive isovector boson, then  $G_Y = 0$ ,  $\rho = 1$ ,  $S_W = \sin\theta_W$  and  $C_W = C_Y = C = 0$ . From (3.39) it is clear that the Standard Model low energy Lagrangian has been reproduced and the Weinberg mass relations (1.27) and (1.28) are obtained from (3.38) and (3.35) respectively i.e.

$$m_W^2 = \sqrt{2}g^2/8G_F \quad \text{and} \quad m_Z^2 = m_W^2/(1 - \sin^2\theta_W) \quad (3.41)$$

These relations have been derived independently of the isoscalar contribution so long as it is small. However, since the value of  $\rho$  is known from experiment to be (see chapter 1)  $\rho = 1.02 \pm 0.02$ , it follows from (3.40) that  $G_Y < 0.04G_W$ . Approximating to the case of one isovector and one isoscalar boson and assuming  $g_W = g_Y$  one obtains the bound  $m_Y > 405$  GeV. However,  $g_Y$  may be smaller than  $g_W$  thereby relaxing the bound on  $m_Y$ . If  $g_W = xg_Y$  then one has  $m_Y > 405/x$  GeV.

### 3.6 The Size of the Weinberg Angle

From (3.9) and (3.25) the magnitude of  $W^3$ -photon mixing is given by

$$\lambda_W^2 = e^2/g^2 = e^2/f_W^2 \approx \sin^2 \theta_W \approx 0.218 \quad (3.42)$$

This is a very large amount of mixing [3.14] by comparison with the analogous situation in QCD where one has  $\gamma$ - $\rho^0$  transitions with  $\lambda_\rho^2 = e^2/f_\rho^2 \approx 1/260$ . However, there are two reasons for thinking that this sort of value for  $\lambda_W$  is not unreasonably large.

Firstly consider duality applied to QCD, which is the hypothesis that the peaks in the cross section for  $e^+e^- \rightarrow$  hadrons due to vector meson resonances can be averaged to approximate the annihilation cross-section into free quark pairs  $\sigma(e^+e^- \rightarrow \sum q\bar{q})$ . One obtains the relation [3.15]

$$\begin{aligned} \sigma &= \frac{4\pi\alpha^2}{3s} 3e_Q^2 \frac{v(3-v^2)}{2} \theta(s-4m^2) \\ &= \sum_j 12\pi^2 \delta(s-M_j^2) M_j^{-1} \Gamma_j(e^+e^-) \end{aligned} \quad (3.43)$$

where  $e_Q$  is the quark charge in units of  $e$ ,  $m$  is the quark mass,  $M_j$  is the mass of resonance  $j$  and  $v = (1 - 4m^2/s)^{1/2}$ . Using equations (3.4) and (3.9) one finds from (3.43)

$$\lambda_\rho^2 = (\alpha/3\pi) \Delta m^2/M_\rho^2 \quad (3.44)$$

where  $\Delta m \equiv M'_\rho - M_\rho$ . In the QHD case one obtains the corresponding relation [3.16]

$$\lambda_W^2 = (\alpha/3\pi) N_C N_H \langle Q \rangle^2 \Delta m^2 / M_W^2 \quad (3.45)$$

where  $\langle Q \rangle^2$  is the average value of the charge of the constituents which equals 1/2 in the haplon model and  $\Delta m \equiv M'_W - M_W$  is the mass difference between the W and its first excited state. Taking for example  $N_C = N_H = 3$  and requiring  $\lambda_W^2 = \sin^2 \theta_W = 0.218$  yields  $\Delta m = 660$  GeV. It follows that for a hypercolour force with a large level spacing compared to  $M_W$ , one expects the  $W^3-\gamma$  coupling to be big and the large experimental value of  $\sin^2 \theta_W$  is not so surprising.

Secondly one can use the W wavefunction to define a radius  $r_W$  for the particle i.e.

$$|\varphi(0)|^2 = (4\pi r_W^3/3)^{-1} \quad (3.46)$$

From equation (3.13) with  $N_C = N_H = 3$  one obtains  $M_W^{-1} \approx 1.4 r_W$ . This sort of correspondence between the size and Compton wavelength of a particle is just like that found in QCD where for example the pion and rho mesons have radii  $\sim 1\text{fm} \sim 1/M \sim 1/\Lambda_{\text{QCD}}$ . One can conclude that the value of  $\sin^2 \theta_W$  is not abnormally large although this explanation relies on being able to treat all these particles as non-relativistic bound states. However, since both of these arguments indicate that  $\sin^2 \theta_W$  is expected to be big because of the large mass scale, one need not be so unduly concerned that  $\lambda_W^2 \gg \lambda_\rho^2$ .

### 3.7 The Z Wavefunction

The  $(W^+, W^3, W^-)$  particles form an exact global SU(2) weak isospin symmetry if one ignores the electromagnetic interaction. However, when the  $W^3$  mixes with the photon to form a Z, the symmetry is no longer exact and the Z is not a pure isovector state. The

extent of the breaking of the SU(2) symmetry is clearly related to the amount of  $W^3-\gamma$  mixing which is determined by  $\lambda_W \approx \sin\theta_W$ . In order to determine the isovector and isoscalar components within the Z it can be seen from (3.31) that at low values of  $q^2$ , the weak neutral current Lagrangian is of the form

$$L \sim (\cos^2\theta_W J^{(3)} - \sin^2\theta_W J^{(Y)})^2 \quad (3.47)$$

where  $J^{(3)}$  and  $J^{(Y)}$  are isovector and isoscalar currents respectively. It is straightforward to show that the same result is true for  $q^2 \rightarrow M_Z^2$  and so in the haplon model the Z-wavefunction may be regarded as being of the form [3.17]

$$Z = \frac{\cos\theta_W}{\sqrt{2}} (\alpha\bar{\alpha} - \beta\bar{\beta}) + \frac{\sin\theta_W}{\sqrt{2}} (\alpha\bar{\alpha} + \beta\bar{\beta}) \quad (3.48)$$

This result will be exploited in Chapter 5 when calculating decays of the Z into isoscalar gauge bosons.

### 3.8 Conclusions

It has been shown in this chapter that composite models in which the weak bosons are bound states can be made to emulate the features of the Standard Model at low energies. If one accepts the W-dominance hypothesis which claims that weak interactions are governed predominantly by single W exchange for low  $q^2$ , then the Weinberg mass relations, the universal couplings of W's to all fermions and the structure of the weak neutral current arise quite naturally from a model with a global SU(2) symmetry. It is necessary in these models to associate the Standard Model Weinberg angle  $\sin^2\theta_W$  with the degree

of  $W^3$ -photon mixing but, as was seen in section 3.6, the magnitude of this parameter is not implausible.

## CHAPTER 4 A SPECTRUM OF COMPOSITE STATES

### 4.1 Introduction

It has been shown in the previous chapter that it is possible to construct composite models of quarks and leptons in which the  $W$  and  $Z$  bosons are bound states of preons which mimic the Standard Model behaviour at low energies. One of the expected consequences of composite  $W$ 's and  $Z$ 's is that there may be a rich spectrum of new bound states with masses of the order of  $M_Z$ . If the constituents of the weak bosons are two charged and hypercoloured fermions, which is the case in the haplon model [2.28] of Section 2.4, it is natural to expect the  $W$ 's and  $Z$ 's should have isovector spin 0 partners and associated neutral isoscalar states. If the scale of the confining hypercolour force  $\Lambda_H$  is not much greater than  $M_Z$ , then radially and orbitally excited states should also be present at energies somewhat greater than  $M_Z$ . In addition, if the constituents of the weak bosons transform as triplets under  $SU(3)$  of colour, then one expects colour octet  $W$ 's and  $Z$ 's to be present with masses in the range 100-200 GeV. In sections 4.2, 4.3 and 4.4, predictions are made for the masses and leading order decay widths of spin 0 and excited states in various models. In section 4.5, coloured bosons are discussed and the results of the chapter are summarized in section 4.6.

### 4.2 The Masses of Composite Weak Bosons

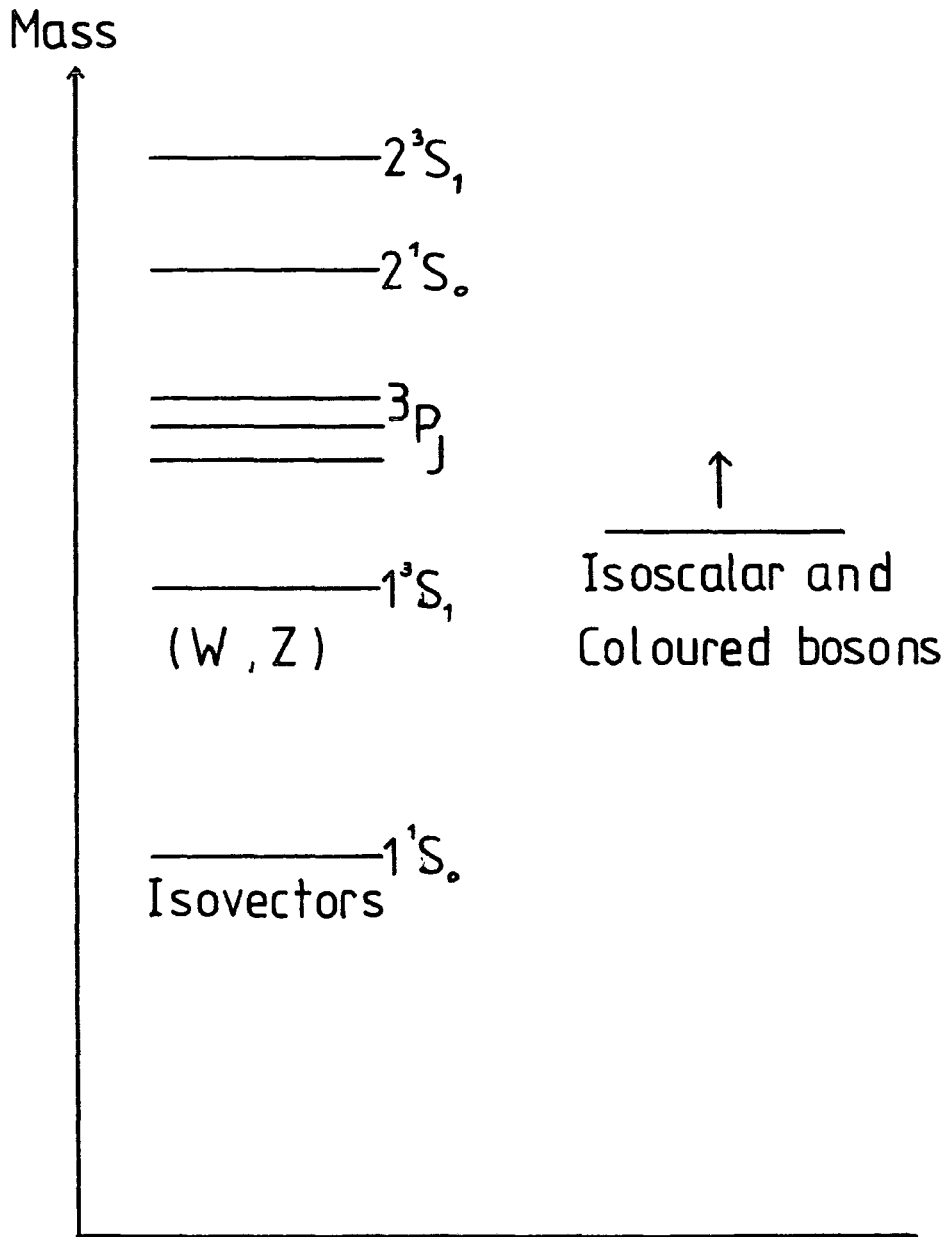
The masses of mesons and baryons in QCD have been described with great success by invoking the similarity of the spin interactions in

QCD and electromagnetism [4.1]. Weak bosons are the mesons of QHD and estimates of the masses of new particles can be made by applying the same techniques to the hypercolour force. In the calculation of the masses and widths of new particles it will be assumed that a composite  $Z$  and its partners can be treated to a reasonable approximation as non-relativistic bound states. This is not a very accurate description of the states since the binding energy is not necessarily small compared to the effective mass of the constituent preons. However, in QCD this sort of approximation has given fairly accurate results, even for the very light quark bound states such as  $\rho$ ,  $\omega$  and  $\phi$  [4.2] and it seems reasonable to hope that the predictions obtained here should hold to better than an order of magnitude.

The spectrum of states predicted is shown in Figure 4.1 and has a similar form to that of the familiar bound states of heavy quarks. The first prediction concerns the spin 0 partners of the  $W$ 's and  $Z$ 's [4.3]. The new charged states have the same mass as the neutral particle since it cannot mix with the photon which has spin one. These particles must be heavier than 15 GeV otherwise the charged bosons would have been observed in  $e^+e^-$  annihilation experiments [4.4]. They will couple very weakly to quarks and leptons since chiral symmetry suppresses the vertex to be  $O(M_f/M_W)$ . In addition, they cannot decay into gluons and hypergluons which are isosinglets.

The precise form of the hypercolour binding potential  $V_H(r)$  is unknown but it is required to be confining with  $V_H(r) \sim r$  as  $r \rightarrow \infty$  and in addition must have the correct asymptotically free behaviour for  $r \rightarrow 0$ . The Richardson parameterization [4.5] generalised to an  $SU(N_H)$  hypercolour potential has these properties and will be used

Figure 4.1



The particles expected in a model where W's and Z's are made of charged, coloured and fermionic constituents (not to scale).

i.e

$$V_H(r) = \frac{N_H^2 - 1}{2N_H} \frac{6\pi\Lambda_H}{11N_H - 2N_C N_F} \left[ \Lambda_H r - \frac{f(\Lambda_H r)}{\Lambda_H r} \right] \quad (4.1)$$

where

$$f(t) \equiv 1 - 4 \int_1^\infty \frac{dq}{q} \frac{e^{-qt}}{[\ln(q^2 - 1)]^2 + \pi^2} \quad (4.2)$$

and  $N_F$  is the number of preon flavours which is taken to be two in all calculations. The Richardson potential depends only upon the hypercolour scale so there are only two free parameters which need to be determined. These are  $\Lambda_H$  and the effective constituent mass  $m$  attained by the preons. In order to determine them, the radial Schrodinger equation

$$-\frac{1}{m} \left[ \frac{d^2}{dr^2} + \frac{2}{r} \frac{d}{dr} \right] R(r) - \left[ E_{nl} - V_H(r) - \frac{l(l+1)}{mr^2} \right] R(r) = 0 \quad (4.3)$$

is solved with  $l = 0$  and two constraints are imposed.

1).  $M_W = M_{\text{Spin Averaged}} + \text{Hyperfine Splitting}$ .

The contribution of the spin-spin hyperfine interaction to the masses of the bosons is treated perturbatively and is given by

$$H = \frac{2}{3m^2} \langle S_1 \cdot S_2 \rangle \langle \nabla^2 V_S(r) \rangle \quad (4.4)$$

where  $V_S(r)$  is the short range  $r^{-1}$  term in the potential (4.1). (The scalar confining part of the potential does not contribute to the hyperfine splitting). Since

$$\langle S_1 \cdot S_2 \rangle = 1/2 \langle (S^2 - S_1^2 - S_2^2) \rangle = 1/2 S(S+1) - 3/4 \quad (4.5)$$

where  $S = S_1 + S_2$  is the total spin of the boson, the mass splitting between the  $S = 1$  and  $S = 0$  states will be

$$\Delta M \equiv M(^3S_1) - M(^1S_0) = \frac{2}{3m^2} \langle \nabla^2 v_S(r) \rangle \quad (4.6)$$

where the expectation value of a function  $g(r)$  is defined to be

$$\langle g(r) \rangle \equiv \int_0^\infty dr g(r) r^2 R_{nl}^2(r) \quad (4.7)$$

The origin of the potential is of course arbitrary and so to fix the mass of the lowest state incorporating (4.6) we have used

$$M_W = 2m - E_{10} - \frac{1}{6m^2} \frac{N_H^2 - 1}{2N_H} \frac{6\pi}{(11N_H - 2N_C N_F)} \left\langle \frac{f'(\Lambda_H r)}{r} \right\rangle \quad (4.8)$$

where  $' \equiv \partial/\partial r$ . Notice that from (4.2)  $f''$  is always negative.

2). The normalization of the 1S radial wavefunction must give the correct amount of  $W^3 - \gamma$  mixing (see Section 3.2) i.e.

$$|R_{1S}(0)|^2 N_C N_H = \frac{4\pi g^2}{e^4} \sin^4 \theta_W \frac{M_W^3}{2} \quad (4.9)$$

Using  $M_W = 80.9 \pm 1.5$  GeV,  $\sin^2 \theta_W = 0.218 \pm 0.010$  and  $e/g \approx \sin \theta_W$  one obtains the bounds

$$7.14 \times 10^6 \leq |R_{1S}(0)|^2 N_C N_H \leq 8.75 \times 10^6 \text{ (GeV)}^3 \quad (4.10)$$

Solving the Schrodinger equation (4.3) for the  $R_{1S}(r)$  wavefunction and  $E_{10}$  eigenvalue and imposing (4.8) and (4.10) determines  $m$  and  $\Lambda_H$

exactly. The range of values which  $m$  and  $\Lambda_H$  may take are displayed in Table 4.1. The values of  $\Lambda_H$  are much lower than the bound  $\Lambda_H > 1$  TeV deduced from the four fermi interaction (see section 2.3). However, it has been suggested by Visnjic [4.6] that the physical scale of compositeness could well be an order of magnitude lower than this because the strength of the effective four fermi interaction must be much less than unity if approximate chiral symmetry is to be preserved so that the fermions have masses very much less than  $\Lambda_H$ . An alternative approach is to assume that the fermions and weak bosons have different compositeness scales with  $\Lambda_f \gg \Lambda_W$ . This idea was proposed by Renard [4.7] to explain both the weak coupling of  $W$ 's to quarks and leptons and also the large degree of mixing between the  $W^3$  and the photon which manifests itself in the high value of  $\lambda_W = \sin\theta_W$ .

The range of masses of the spin 0 partners of  $W$  and  $Z$  are shown in Table 4.2. It can be seen that the different spin states are unlikely to be degenerate in mass and suggests that perhaps the effects of such pseudoscalars may soon be evident in  $e^+e^-$  annihilation experiments.

There are no clear experimental bounds on the mass of a spin 0 isoscalar boson ( $U$ ). However, the production of such a particle was offered as an explanation of the radiative decays  $Z \rightarrow e^+e^-\gamma$  and  $Z \rightarrow \mu^+\mu^-\gamma$  [2.21, 2.22] at an anomalously high rate. The idea involved the radiative decay  $Z \rightarrow U\gamma$  followed by  $U \rightarrow l^+l^-$ . In [4.8, 4.9] the  $U$  had a mass of about 50 GeV whilst in [4.10]  $M_U \approx M_Z$ . The experimental bound from  $e^+e^-$  annihilation experiments is  $M_U > 46.7$  GeV [4.11].

The experimental determination of the value of  $g = 1.02 \pm 0.02$

Table 4.1

Ranges of  $\Lambda_H$ ,  $m$  and  $E_{10}$  which give the correct  $W$  mass consistent with equation (4.10).

$N_H$	$N_C$	$ R_{1S}(0) ^2 \text{ (GeV)}^3$	$\Lambda_H \text{ GeV}$	Constituent Mass $m \text{ GeV}$	Energy $E_{10} \text{ GeV}$
2	1	$3.57 \times 10^6 - 4.37 \times 10^6$	138 - 147	133 - 140	199 - 214
2	3	$1.19 \times 10^6 - 1.46 \times 10^6$	67 - 72	78 - 82	97 - 107
3	1	$2.38 \times 10^6 - 2.91 \times 10^6$	112 - 121	114 - 122	162 - 177
3	3	$7.92 \times 10^5 - 9.71 \times 10^5$	61 - 67	76 - 80	83 - 94
4	1	$1.78 \times 10^6 - 2.18 \times 10^6$	99 - 107	105 - 111	141 - 154
4	3	$5.94 \times 10^5 - 7.28 \times 10^5$	56 - 61	72 - 76	73 - 82

Table 4.2

Spin averaged masses, Hyperfine splittings and pseudoscalar masses obtained with the parameter ranges of Table 4.1.

$N_H$	$N_C$	$M_{10}^{SA} \text{ GeV}$	$m_H \text{ GeV}$	$M(1^1S_0) \text{ GeV}$
2	1	65 - 66	60 - 66	15 - 21
2	3	57 - 59	82 - 87	0 - 0
3	1	66 - 66	58 - 62	19 - 23
3	3	66 - 68	54 - 59	22 - 28
4	1	67 - 68	52 - 57	24 - 29
4	3	70 - 71	41 - 46	36 - 40

constrains an  $S=1$  isoscalar to have either a very large mass or a very small coupling (see section 3.5). There are no entirely satisfactory explanations of why this particle should be so much heavier than the  $Z$ . In the analogous QCD case, the isovector  $\rho$  and isoscalar  $\omega$  are almost degenerate in mass. The large mass difference is usually attributed to hypergluon annihilation effects. However, there is a second possibility if the constituents of the  $W$  and  $Z$  are scalars. In this case the  $W$  particles are  $P$ -waves and so have an antisymmetric spatial wavefunction. Bose statistics requires that the total wavefunction be symmetric. Hence the isospin wavefunction must be antisymmetric but an isoscalar state has a symmetric isospin wavefunction and so no such state with a low mass can exist. The drawback to this idea is that if the boson constituents have spin 0 then the value of the  $W$  wavefunction at the origin is zero in a non relativistic approximation since the  $W$  is a  $P$ -wave. However, the wavefunction is proportional to  $\sin^2\theta_W$  and so the large magnitude of this parameter must stem solely from relativistic corrections to the value of the wavefunction. This seems unlikely and the most common view is that weak bosons are made from fermionic constituents.

### 4.3 Excited States

Turning now to radially and orbitally excited states of weak bosons, one can estimate their masses by extending the method used in the previous section to predict the pseudoscalar masses. For radial excitations, since  $m$  and  $\Lambda_H$  have been fixed, it is straightforward to compute the energy eigenvalue  $E_{20}$  the spin averaged mass  $M_{20}^{SA}$  and the  $R_{2S}(r)$  wavefunction. The hyperfine splitting is then calculated from

equation (4.6) to give values for the  $2^1S_0$  and  $2^3S_1$  states. The results are shown in Tables 4.3 and 4.4 for various values of  $N_C$  and  $N_H$ . It can be seen that in all cases the masses are much heavier than those of the ground state particles.

The masses of the first orbital excitations (P-waves) can be calculated by noting that for a vectorlike potential one obtains contributions to the particle masses [4.12, 4.13]

$$m_H = (2/3m^2) \langle \nabla^2 V_H(r) \rangle \quad (4.11)$$

$$m_{SO} = (3/2m^2) \langle V'_H(r)/r \rangle \quad (4.12)$$

$$m_T = (-1/m^2) \langle V''_H(r) - V'_H(r)/r \rangle \quad (4.13)$$

where  $m_H$ ,  $m_{SO}$  and  $m_T$  are the mass shifts generated by the hyperfine, spin orbit and tensor forces respectively. Using the short distance part of the Richardson Potential one has

$$m_H = -2c/3m^2 \langle f''(\Lambda_H r)/r \rangle \quad (4.14)$$

$$m_{SO} = 3c/2m^2 \langle f(\Lambda_H r)/r^3 - f'(\Lambda_H r)/r^2 \rangle \quad (4.15)$$

$$m_T = c/m^2 \langle 3f(\Lambda_H r)/r^3 - 3f'(\Lambda_H r)/r^2 + f''(\Lambda_H r)/r \rangle \quad (4.16)$$

where  $' \equiv \partial/\partial r$  and

$$c \equiv \frac{N_H^2 - 1}{2N_H} \frac{6\pi}{(11N_H - 2N_C N_F)} \quad (4.17)$$

In addition to these effects there is also a contribution to the spin-orbit force from the long distance confining scalar potential which is the hyperchromic analogue of the Thomas precession term in atomic physics. The contribution from this term is [4.12, 4.13, 4.14]

$$-1/2m^2 \langle V'_L(r)/r \rangle \quad (4.18)$$

Table 4.3

Radially excited wavefunctions and energy eigenvalues obtained using the parameters of Table 4.1.

$N_H$	$N_C$	$ R_{2S}(0) ^2 \text{ (GeV)}^3$	Energy $E_{20} \text{ GeV}$
2	1	$2.90 \times 10^6 - 3.48 \times 10^6$	436 - 465
2	3	$8.69 \times 10^5 - 1.05 \times 10^6$	269 - 292
3	1	$1.87 \times 10^6 - 2.34 \times 10^6$	364 - 396
3	3	$5.77 \times 10^5 - 7.20 \times 10^5$	218 - 243
4	1	$1.40 \times 10^6 - 1.72 \times 10^6$	321 - 350
4	3	$4.17 \times 10^5 - 5.24 \times 10^6$	188 - 208

Table 4.4

Predicted hyperfine splittings and masses of radially excited spin 0 and spin 1 states.

$N_H$	$N_C$	$M_{20}^{SA} \text{ GeV}$	$m_H \text{ GeV}$	$M(2^1S_0) \text{ GeV}$	$M(2^3S_1) \text{ GeV}$
2	1	301 - 316	43 - 47	269 - 281	312 - 328
2	3	231 - 242	56 - 62	189 - 196	245 - 257
3	1	268 - 285	40 - 44	238 - 252	278 - 296
3	3	203 - 215	35 - 39	177 - 186	212 - 225
4	1	248 - 263	36 - 40	221 - 233	257 - 273
4	3	186 - 196	26 - 29	167 - 174	192 - 203

where  $V_L(r)$  is the linear confining term in the hypercolour potential. For the Richardson potential (4.1) one has  $V_L(r) = c\Lambda^2 r$  so that in total

$$m_{SO} = 3c/2m^2 \langle f(\Lambda_H r)/r^3 - f'(\Lambda_H r)/r^2 - \Lambda^2/3r \rangle \quad (4.19)$$

The full expression for the particle masses is

$$m(^{2S+1}L_J) = m_{SA} + m_H \langle S_1 \cdot S_2 \rangle + m_{SO} \langle L \cdot S \rangle + m_T \langle T \rangle \quad (4.20)$$

where  $m_{SA}$  is the spin averaged mass,  $\langle S_1 \cdot S_2 \rangle = 1/2 (S(S+1) - 3/2)$  and

$$\langle T \rangle = - \langle L \cdot S \rangle^2 - 1/2 \langle L \cdot S \rangle + 1/3 \langle L^2 \rangle \langle S^2 \rangle / (2L+3)(2L-1) \quad (4.21)$$

For the P-wave  $L=1$  states one obtains

$$m(^3P_0) = m_{SA} + 1/4 m_H - 2 m_{SO} - 1/3 m_T \quad (4.22)$$

$$m(^3P_1) = m_{SA} + 1/4 m_H - m_{SO} + 1/6 m_T \quad (4.23)$$

$$m(^3P_2) = m_{SA} + 1/4 m_H + m_{SO} - 1/30 m_T \quad (4.24)$$

$$m(^1P_1) = m_{SA} - 3/4 m_H \quad (4.25)$$

The energy eigenvalues  $E_{21}$ , the spin averaged mass  $M_{21}^{SA}$  and the  $R_{21}(r)$  wavefunction are calculated in the same way as for the radial excitations. The results for the P-wave particles are shown in Tables 4.5, 4.6 and 4.7 for various choices of  $N_C$  and  $N_H$ . The pattern of the masses is similar to that in the P-wave charmonium states in QCD. A typical mass spectrum taking  $N_C = N_H = 3$  is shown in Figure 4.2. These results differ from those of Grosser et.al. [4.15] who obtain an inverted spectrum of P-states i.e. the  $^3P_2$  state is the lightest. However they assume a very small hyperfine splitting between the S-wave states which has the effect of emphasizing the long range scalar

Table 4.5

Orbitally excited wavefunctions, energy eigenvalues and spin-averaged masses obtained using the parameters of Table 4.1.

$N_H$	$N_C$	$ R'_{2P}(0) ^2 \text{ (GeV)}^5$	$E_{21} \text{ GeV}$	$M_{21}^{SA} \text{ GeV}$
2	1	$1.38 \times 10^{10} - 1.86 \times 10^{10}$	350 - 375	217 - 226
2	3	$1.81 \times 10^9 - 2.53 \times 10^9$	213 - 232	175 - 182
3	1	$6.64 \times 10^9 - 9.66 \times 10^9$	293 - 319	197 - 208
3	3	$9.06 \times 10^8 - 1.38 \times 10^9$	173 - 194	158 - 166
4	1	$4.05 \times 10^9 - 5.62 \times 10^9$	258 - 281	185 - 194
4	3	$5.52 \times 10^8 - 7.96 \times 10^8$	150 - 166	148 - 154

Table 4.6

Contributions to P-wave mass splittings from hyperfine, spin-orbit and tensor interactions given by equations (4.11) - (4.19).

$N_H$	$N_C$	$m_H \text{ GeV}$	$m_{SO} \text{ GeV}$	$m_T \text{ GeV}$
2	1	4 - 5	3 - 3	58 - 63
2	3	7 - 7	21 - 23	79 - 88
3	1	4 - 5	6 - 6	55 - 61
3	3	4 - 5	11 - 13	48 - 56
4	1	4 - 4	6 - 6	49 - 54
4	3	3 - 3	8 - 9	37 - 41

Table 4.7

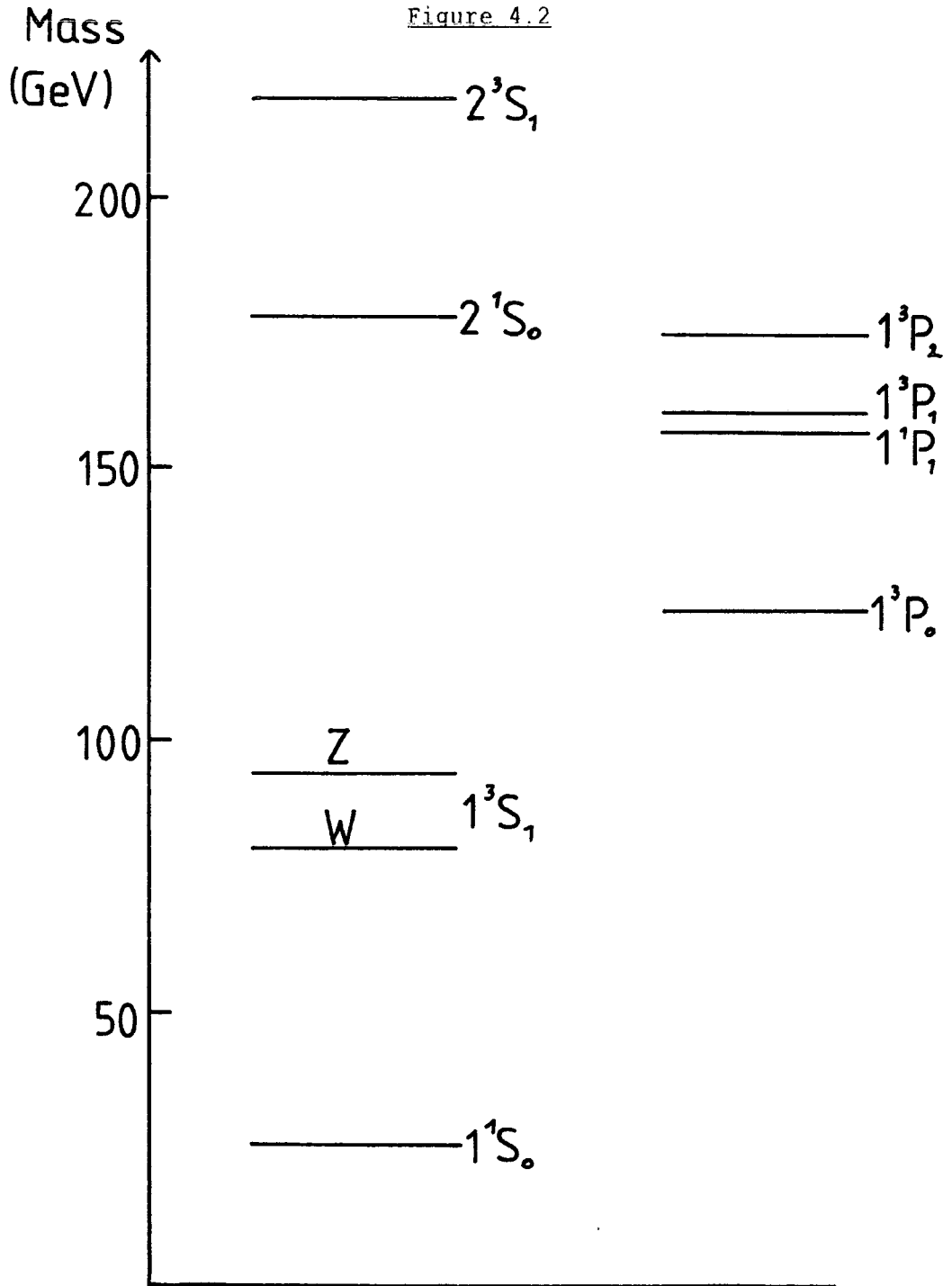
Predicted masses of orbitally excited states given by equations (4.20) - (4.25) using the mass splittings of Table 4.6.

---

$N_H$	$N_C$	$m(^3P_0)$ GeV	$m(^3P_1)$ GeV	$m(^3P_2)$ GeV	$m(^1P_1)$ GeV
2	1	192 - 199	225 - 235	219 - 228	214 - 223
2	3	109 - 109	169 - 176	195 - 204	170 - 177
3	1	168 - 177	202 - 213	202 - 213	194 - 205
3	3	120 - 123	156 - 163	169 - 178	155 - 163
4	1	158 - 165	188 - 198	190 - 199	182 - 191
4	3	120 - 123	146 - 152	156 - 163	146 - 152

---

Figure 4.2



The predicted mass spectrum of isovector states in a model with  $N_C = N_H = 3$ .

part of the potential. Hence  $m_{SO}$  is negative in their calculations and so they obtain  $m(^3P_2) < m(^3P_1) < m(^3P_0)$ .

#### 4.4 Decay Widths of New States

The states whose masses were calculated in sections 4.2 and 4.3 were all isovectors and, in consequence, will not decay into pure isoscalar states because of isospin symmetry. Hence the leading order decays of these states are  $^3P_J \rightarrow Z\gamma$  and  $^3P_1 \rightarrow hh\gamma$  where  $h$  is a hypergluon. The hypergluons will fragment into quarks and leptons and will eventually form hadrons. In order to obtain an estimate of the decay rates, the standard leading order, non relativistic bound state quarkonia decay formulae are generalised to an  $SU(N_H)$  hypercolour force (see [4.16] for the quarkonium non-relativistic bound state formalism). Although the use of perturbation theory is questionable for the large values of  $\alpha_H$ , it would be very suprising if higher order contributions were to conspire to change the widths by orders of magitude. One has for an  $SU(N_H)$  hypercolour force [4.17]

$$\Gamma(^3P_1 \rightarrow hh\gamma) = \frac{1}{\pi} \frac{(N_H^2 - 1) N_C}{N_H} \frac{\alpha_H^2 \alpha}{M^4} |R'_{2P}(0)|^2 \left[ \frac{2348}{3} - \frac{317\pi^2}{4} \right] \quad (4.26)$$

and [4.18]

$$\Gamma(^3P_J \rightarrow Z\gamma) = (1/9) \alpha \omega^3 \sin^2 \theta_W |I_1|^2 \quad (4.27)$$

where  $\omega$  is the photon momentum and

$$I_1 = \int_0^\infty r^3 R_{1S}(r) R_{1P}(r) dr \quad (4.28)$$

Notice that the radiative decays to  $Z\gamma$  are suppressed by  $\sin^2 \theta_W$

because the  $Z$  has only a small isoscalar component (see section 3.7).

The values of these widths are shown in Tables 4.8 and 4.9. The decay  ${}^3P_1 \rightarrow hh\gamma$  contributes appreciably to the width of the axial vector state. A characteristic feature of all these decays is the emission of a photon. Two events with a photon balanced by missing energy have been detected by UA1 [4.19] in the 1983/84 run of the CERN collider. However, these isovector particles cannot be made by gluon fusion since gluons are isoscalar and so cannot be easily produced. The situation is entirely different for any isoscalar particle in the 100 - 200 GeV energy range since they can be produced from gluon fusion. Unfortunately such a particle would also be able to decay into hypergluons and so would have such a broad width that it could not be observed as a single particle.

#### 4.5 Coloured Bosons

It is possible that the constituents of  $W$ 's and  $Z$ 's carry colour quantum numbers as well as charge and hypercolour. In this section it will be assumed that the haplons  $\alpha$  and  $\beta$ , which bind to form weak bosons, are colour triplets under  $SU(3)_{\text{Colour}}$ . Because the  $W$ 's and  $Z$ 's have a large mass and are very tightly bound, QCD, which is an asymptotically free theory at sufficiently small distances, is just a weak perturbation at ranges of the order of  $1/\Lambda_H$  which are very much less than typical QCD distances ( $O(1/\Lambda_C)$ ). Hence the haplons can form colour octet  $W$ 's [4.20, 4.21]. The mass splitting between these states can be estimated by considering the colour force between haplons

Table 4.8

Radiative decay widths of composite P-wave states given by equations (4.27) and (4.28). All widths are given in MeV.

$N_H$	$N_C$	$ I_1 ^2$	$\Gamma(^3P_0 \rightarrow Z\gamma)$	$\Gamma(^3P_1 \rightarrow Z\gamma)$	$\Gamma(^3P_2 \rightarrow Z\gamma)$
2	1	$1.21 \times 10^{-4} - 1.37 \times 10^{-4}$	80 - 94	270 - 320	180 - 220
2	3	$2.64 \times 10^{-4} - 3.10 \times 10^{-4}$	0.2 - 0.2	63 - 76	210 - 250
3	1	$1.50 \times 10^{-4} - 1.80 \times 10^{-4}$	35 - 45	160 - 200	160 - 200
3	3	$3.24 \times 10^{-4} - 3.82 \times 10^{-4}$	1.8 - 2.1	38 - 48	78 - 103
4	1	$1.99 \times 10^{-4} - 2.17 \times 10^{-4}$	24 - 33	110 - 150	120 - 150
4	3	$3.98 \times 10^{-4} - 4.84 \times 10^{-4}$	2.2 - 2.6	25 - 31	48 - 59

Table 4.9

The decay width in MeV for  $^3P_1 \rightarrow hh\gamma$  given by equation (4.26).

$N_H$	$N_C$	$\alpha_H$	$\Gamma(^3P_1 \rightarrow hh\gamma)$
2	1	1.61 - 1.65	24.3 - 29.0
2	3	1.89 - 1.94	41.5 - 51.9
3	1	0.90 - 0.92	10.0 - 12.3
3	3	0.89 - 0.93	11.3 - 15.7
4	1	0.62 - 0.63	5.4 - 6.3
4	3	0.57 - 0.60	5.2 - 7.0

$$\begin{aligned}
V_C(R) &= T_1 \cdot T_2 \alpha_S / R = 1/2 (T^2 - T_1^2 - T_2^2) \alpha_S / R & (4.29) \\
&= -4/3 \alpha_S / R & \text{Singlet} \\
&= 1/6 \alpha_S / R & \text{Octet}
\end{aligned}$$

where  $T_i$  are SU(3) generators and R is the radius of the bound state W's and Z's. Hence one has

$$\begin{aligned}
M(\text{Singlet}) &= M_0 - 4/3 \alpha_S \langle 1/R \rangle \\
M(\text{Octet}) &= M_0 + 1/6 \alpha_S \langle 1/R \rangle
\end{aligned}$$

whereupon

$$M_8 - M = 3/2 \alpha_S \langle 1/R \rangle \quad (4.30)$$

If  $\langle 1/R \rangle \sim \Lambda_H$  then for values of  $\Lambda_H$  between 100 and 500 GeV, one expects coloured weak bosons in the range 100-180 GeV. The  $W_8^+$  and  $Z_8$  are expected to be almost degenerate in mass because the  $Z_8$  does not mix with either a photon or a gluon. However, the coloured isoscalar states can mix with gluons and so are expected to be heavier than  $W_8$ ,  $Z_8$ . The presence of coloured bosons necessarily demands that there be colour octet leptons [4.21]. This is because colour singlet leptons are made from one constituent of the W (an  $\alpha$  or  $\beta$ ) and a scalar  $y$  (see section 2.4 for details). If  $\alpha$ ,  $\beta$  are SU(3) triplets then  $y$  must be in the conjugate  $\bar{3}$  representation and hence octet ( $\alpha y$ ) and ( $\beta y$ ) states can be formed too. The same argument does not hold for the quarks ( $\alpha x$ ) and ( $\beta x$ ) since the scalar constituent  $x$  need not carry colour. However if it did there would be exotic colour sextet quarks formed.

Coloured gauge bosons have been used to explain the "monojet" and "W + jet" events detected at the CERN collider [4.19, 4.22]. The monojets occur when an energetic jet is found in one half of the

detector with no observed particle balancing its momentum in the other half. In a coloured boson scenario this could be due to the production and decay of a  $Z_8$ . i.e.  $Z_8 \rightarrow Zq \rightarrow v\bar{v}q$  so that only one final state jet will be observed. Similarly  $W_8^+ \rightarrow W^+g$  can account for the W plus jet events. However, there are many other interpretations and the Standard Model itself can provide possible explanations for at least some of the events [4.23, 4.24].

#### 4.6 Summary

The hypothesis that the W and Z particles are composite implies the existence of many more states. A degenerate pseudoscalar isotriplet is predicted at a mass of about 20-40 GeV. Orbital excitations of W and Z should occur in the 100-200 GeV mass region and, because they are isovectors, their preferred decays are into photons. The radial excitations are expected to have higher masses because the 1S - 2S mass splitting is found to be large. The only experimental information on the masses of the isoscalars is the bound on the  $^3S_1$  state from measurements of  $\rho$ . Spin 0 isoscalars and their coloured partners have been introduced as a possible explanation for the anomalous events observed at the CERN collider [4.8, 4.9, 4.10, 4.25]

Coloured constituents of W's and Z's imply coloured partners for the bosons in the 100-200 GeV mass range and also coloured leptons. These coloured particles have also been used to try and explain the strange collider events. However, there is no really convincing evidence that any of these explanations involving new bosons is correct.

In conclusion, although many new states are predicted if the weak bosons are composite, there is no experimental evidence to indicate their presence.

## CHAPTER 5 THE WIDTH OF THE Z IN COMPOSITE MODELS

### 5.1 Introduction

It has been shown in Chapter 4 that one can attempt to find compositeness by looking for new particles. In addition one might also be concerned that anomalously large contributions from a composite Z may add to the Standard Model decays and might exceed the present experimental bound on the width. In this chapter this question is examined in detail and a comparison is made between the theoretical predictions and experimental results. It is necessary to begin with a summary of the results of Z decays predicted by the Standard Weinberg-Salam Model of weak interactions.

### 5.2 Standard Model Z Decays

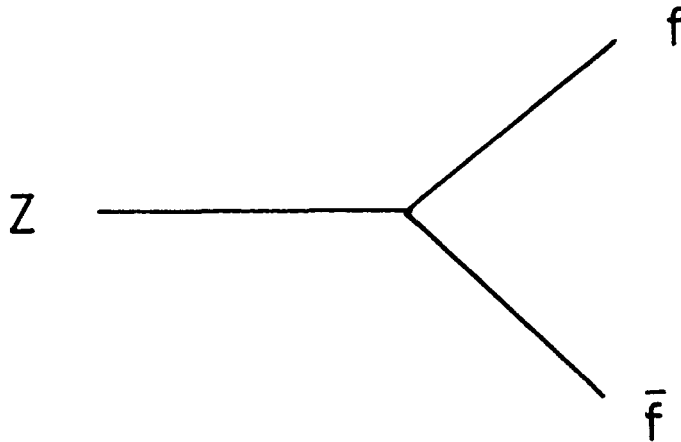
The leading order decays of the Z in the Standard Model are into fermion antifermion pairs  $q\bar{q}$ ,  $l^+l^-$  and  $\nu\bar{\nu}$  (see Figure 5.1). The width is given by [5.1]

$$\Gamma(Z \rightarrow f\bar{f}) = \frac{G_F M_Z^3 N_C \sqrt{2}}{12\pi} \left[ 1 - \frac{4m^2}{M_Z^2} \right]^{1/2} \quad (5.1)$$
$$\times \left[ (a^2 + b^2) [1 - (m/M_Z)^2] + 3(a^2 - b^2) \frac{m^2}{M_Z^2} \right]$$

where  $m$  is the mass of the fermions and  $N_C = 3$  for quarks and 1 for leptons. The parameters  $a$  and  $b$  are defined by

$$a \equiv T_f^3 - 2\sin^2\theta_W Q_f \quad b \equiv T_f^3 \quad (5.2)$$

Figure 5.1



Standard Model decay of the Z into fermion-antifermion pairs.

where  $T_f^3$  is the third component of weak isospin and  $Q_f$  is the charge of the fermions in units of  $e$ . It follows that for left-handed fermions one obtains

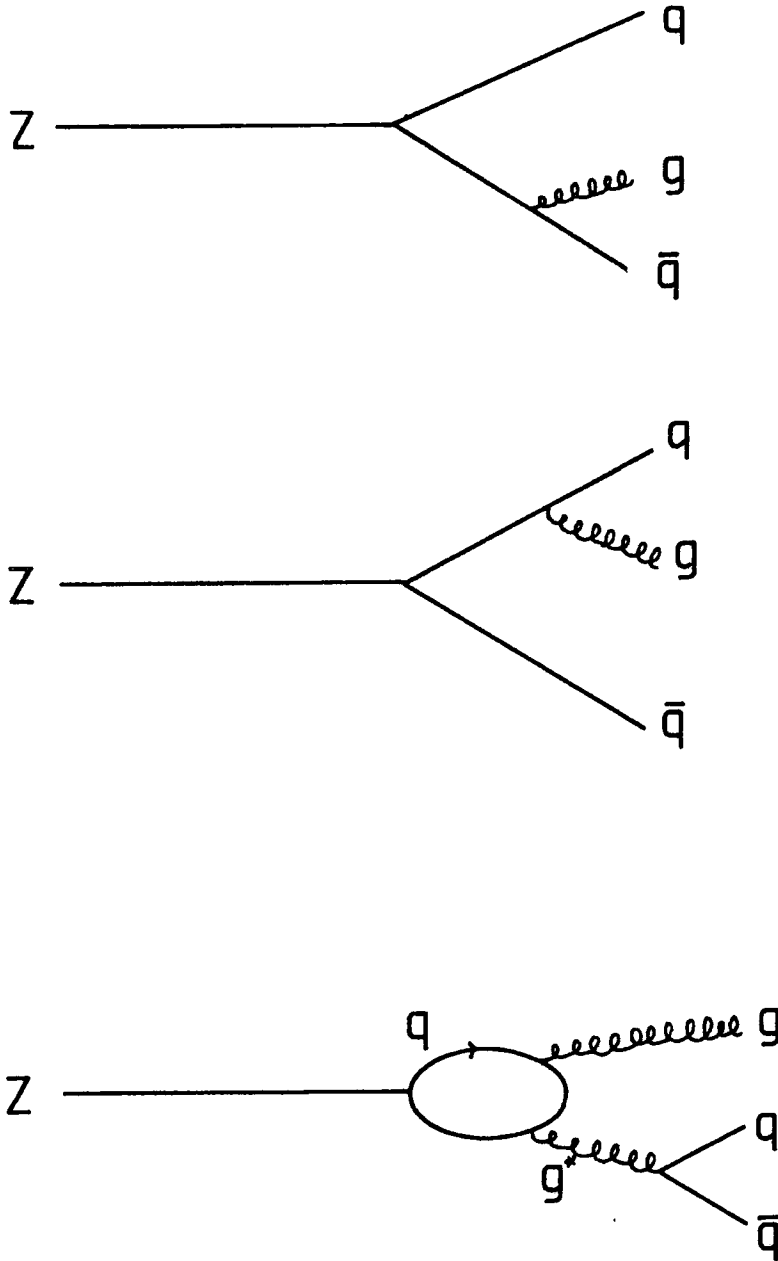
f	$Q_f$	$T_f^3$	a	b	$\Gamma$ (MeV)
u,c	2/3	1/2	$1/2 - 4/3 \sin^2 \theta_W$	1/2	321
t	2/3	1/2	$1/2 - 4/3 \sin^2 \theta_W$	1/2	104
d,s,b	-1/3	-1/2	$-1/2 + 2/3 \sin^2 \theta_W$	-1/2	411
$\nu_e, \nu_\mu, \nu_\tau$	0	1/2	1/2	1/2	182
$e^-, \mu^-, \tau^-$	-1	-1/2	$-1/2 + 2 \sin^2 \theta_W$	-1/2	93

using a top quark mass of 40 GeV,  $\sin^2 \theta_W = 0.218$  and  $M_Z = 94$  GeV. This gives a total Z width of 2.8 GeV. The most important radiative correction is  $Z \rightarrow q\bar{q}g$  (see Figure 5.2). The width for this decay is given by [5.2]

$$\begin{aligned}
 \Gamma(Z \rightarrow q\bar{q}g) &= \Gamma(Z \rightarrow q\bar{q}) \frac{4\alpha_S}{3\pi} \left[ \log^2 \frac{\epsilon}{1-\epsilon} + \frac{3}{2}(1-2\epsilon) - \frac{\pi^2}{6} \right. \\
 &\quad \left. + \frac{1}{4} - \frac{(5+3\epsilon)(1-3\epsilon)}{4} + 2 \operatorname{Li}_2 \frac{\epsilon}{1-\epsilon} \right] \\
 &= \Gamma(Z \rightarrow q\bar{q}) \frac{4\alpha_S}{3\pi} \left[ \log^2 \epsilon - \frac{3}{2} |\log \epsilon| + \frac{5}{4} - \frac{\pi^2}{6} + \epsilon \log \epsilon + 2\epsilon \right] \\
 &\quad + \text{higher order terms in } \epsilon
 \end{aligned} \tag{5.3}$$

where  $\operatorname{Li}_2(z) = -\int_0^z dt (1/t) \log(1-t)$  and  $\epsilon$  is the minimum energy fraction which can be carried by the gluon. Taking  $\epsilon = 0.1$ , one obtains  $\Gamma(Z \rightarrow q\bar{q}g) \approx 150$  MeV i.e about 5% of the total Z width. Z decays into gauge bosons take place only via the loop diagrams of

Figure 5.2



Leading order Feynman diagrams for the decay  $Z \rightarrow q \bar{q} g$  in the Standard Model.

Figure 5.3 and they are all very much suppressed. Their widths are [5.3]

$$\begin{aligned}\Gamma(Z \rightarrow ggg) &\approx 3.4 \times 10^{-5} \text{ GeV} \\ \Gamma(Z \rightarrow gg\gamma) &\approx 1.1 \times 10^{-7} \text{ GeV} \\ \Gamma(Z \rightarrow \gamma\gamma\gamma) &\approx 1.4 \times 10^{-9} \text{ GeV}\end{aligned}\tag{5.4}$$

### 5.3 Anomalous Decays into Gauge Bosons

It has been pointed out by Renard [5.4] that in models where the  $Z$  is made of light, charged and coloured fermionic preons, its decays into gauge bosons  $Z \rightarrow ggg$ ,  $gg\gamma$  and  $\gamma\gamma\gamma$  could be anomalously large. The diagrams giving the additional contributions to the width, which are shown in Figure 5.4, couple the gauge bosons to a preon loop. Using the haplon model of section 2.4 and the standard quarkonium non-relativistic bound state decay formulae [4.17] applied to QHD, one obtains for the decay widths [5.4]

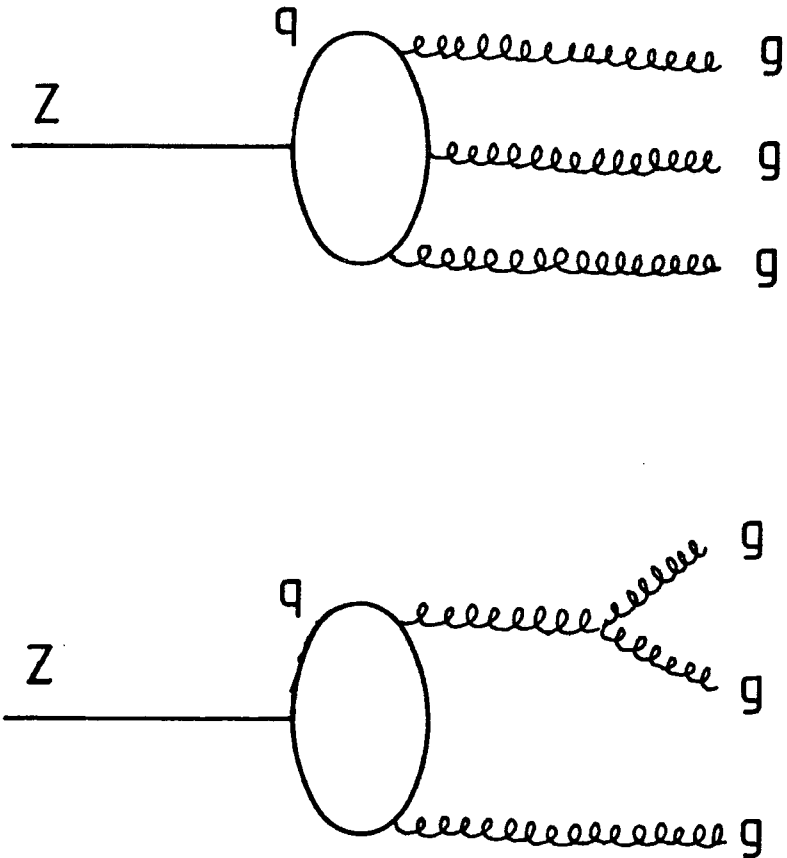
$$\Gamma(Z \rightarrow ggg) = \frac{80}{243\pi} N_C N_H (\pi^2 - 9) \alpha_S^3 \frac{|R_{1S}(0)|^2}{M_Z^2} \sin^2 \theta_W \tag{5.5}$$

$$\Gamma(Z \rightarrow gg\gamma) = \frac{16}{81\pi} N_C N_H (\pi^2 - 9) \alpha_S^2 \alpha \frac{|R_{1S}(0)|^2}{M_Z^2} \cos^2 \theta_W \tag{5.6}$$

$$\Gamma(Z \rightarrow \gamma\gamma\gamma) = \frac{1}{18\pi} N_C N_H (\pi^2 - 9) \alpha^3 \frac{|R_{1S}(0)|^2}{M_Z^2} \cos^2 \theta_W \tag{5.7}$$

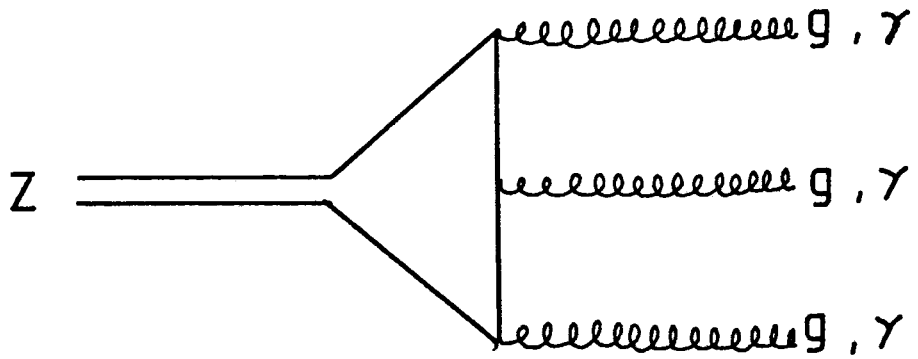
where the preons  $\alpha$  and  $\beta$  have charges  $1/2$  and  $-1/2$  respectively in units of  $e$ . The factors involving  $\sin\theta_W$  and  $\cos\theta_W$  arise because the final states are all purely isoscalar whereas the  $Z$  wavefunction is

Figure 5.3



Leading order Feynman diagrams for the decay  $Z \rightarrow ggg$  in the Standard Model.

Figure 5.4



Anomalous contributions to the decays  $Z \rightarrow ggg$ ,  $gg\gamma$ ,  $\gamma\gamma\gamma$  where the Z is made of coloured fermionic constituents.

predominantly isovector [3.17] as was seen in section 3.7. The magnitude of these widths are given in Table 5.1 and a comparison with the Standard Model values of section 5.2 shows that the above contributions constitute by far the most important terms. Unfortunately the decays still represent only a small fraction of the total width and so cannot easily be detected by experimental determination of the Z width. One consequence of the extra diagrams is that production of Z's will be enhanced by the mechanisms  $gg \rightarrow Zg$  and  $gg \rightarrow Z\gamma$ . These effects have been investigated by Renard [5.5] and Leurer et al. [5.6] but without the isospin suppression factors.

In addition to the above decay channels, there are also possible enhancements in the modes  $Z \rightarrow 1^+ 1^- \gamma$ ,  $q\bar{q}\gamma$  and  $q\bar{q}g$ . Renard [5.4] has suggested that the latter decay  $Z \rightarrow q\bar{q}g$  might substantially increase the width of the Z. The additional composite model diagram is that of Figure 5.5 and occurs because parity violation in the Z's coupling to preons is assumed to be the same as that in fermion couplings. This enables it to decay through a  $1^{++}$  component [5.4]. Of course the Z cannot decay into two real gluons, the  $1^{++}$  component being forbidden by Bose statistics (Yang's theorem [5.7]) and  $1^{--}$  by charge conjugation. The aim of this section is to try and quantify this observation, using simple potential models and various rough bounds on the mass of the next radially excited Z' state [5.8].

One obtains [5.9] for the diagram in Figure 5.5

$$\Gamma(Z \rightarrow q\bar{q}g) = N_F N_C N_H \frac{256\alpha_S^3}{27\pi M_Z^4} |R'_{2P}(0)|^2 \log \left[ \frac{4m^2}{4m^2 - M_Z^2} \right] \sin^2\theta_W \quad (5.8)$$

where  $N_F$  is the number of quark flavours into which the Z will decay. It is assumed throughout that  $N_F=5$  since the decay into  $t\bar{t}g$  is much

Table 5.1

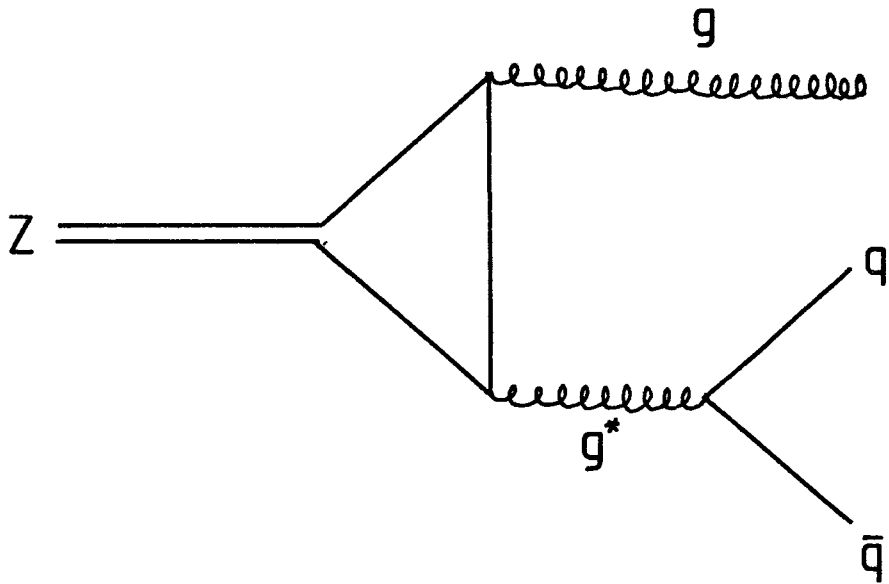
The widths  $\Gamma(Z \rightarrow ggg, gg\gamma, \gamma\gamma\gamma)$  for an elementary and composite Z.

---

	Standard Model	Composite Model
$\Gamma(Z \rightarrow ggg)$ (GeV)	$3.4 \times 10^{-5}$	$6.1 \times 10^{-2}$
$\Gamma(Z \rightarrow gg\gamma)$ (GeV)	$1.1 \times 10^{-7}$	$6.3 \times 10^{-3}$
$\Gamma(Z \rightarrow \gamma\gamma\gamma)$ (GeV)	$1.4 \times 10^{-9}$	$4.2 \times 10^{-6}$

---

Figure 5.5



Additional diagram for a composite  $Z \rightarrow q\bar{q}g$  coming from the  $1^{++}$  component of the Z.

reduced by phase space.  $R'_{2P}(r)$  is the derivative of the radial wavefunction in the  $1^{++}$  state. Again the suppression factor  $2\sin^2\theta_W$  occurs because  $q\bar{q}g$  is a purely isoscalar state. Although this wavefunction is not known, the magnitude of the  $W^3-\gamma$  mixing (see Figure 3.3) relates the S-wave radial wavefunction at the origin to the Weinberg angle  $\theta_W$  as was shown in chapter 3. Squaring equation (3.13) yields

$$\sin^4\theta_W = (e^2/g)^2 N_C N_H (2/M_W^3) |R_{1S}(0)|^2/4\pi \quad (5.9)$$

so one needs to determine the ratio

$$K \equiv \frac{1}{4m^2} \frac{|R'_{2P}(0)|^2}{|R_{1S}(0)|^2} \quad (5.10)$$

Combining (5.8) - (5.10) one obtains

$$\Gamma(Z \rightarrow q\bar{q}g) = N_F \frac{2048\alpha_S^3}{27M_Z^4} \frac{g^2}{e^4} M_W^3 m^2 K \sin^6\theta_W \log \left[ 1 + \frac{M_Z^2}{\epsilon(\epsilon + 2M_Z)} \right] \quad (5.11)$$

where  $m$  is the effective constituent mass of the preons and  $\epsilon$  is the binding energy of the bound state:  $\epsilon = 2m - M_Z$ . To estimate  $\epsilon$  and  $K$ , the results of Tables 4.1 and 4.5 can be used. Values of  $\Gamma$  obtained in this way are given in Table 5.2.

Alternatively, one can take the effective potential between the preons to be of the form

$$V(r) = \beta r^\nu \quad (5.12)$$

with  $\nu > -2$  to keep  $r^2 R(r)$  non-singular at the origin. Then in the WKB approximation [5.10] the energy eigenvalues are [5.11]

Table 5.2

Values of  $\Gamma(Z \rightarrow q\bar{q}g)$  using equation (5.11) and Tables 4.1 and 4.5 to estimate the binding energy  $\epsilon$  and  $K$  defined by (5.10).

---

$N_H$	$N_C$	$K$	$\epsilon$ (GeV)	$\Gamma(Z \rightarrow q\bar{q}g)$ GeV
2	3	0.058 - 0.059	87.9 - 97.5	0.75 - 0.78
3	3	0.047 - 0.050	74.7 - 85.5	0.67 - 0.75
4	3	0.042 - 0.045	66.8 - 75.4	0.63 - 0.72

---

$$E_{nl} = \beta^{2q} m^{-vq} [ A(v) (n + 1/2 - 1/4) ]^{2vq} \quad v > 0 \quad (5.13)$$

$$|\beta|^{2q} m^{-vq} [ \check{A}(v) (n - q/2(1 + v - 2l)) ]^{2vq} \quad -2 < v < 0$$

where  $q \equiv (2 + v)^{-1}$  and

$$A(v) \equiv \frac{2v\sqrt{\pi} \Gamma(3/2 + 1/v)}{\Gamma(1/v)} \quad , \quad \check{A}(v) \equiv \frac{2|v|\sqrt{\pi} \Gamma(1 - 1/v)}{\Gamma(-1/2 - 1/v)} \quad (5.14)$$

Introducing the mass difference between the Z and its first radially excited state,

$$\Delta M \equiv M'_Z - M_Z = E_{20} - E_{10} \quad (5.15)$$

then  $\epsilon = E_{10}$  is given by

$$\epsilon = \Delta M \frac{(3/4)^{2vq}}{(7/4)^{2vq} - (3/4)^{2vq}} \quad v > 0 \quad (5.16)$$

$$= \Delta M \frac{(1 - p)^{2vq}}{(2 - p)^{2vq} - (1 - p)^{2vq}} \quad -2 < v < 0$$

where  $p \equiv 1/2(1+v)(2+v)^{-1}$ .  $\beta$  can now be written in terms of  $v$  and  $\Delta M$

$$\beta = (\Delta M)^{1/2q} m^{v/2} [A(v)]^{-v} [ (7/4)^{2vq} - (3/4)^{2vq} ]^{-1/2q} \quad v > 0$$

$$= (\Delta M)^{1/2q} m^{v/2} [\check{A}(v)]^{-v} [ (2-p)^{2vq} - (1-p)^{2vq} ]^{-1/2q} \quad -2 < v < 0$$

Similarly, to evaluate K one uses [5.11]

$$\left| \frac{d^l}{dr^l} R_{nl}(0) \right|^2 = \frac{1}{\pi} \left[ \frac{l!}{(2l+1)!!} \right]^2 \frac{d}{dn} (mE_{nl}) (mE_{nl})^{1+1/2} \quad v > 0 \quad (5.17)$$

$$= q \left[ \frac{l! q^{q(2l+1)}}{\Gamma[q(2l+1)+1]} \right]^2 \frac{d}{dn} (mE_{nl}) (m|\beta|)^{q(2l+1)} \quad -2 < v < 0$$

giving

$$\begin{aligned}
 K &= \frac{\Delta M}{m} \frac{3^{(4\nu - 6)q}}{4^{(3\nu + 2)q}} \left[ (7/4)^{2\nu q} - (3/4)^{2\nu q} \right]^{-1} \quad \nu > 0 \quad (5.18) \\
 &= \frac{\Delta M}{4m} q^{q(6+\nu)+1} \left[ \Gamma(q)/\Gamma(3q + 1) \right]^2 \tilde{\chi}(\nu)^{-2\nu q} \left[ \frac{2 - q/2(\nu - 1)}{1 - q/2(\nu + 1)} \right]^{2\nu q - 1} \\
 &\quad \times \left[ (2 - p)^{2\nu q} - (1 - p)^{2\nu q} \right]^{-1} \quad -2 < \nu < 0
 \end{aligned}$$

Thus  $\epsilon$  and  $K$  depend only upon  $\Delta M$  and  $\nu$ .

The next stage of the calculation involves trying to estimate bounds for  $\Delta M$ . The results of Table 4.4 give values for  $\Delta M$  ranging between 114 and 178 GeV. In models where  $W$ 's and  $Z$ 's have right-handed couplings, it seems likely that  $M'_Z > M_{WR}$  the mass of the lightest right-handed vector boson. The experimental limit from  $\mu$  decay is  $M_{WR} > 400$  GeV [5.12], giving  $\Delta M > 305$  GeV. As a third alternative, one can use the  $W$ -dominance of the weak current. Demanding that the low energy coupling relations be satisfied by the  $W$ -dominance model with two  $W$  bosons gives [3.13]

$$\frac{g_W^2}{M_W^2} + \frac{g'_W{}^2}{M'_W{}^2} = \frac{8G_F}{\sqrt{2}} \quad \text{Charged Current} \quad (5.19)$$

$$\frac{\lambda_W g_W}{M_W^2} + \frac{\lambda'_W g'_W}{M'_W{}^2} = \frac{8G_F \sin^2 \theta_W}{e\sqrt{2}} \quad \text{Neutral Current} \quad (5.20)$$

$$\lambda_W g_W + \lambda'_W g'_W = e \quad \text{Electromagnetic Current} \quad (5.21)$$

where  $\lambda_W$  is the  $W - \gamma$  mixing and  $g_W$  the  $W$ -fermion coupling. In

addition duality [3.16] gives

$$\lambda_W M_W = \lambda'_W M'_W \quad (5.22)$$

Introducing  $x = g'_W/g_W$ ,  $r = M_W/M'_W$  and  $c = 8G_F \sin^2 \theta_W M_W^2 / (e^2 \sqrt{2})$  relations (5.19) - (5.22) imply

$$r^3 - cr + (1-c)/x = 0 \quad (5.23)$$

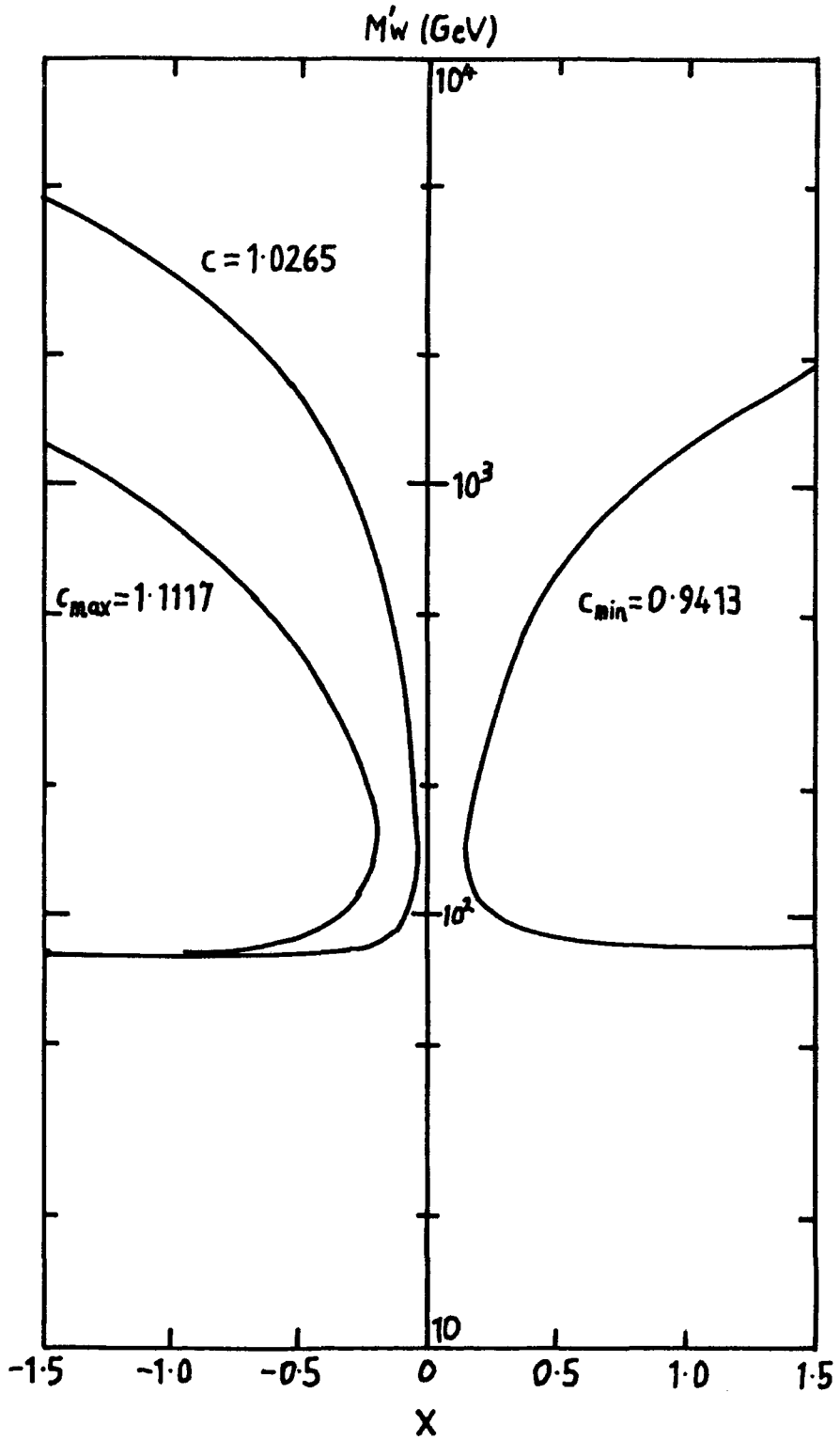
The experimental values  $M_W = 80.9 \pm 1.5$  GeV,  $\sin^2 \theta_W = 0.218 \pm 0.010$  imply  $c = 1.062 \pm 0.085$ . Solutions of (5.23) within these bounds are shown in Figure 5.6. If W and W' couple with the same strength i.e.  $|x| = 1$ , then apart from the solution with  $M_W \approx M'_W$  which is rejected as it would mean that there was little binding energy and almost a continuum of W and Z states, one needs  $M'_W > 820$  GeV and  $\Delta M > 725$  GeV if  $M'_Z > M'_W$ . Only if the W' is very weakly coupled can it have a low mass. Finally, it is noted that no other W or Z particles have been detected at the CERN collider, though there may possibly be structure in the 130 - 150 GeV mass region [4.22]. In conclusion, it seems unlikely that  $\Delta M < 40$  GeV. Fortunately, as will be seen, these bounds are not critical for the decay estimates.

More important is the value of  $v$  in the potential. This can be estimated very approximately by making a comparison of the Z with the QCD charmonium system. A good description of these states has been obtained using potentials of the form

$$V(r) = -a/r + br \quad (5.24)$$

where  $a = (4/3)\alpha_S \approx 0.51$  and  $b \approx 0.17$  (GeV)<sup>2</sup> is the string tension, which is related to the slope of the Regge trajectory  $\alpha'$  by [5.13]

Figure 5.6



The mass of the excited  $W'$  boson as a function of its coupling ( $g'_W = xg_W$ ) to satisfy equation (5.23) for various values of  $c$ .

$$b = 1/(2\pi\alpha') \quad (5.25)$$

Since radial and orbital excitations have comparable masses,  $\alpha' \approx 1/(M'^2 - M^2)$  giving

$$2\pi b \approx M'^2 - M^2 = \Delta M(\Delta M + 2M_Z). \quad (5.26)$$

It is thus convenient to introduce the dimensionless ratio of the potential parameters

$$y = \frac{b}{a\Delta M(\Delta M + 2M_Z)} \quad (5.27)$$

It is found that for charmonium  $y \approx 0.083$ . For the Z, a and b are estimated by finding the value of  $\beta$  needed to generate the spectrum of Z states with  $\nu = -1$  and  $+1$  respectively. It is found that  $y = 0.073$  for  $\Delta M = 100$  GeV, 0.108 for  $\Delta M = 500$  GeV and 0.122 for  $\Delta M = 1$  TeV. Using instead the Richardson Potential [4.5] of (4.1) and the values for  $\Delta M$  from Table 4.4 with  $N_C=3$ ,  $y$  ranged between 0.073 and 0.091 (see Table 5.3). All these values are very similar to those for charmonium which suggests that with appropriate scaling, the shape of the effective potential which binds the preons is not very different from the QCD potential. Furthermore, it is known that for charmonium the power  $\nu$ , arising from the combination of powers in (5.24) is  $\nu \approx 0$  [5.11]. This is because confinement precludes the wavefunction penetrating very far into the large  $r$  region where the  $br$  term dominates. This seems likely to be a feature of any model in which the constituents acquire large effective masses through confinement, so one expects that probably  $\nu \approx 0$  for the Z system too.

Table 5.3

Values of  $y$  defined by equation (5.27) using the values of  $\Delta M$  obtained from Table 4.4. The parameters  $a$  and  $b$  are the appropriate terms in the Richardson potential specified by (4.1) and Table 4.1.

$N_H$	$N_C$	$y$
2	3	0.073 - 0.075
3	3	0.083 - 0.088
4	3	0.088 - 0.091

In Figure 5.7 the results on the width of  $Z \rightarrow q\bar{q}g$  via the diagrams of Figure 5.5 from equation (5.11) are shown as a function of  $\Delta M$  for various possible values of  $v$ . It can be seen that for any  $\Delta M > 40$  GeV and  $v > 0$  one has  $\Gamma > 0.3$  GeV. The value of  $\Delta M$  is of little importance but  $\Gamma$  increases with  $v$ . It is hard to see how a confining potential can have a negative value of  $v$  and the comparison with charmonium suggests that  $v \approx 0$  is quite likely. It is possible however that  $v > 0$  if  $M_Z < \Lambda_H$  whereupon the effects of confinement may be more significant than in charmonium. Notice that the values of  $\Gamma$  in Table 5.2 obtained from (5.8) and (5.13) and the data from Tables 4.1 and 4.5 using the Richardson Potential (4.1) correspond to values of  $v$  in the range  $0.4 \leq v \leq 0.6$ .

#### 5.4 Experimental Results

The latest experimental bound on the Z width is [1.15]

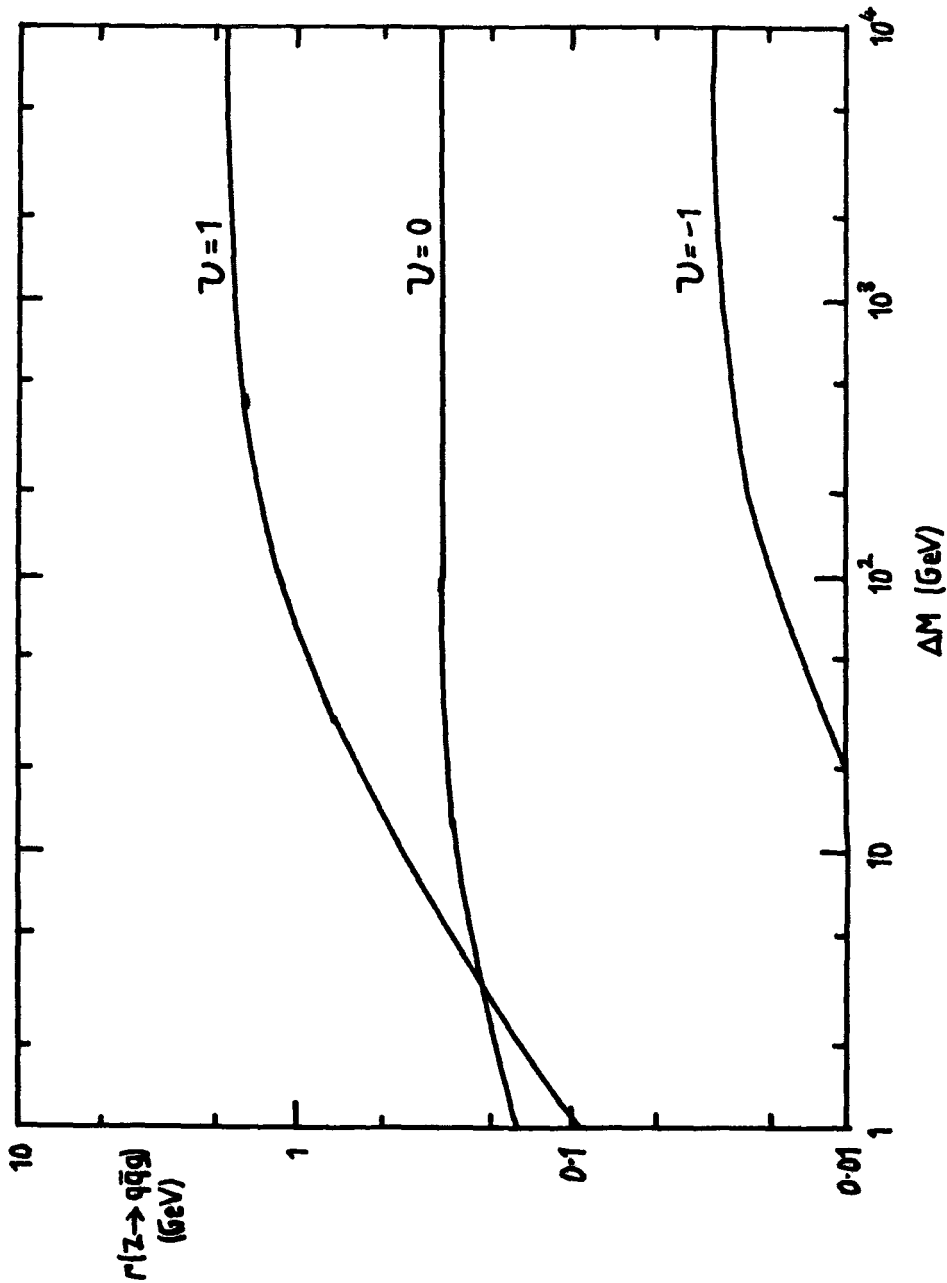
$$\Gamma = 2.7 \begin{matrix} + 2.2 \\ - 1.7 \end{matrix} \text{ GeV} \quad \text{UA2} \quad (5.28)$$

which is not necessarily in disagreement with the results of the last section although a composite Z would produce an increased fraction of three jet events. An indirect determination of the Z width using production rates and assuming a Standard Model width for the W gives [1.15]

$$\Gamma < 3.3 \pm 1.3 \text{ GeV} \quad (5.29)$$

It can be seen from these values that  $v$  cannot be close to 1. One may conclude that in decays of the Z, there should be at least a small rise in the branching ratio into three hadronic jets.

Figure 5.7



The decay width  $\Gamma(Z \rightarrow q\bar{q}g)$  via Figure 5.5 predicted by equation (5.11) as a function of the mass difference  $\Delta M = M'_Z - M_Z$  for different effective potentials. Note the insensitivity of  $\Gamma$  to the value of  $\Delta M$ .

The corresponding leptonic decay  $Z \rightarrow \gamma^* \gamma \rightarrow e^+ e^- \gamma$  has a width

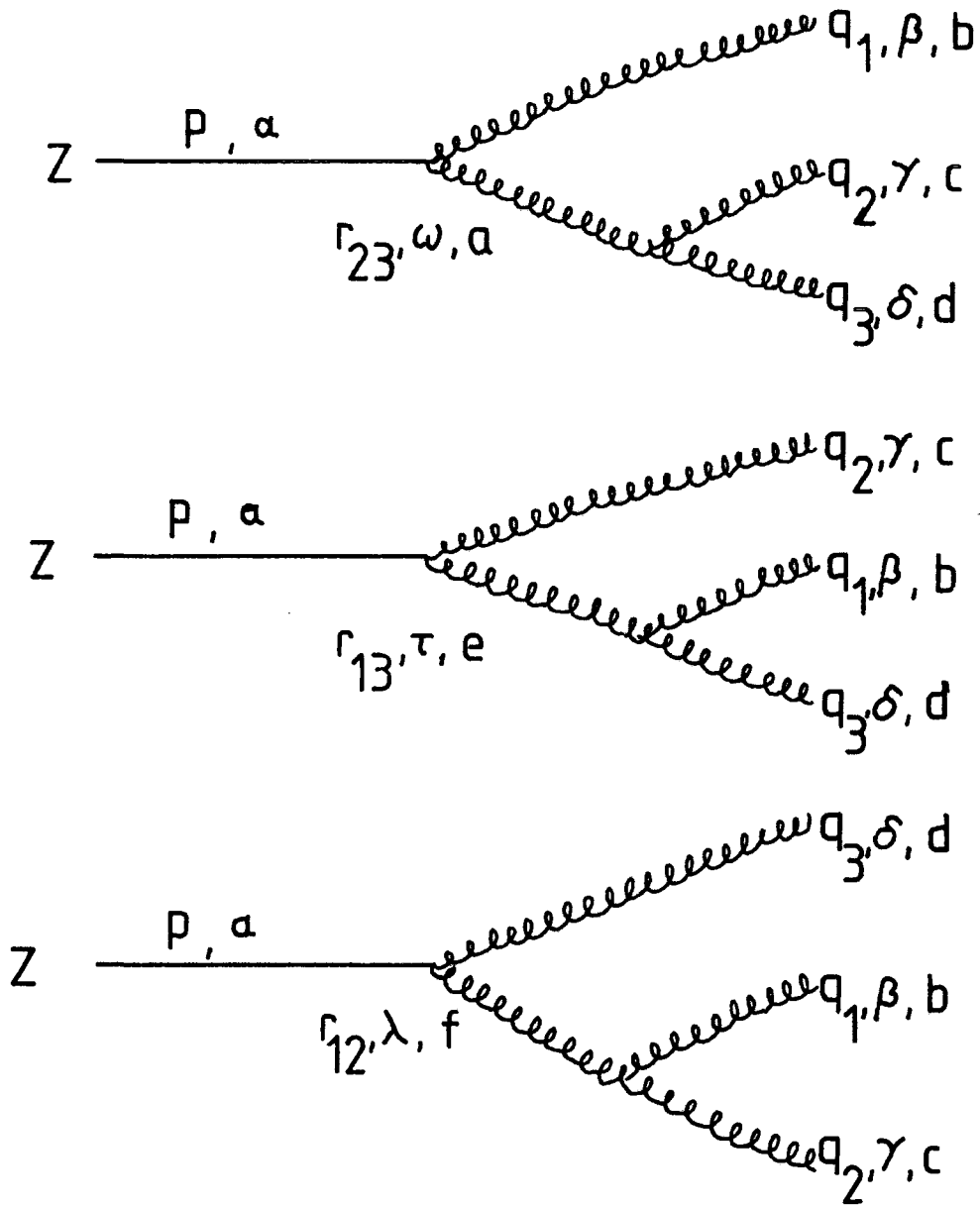
$$\Gamma(Z \rightarrow e^+ e^- \gamma) = \Gamma(Z \rightarrow q \bar{q} g) \frac{3\alpha^3}{16N_F \alpha_S^3} \sim 5 \text{ keV} \quad (5.30)$$

so this mechanism certainly could not account for the anomalously high rate of  $Z \rightarrow l^+ l^- \gamma$  events (0(25%)) observed during the 1983/84 run of the CERN collider [2.21, 2.22]. In fact any model in which the constituents carry colour as well as charge will find it hard to explain how these events can provide such a substantial contribution to the total width (see [5.14] for a summary of the interpretations of  $Z \rightarrow l^+ l^- \gamma$  events). However, more recent runs at CERN suggest that the  $l^+ l^- \gamma$  rate may not be such a large fraction after all [2.25, 2.26]. In this case the Standard Model bremsstrahlung width of about 1 MeV may be sufficient to explain the data, possibly with a very small contribution from (5.30) too.

### 5.5 Effective Interactions

An alternative method of calculating the widths of composite particles is to regard their decays as effective point interactions (see for example [5.15]). Hence the decay  $Z \rightarrow g^* g \rightarrow g g g$  can be treated as if it proceeded through the diagrams of Figure 5.8 and  $Z \rightarrow g^* g \rightarrow q \bar{q} g$  through Figure 5.9. One is treating these interactions in the same sort of way that weak interactions were originally formulated at low energies in terms of a pointlike four fermion vertex. This is a good approximation for weak interactions because the masses of the propagating W and Z bosons are much larger than the centre of mass energies in the decays. In the case being

Figure 5.8



Diagrams for the decay  $Z \rightarrow ggg$  via an effective  $Zgg$  vertex.

Figure 5.9

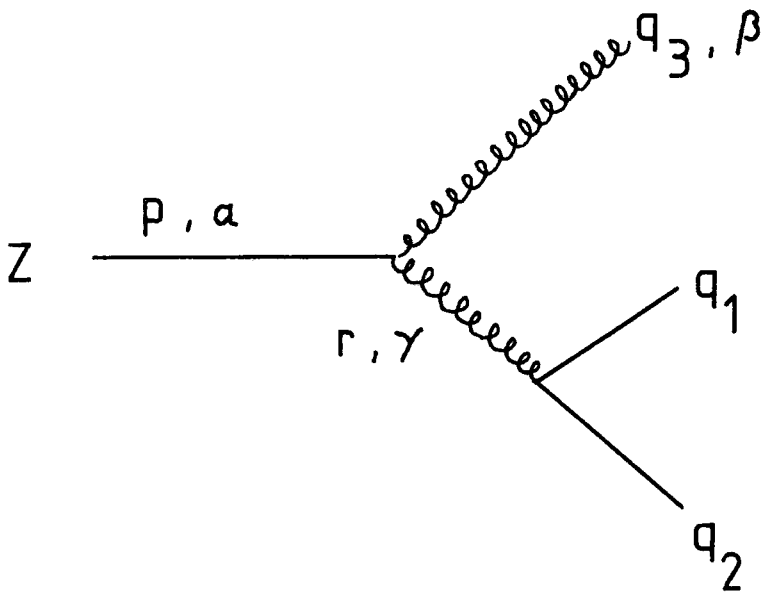


Diagram for the decay  $Z \rightarrow q\bar{q}g$  via an effective  $Zqg$  vertex.

considered here this condition is not satisfied since one assumes in these models that  $\Lambda_H$  is of the order of  $M_Z$ . However, it is useful to compare the results obtained from this method with those from non-relativistic potential models since one can be more confident of the results if the two methods are in agreement.

One requires the interaction term to be invariant under  $SU(3)_C$  since this is assumed to be an exact gauge symmetry. Because the overall dimension of the Lagrangian is (mass)<sup>4</sup> one looks for terms of lowest dimension  $n$  so that the dimensional constant behaves like  $\Lambda^{4-n}$  [5.16]. The operator of lowest dimension (dimension 6) in an effective Lagrangian to describe such an effective interaction for  $Z \rightarrow g^* g$  is

$$L = C \sigma^{\mu\nu} Z_{\mu\nu} G_{\rho\sigma}^a G_a^{\rho\sigma} \quad (5.31)$$

where  $Z_{\mu\nu}$  and  $G_{\rho\sigma}^a$  are the usual gauge boson field strength tensors. One estimates  $C \approx g_S^2/\Lambda_H^2$  by dimensional analysis and since there must be two gluon couplings within the  $Zgg^*$  vertex. In the following calculations it is assumed that  $C = g_S^2/\Lambda_H^2$  since changing  $C$  is equivalent to varying  $\Lambda_H$  so that no generality has been lost. The tensor  $\sigma_{\mu\nu}$  is defined in the usual way to be

$$\sigma_{\mu\nu} = i/2 [ \gamma_\mu , \gamma_\nu ] = i/2 ( \gamma_\mu \gamma_\nu - \gamma_\nu \gamma_\mu ) \quad (5.32)$$

$\sigma_{\mu\nu}$  is selected in preference to momentum operators so that the dimension of the operator is as low as possible. Using (5.31) one can derive the vertex factor  $V$  for  $Z \rightarrow g^* g$  via Figure 5.8a

$$V = 2g_S^2/\Lambda_H^2 ( \not{p}\gamma^\alpha - \gamma^\alpha\not{p} ) ( (q_1 \cdot r_{23}) g^{\beta\omega} - q_1^\omega r_{23}^\beta ) \quad (5.33)$$

The amplitude for the above process can now easily be written down using standard Feynman rules [5.17]

$$\begin{aligned}
 M = & \epsilon^{\alpha(p)} \epsilon^{*\beta(q_1)} \epsilon^{*\gamma(q_2)} \epsilon^{*\delta(q_3)} C_{q_S} (\not{p}\gamma^\alpha - \gamma^\alpha \not{p}) \\
 & \times (\delta^{ab}/\sqrt{2}) (1/r_{23}^2) f^{acd} ((q_1 \cdot r_{23}) g^{\beta\omega} - q_1^\omega r_{23}^\beta) \\
 & \times (g^{\omega\gamma} (r_{23} + q_2)^\delta + g^{\gamma\delta} (q_3 - q_2)^\omega - g^{\omega\delta} (q_3 + r_{23})^\gamma) \quad (5.34) \\
 & + \text{similar terms from Figures 5.8b and 5.8c}
 \end{aligned}$$

Squaring this amplitude in the usual way gives

$$\begin{aligned}
 |M|^2 = & 768\pi \alpha_S^4 g_S^4 M_Z^4 (1/\Lambda_H^4) (1/xyz) \quad (5.35) \\
 & [ 10(x + y + z) + 7/2(xy/z + xz/y + yz/x) + 5(x^2/y + x^2/z \\
 & + y^2/x + y^2/z + z^2/x + z^2/y) + 2(x^3/yz + y^3/xz + z^3/xy) ]
 \end{aligned}$$

where

$$x \equiv 1 - 2E_1/M_Z, \quad y \equiv 1 - 2E_2/M_Z, \quad z \equiv 1 - 2E_3/M_Z \quad (5.36)$$

and  $E_i$  are the final state gluon energies. Note that  $x + y + z = 1$  so that  $|M|^2$  is a function of  $x$  and  $y$  only. The double differential decay width for three massless final state particles is given by [5.2]

$$\frac{d^2\Gamma}{dx dy} = \frac{M_Z}{256\pi^3} \langle |M|^2 \rangle \quad (5.37)$$

In order to prevent infra-red divergences, a cutoff  $\epsilon$  is imposed on  $x$  and  $y$  so that

$$\begin{aligned}
 \epsilon & \leq x \leq 1 - 2\epsilon \quad (5.38) \\
 \epsilon & \leq y \leq 1 - x - \epsilon
 \end{aligned}$$

where  $\epsilon$  is the minimum fraction of the total energy carried by a gluon. Integrating (5.37) with respect to  $x$  and  $y$  using the limits given in (5.38) yields the following expression for  $\Gamma$

$$\Gamma(Z \rightarrow ggg) = \frac{8\alpha_S^3}{\Lambda_H^4} M_Z^5 \left[ 283/24 - 145\epsilon/4 - 29\epsilon^2/8 + 75\epsilon^3/4 \right. \\ \left. + [ - 41/4 + 18\epsilon + 15\epsilon^2/2 - 5\epsilon^3 ] \log ((1 - 2\epsilon)/\epsilon) \right. \\ \left. + 12 \int_{2\epsilon}^{1-\epsilon} ds [ \log ((s - \epsilon)/\epsilon) ] / s \right] \quad (5.39)$$

One obtains the values of  $\Gamma$  as a function of  $\Lambda_H$  shown in Figure 5.10 for various values of  $\epsilon$ . It can be seen that if  $\Lambda_H$  is of the order of  $M_Z$  or is given by the values obtained in Table 4.1 then  $\Gamma$  takes large values in this calculation.

In the calculation of the width for  $Z \rightarrow g^* g \rightarrow q\bar{q}g$  the amplitude can be written down using (5.31), (5.33) and the usual Feynman rules

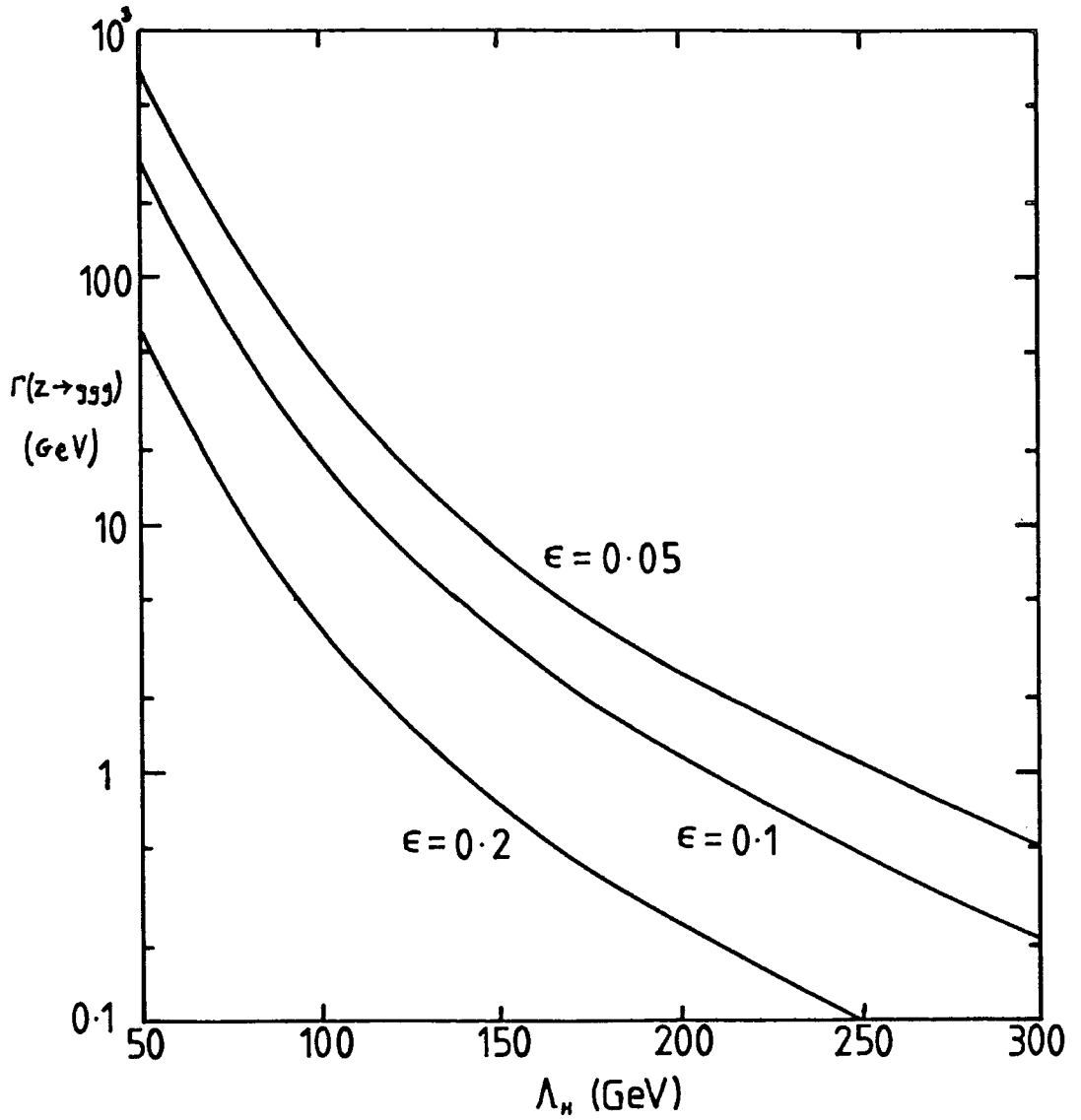
$$M = \bar{u}(q_1) g_S \gamma^\delta v(q_2) (g^{\delta\gamma}/r^2) 2C (\not{p}\gamma^\alpha - \gamma^\alpha\not{p}) \\ \times ((q_3 \cdot r)g^{\beta\gamma} - q_3^\gamma r^\beta) \epsilon^\alpha(p) \epsilon^{*\beta}(q_3) (\delta^{ab}/\sqrt{2}) T_{ij}^b \quad (5.40)$$

Squaring (5.40), averaging over initial spins and summing over final states yields

$$|M|^2 = 128\pi \alpha_S M_Z^4 (g_S^4/\Lambda_H^4) \frac{x^2 + y^2}{z} \quad (5.41)$$

In the same way as the previous calculation using equation (5.37) for the doubly differential decay width and integrating  $x$  and  $y$  between the limits given in (5.38) gives

Figure 5.10



The decay width  $\Gamma(Z \rightarrow ggg)$  via the diagrams of Figure 5.8 as a function of the hypercolour scale  $\Lambda_H$  for different values of the energy cutoff  $\epsilon$ .  $C$  is taken to be  $(g_S/\Lambda_H)^2$  and  $\alpha_S = 0.14$ .

$$\Gamma(Z \rightarrow q\bar{q}g) = N_F \frac{8\alpha_S^3}{\Lambda_H^4} M_Z^5 \left[ -11/9 + 19\epsilon/3 - 29\epsilon^2/3 + 5\epsilon^3 + [2/3 - 2\epsilon + 2\epsilon^2 - 4/3\epsilon^3] \log((1 - 2\epsilon)/\epsilon) \right] \quad (5.42)$$

The results for  $\Gamma$  as a function of  $\Lambda_H$  are displayed in Figure 5.11 (with  $N_F=5$ ) and again it can be seen that with the assumed value for  $C$  (based on dimensional arguments) the widths are similar to those obtained from the potential model calculation. This gives one some confidence to calculate the corresponding decays into hypergluons by these methods.

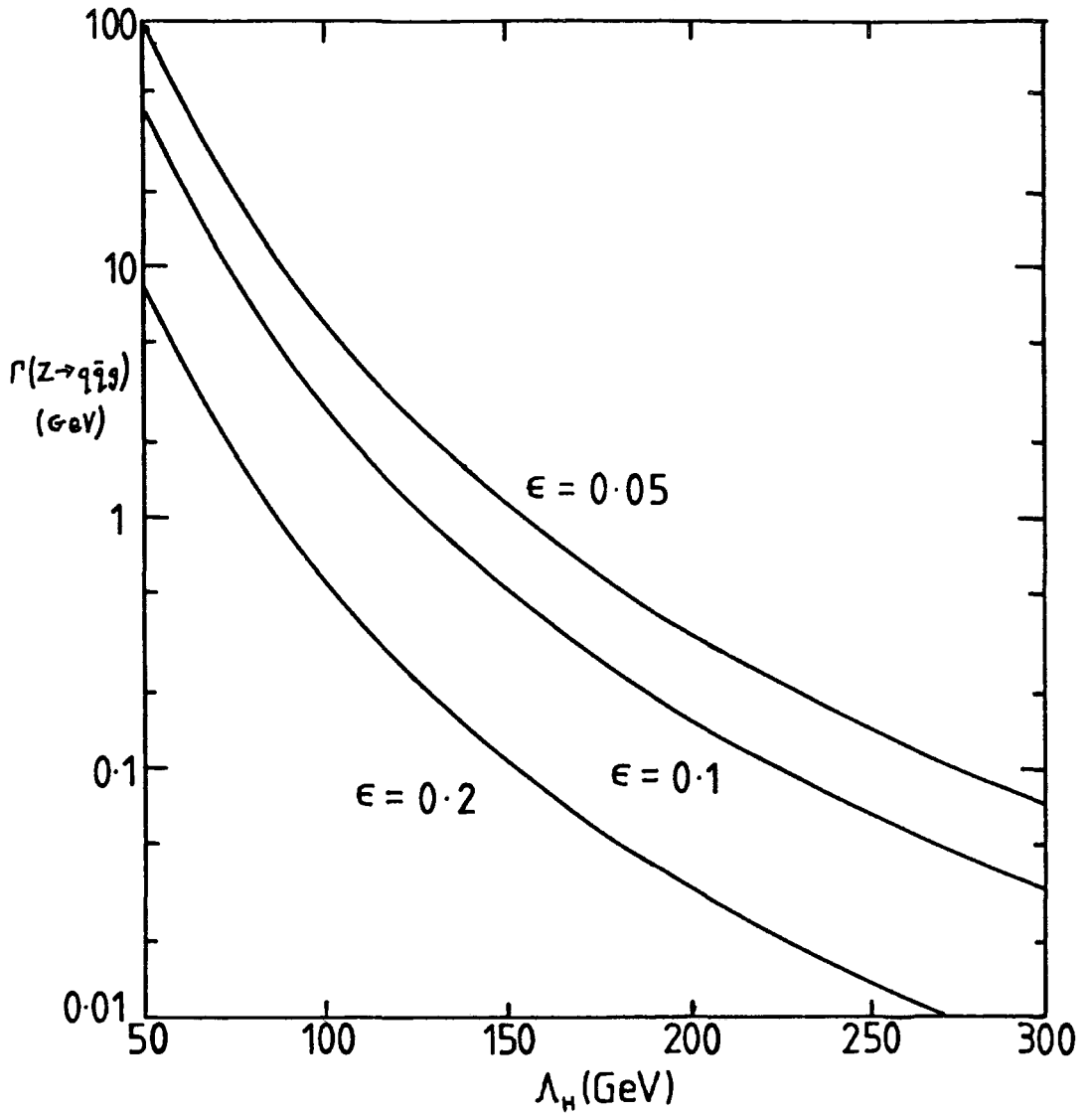
### 5.6 Hypergluon Decays

In addition to the decays of sections 5.3 and 5.5, a composite  $Z$  will have new decay modes into hypergluons - the gauge bosons of the hypercolour force. These new decays include  $Z \rightarrow hhh$ ,  $hh\gamma$  and  $h\bar{p}p$  where  $h$  is a hypergluon and  $p$  is a preon. The hypergluons and preons will fragment into quarks and leptons and will eventually form hadrons. The intention of this section is to show that the partial width of the  $Z$  into these channels seems almost certain to be so large that this type of model can already be ruled out by the current experimental bound on the  $Z$  width.

In order to estimate hypergluon decay widths, non-relativistic bound state models are used, with the confining Richardson Potential given by equation (4.1). This potential has the advantage of having only one free parameter  $\Lambda_H$  (since  $N_F$  is fixed to be 2 in the haplon model). Clearly this is an inadequate description of the  $Z$  system and



Figure 5.11



The decay width  $\Gamma(Z \rightarrow q\bar{q}g)$  via Figure 5.9 as a function of the hypercolour scale  $\Lambda_H$  for different values of the energy cutoff  $\epsilon$ .  $C$  is taken to be  $(g_S/\Lambda_H)^2$  and  $\alpha_S = 0.14$ .

may not give a very good approximation. However, one can obtain some feeling for how close this approach is likely to come to the correct answer by considering analogous decays in QCD i.e.  $\omega, \phi \rightarrow ggg$ . In this case the potential is given by

$$V(r) = \frac{8\pi}{33 - 2N_F} \Lambda_C \left[ \Lambda_C r - \frac{f(\Lambda_C r)}{\Lambda_C r} \right] \quad (5.43)$$

and the width is given by

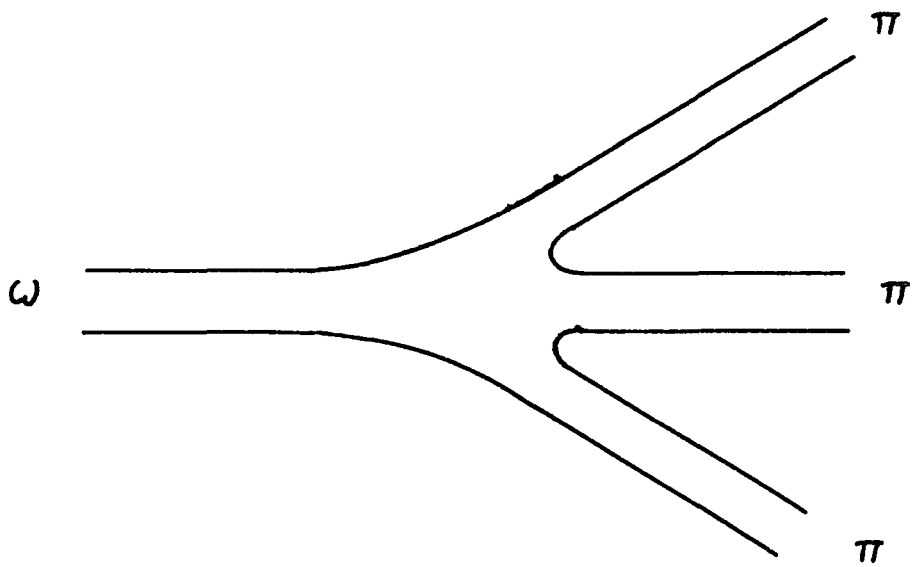
$$\Gamma(\omega \rightarrow ggg) = \frac{80}{81\pi} (\pi^2 - 9) \alpha_S^3 \frac{|R_{1S}(0)|^2}{M_\omega^2} \quad (5.44)$$

where  $|R_{1S}(0)|^2$  is the value of the wavefunction at the origin squared. This is obtained by solving the Schrodinger equation (4.3) with the potential (5.43) with  $N_F = 3$ . Note that because of confinement the gluons fragment into hadrons but will not form jets because the energy is so small. These decays could be quite a substantial fraction of the  $3\pi$  width since each gluon can fragment to form a  $\pi$  meson although the Zweig allowed  $\omega \rightarrow 3\pi$  "fall apart" decay shown in Figure 5.12 is presumably the dominant decay of the  $\omega$ .

The results are shown in Table 5.4 for values of  $\Lambda_C$  within the commonly accepted range and are to be compared with the experimental widths for  $\omega, \phi \rightarrow \pi\pi\pi$  of 10 and 0.6 MeV [3.3] so that when allowance is made for Figure 5.12, the approximation seems to hold to within a factor of about 2 or 3.

Returning to the Z decays, one uses the non-relativistic bound state quarkonia decay formulae [4.17, 5.8] generalised to an  $SU(N_H)$  hypercolour force and applied to preons with zero current masses to obtain

Figure 5.12



The "fall apart" decay  $\omega \rightarrow 3\pi$  which is expected to be the dominant contribution to the total  $\omega$  width.

Table 5.4

The gluon decay width of the  $\omega$  given by equation (5.44) for various values of  $\Lambda_C$ .

$\Lambda_C$ MeV	$ R_{1S}(0) ^2$ (GeV) <sup>3</sup>	$\Gamma(\omega \rightarrow ggg)$ MeV
200	0.051	2.8
250	0.076	6.8
300	0.107	15.0

$$\Gamma(Z \rightarrow hhh) = \frac{2}{9\pi} (\pi^2 - 9) \frac{(N_H^2 - 4)(N_H^2 - 1)}{N_H^2} N_C \alpha_H^3 \frac{|R_{1S}(0)|^2}{M_Z^2} \sin^2 \theta_W \quad (5.45)$$

$$\Gamma(Z \rightarrow hh\gamma) = \frac{2}{9\pi} (\pi^2 - 9) \frac{(N_H^2 - 1)}{N_H} N_C \alpha_H^2 \alpha \frac{|R_{1S}(0)|^2}{M_Z^2} \cos^2 \theta_W \quad (5.46)$$

$$\Gamma(Z \rightarrow hpp\bar{p}) = \frac{32}{3\pi} (\pi^2 - 9) \frac{(N_H^2 - 1)}{N_H} N_C^2 N_F \alpha_H^3 \frac{|R_{2P}(0)|^2}{M_Z^4} \sin^2 \theta_W \log \frac{4m^2}{4m^2 - M_Z^2} \quad (5.47)$$

where

$$\alpha_H(q^2) = \frac{12\pi}{(11N_H - 2N_C N_F)} \frac{1}{\log(1 + q^2/\Lambda_H^2)} \quad (5.48)$$

and  $N_F = 2$  in the haplon model. The value of the wavefunction is related to the magnitude of  $W$ - $\gamma$  mixing by (5.9). Hence, following the method described in section 4.2 and using the bound (4.10) one can solve the Schrodinger equation (4.3) and for given values of  $N_H$  and  $N_C$  the value of  $\Lambda_H$  in (5.48) is determined. This fixes the coupling  $\alpha_H$  in (5.48) and hence  $\Gamma$  can be calculated from (5.45) - (5.47). The results are displayed in Table 5.5. The possible ranges of  $\Lambda_H$  and  $\Gamma$  stem from the uncertainty in (4.10). The hypercolour factor ( $d^{abc}$ ) automatically ensures that  $\Gamma(Z \rightarrow hhh)$  is zero for an  $SU(2)$  hypercolour force. However, for all values of the parameters it can be seen that the sum of the widths  $\Gamma(Z \rightarrow hhh)$  and  $\Gamma(Z \rightarrow hpp\bar{p})$  is more than an order of magnitude greater than the amount allowed by experiment (see (5.28) and (5.29)).

One might query the validity of these results by arguing that the

Table 5.5

The hypergluon decay widths of the Z given by equations (5.45) - (5.47) for various values of  $N_C$  and  $N_H$ .  $\alpha_H$  is given by equation (5.48) and the values for  $\Lambda_H$  are taken from Table 4.1. All widths are in GeV.

$N_H$	$N_C$	$\Gamma(Z \rightarrow hhh)$	$\Gamma(Z \rightarrow hh\gamma)$	$\Gamma(Z \rightarrow hpp\bar{p})$
2	1	0 - 0	6.1 - 9.5	$6.8 \times 10^3 - 1.2 \times 10^4$
2	3	0 - 0	2.4 - 5.1	$6.2 \times 10^3 - 1.7 \times 10^4$
3	1	204 - 396	1.4 - 2.3	$7.0 \times 10^2 - 1.2 \times 10^3$
3	3	44 - 83	0.5 - 0.8	460 - 820
4	1	87 - 167	0.5 - 0.9	161 - 285
4	3	19 - 33	0.2 - 0.3	99 - 169

large values of  $\alpha_H$  and the limited phase space available for the hypergluon jets make the leading order perturbation theory invalid. However, it would be remarkable if higher order contributions conspired to reduce the magnitude of the width by a substantial amount. Even fixing  $\alpha_H$  to be as low as 0.5 leads to very large contributions to the total Z width (see Table 5.6). In addition there is the evidence of the QCD result which encourages one to believe these results to better than an order of magnitude.

Using the effective Lagrangian techniques to evaluate hypergluon decay widths, one simply replaces  $\alpha_S$  by  $\alpha_H$  and the colour factor 12 by  $N_H(N_H^2 - 1)/2$  in (5.39) and the colour factor 2 by  $N_C(N_H^2 - 1)/4$  in (5.42) to obtain widths for  $Z \rightarrow hhh$  and  $Z \rightarrow hp\bar{p}$ . The results are displayed in Figures 5.13 and 5.14 with  $\alpha_H = 0.5$  and  $N_C = N_H = 3$  for various values of the cutoff  $\epsilon$ . The values obtained easily exceed the experimental bounds on the Z width ((5.28) and (5.29)) if  $\Lambda_H$  is of the order of  $M_Z$ .

It should be stressed that the results obtained in this chapter can only be valid for  $\Lambda_H \sim O(M_Z)$ . In this case one can reasonably expect that the chiral symmetry preserving mechanism (see section 2.2) only effects the quarks and lepton masses but not that of the Z. This is not the case when  $\Lambda_H \gg M_Z$  when the mechanism which keeps the composite particles unnaturally light may also suppress their decay widths.

### 5.7 Summary

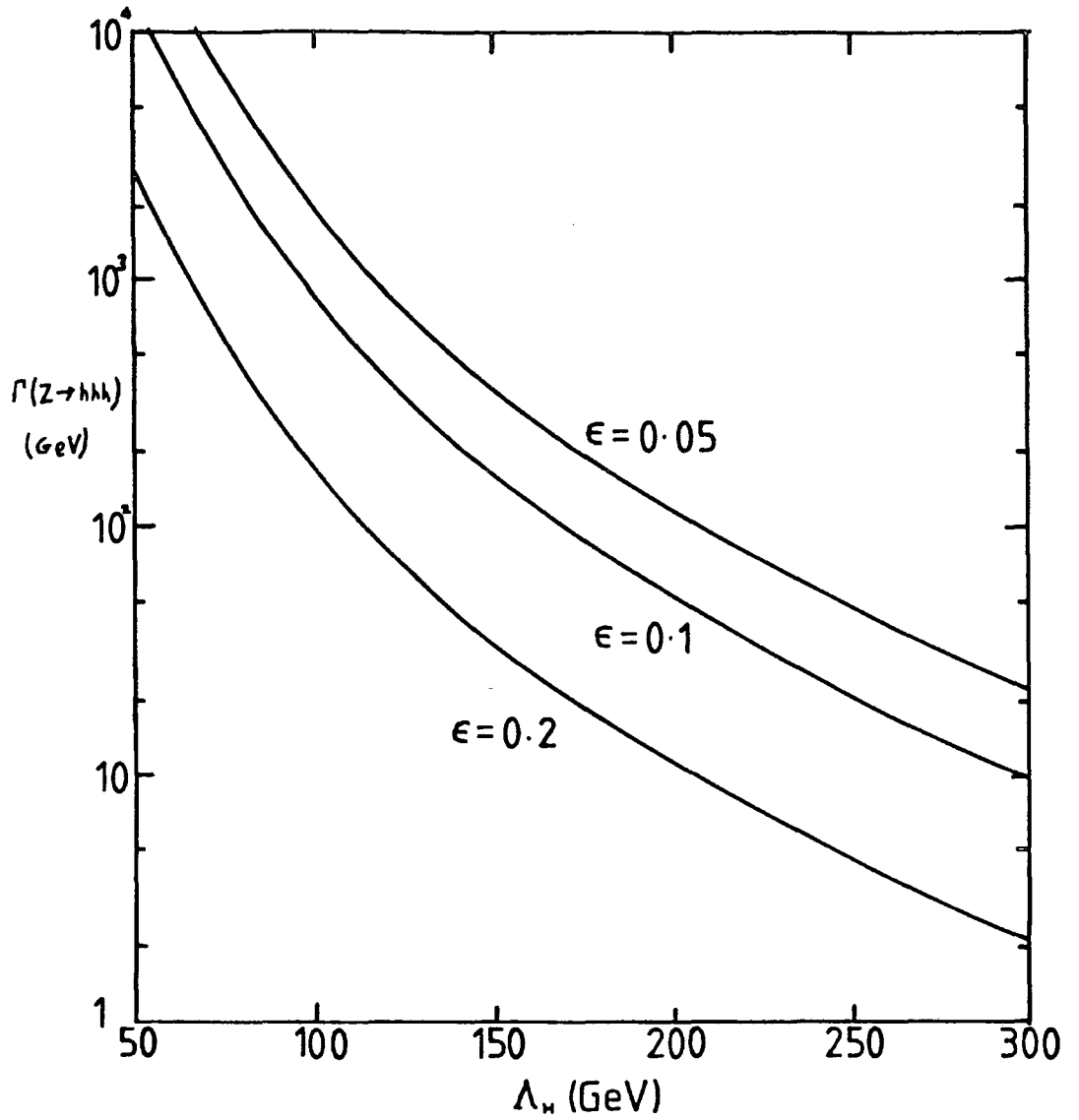
It has been seen that the decay width of the Z will be enhanced relative to the Standard Model value of 2.8 GeV in composite models

Table 5.6

The hypergluon decay widths of the  $Z$  fixing  $\alpha_H = 0.5$  in equations (5.45) - (5.47). All widths are in GeV.

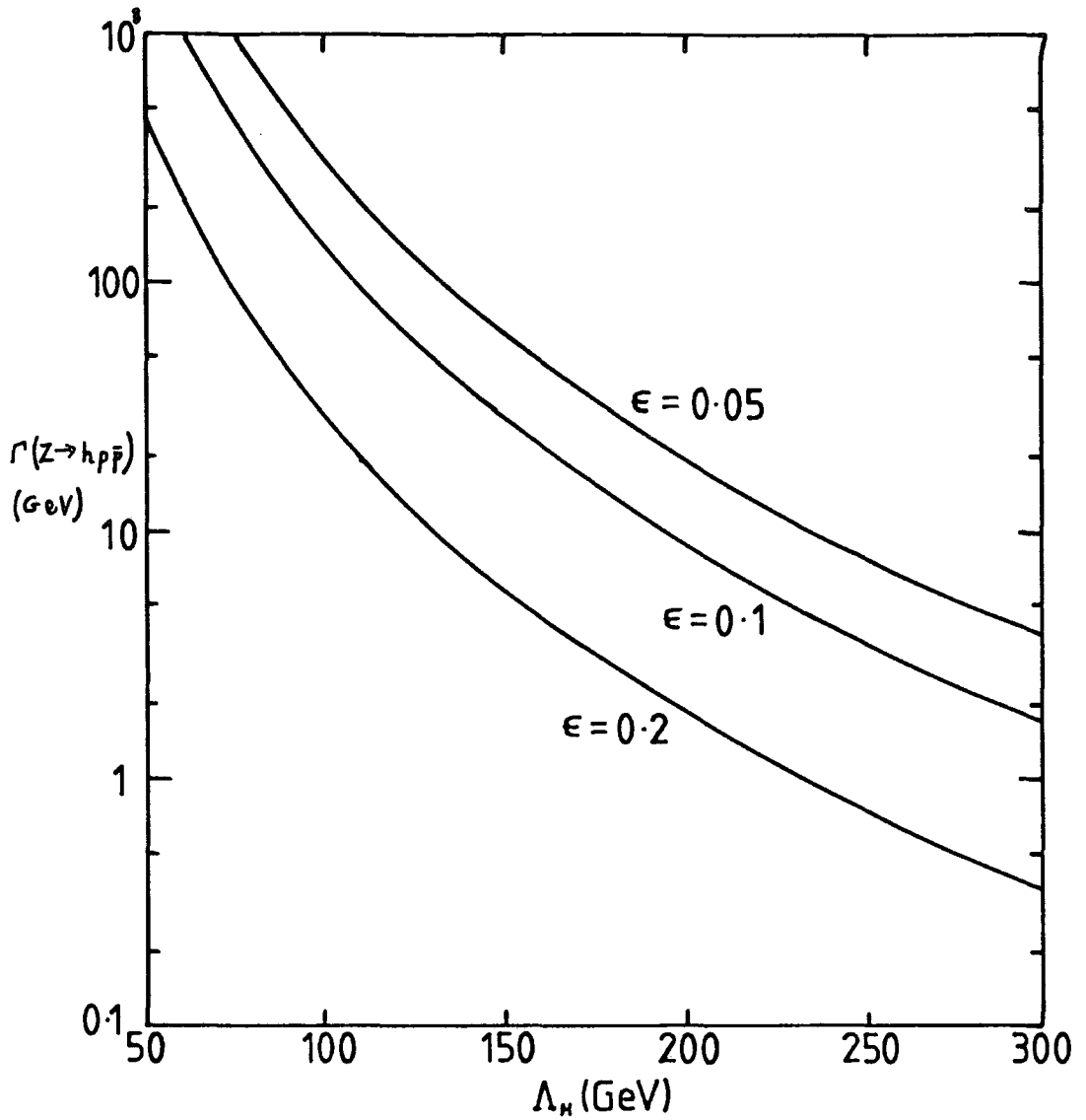
$N_H$	$N_C$	$\Gamma(Z \rightarrow hhh)$	$\Gamma(Z \rightarrow hh\gamma)$	$\Gamma(Z \rightarrow hp\bar{p})$
2	1	0 - 0	0.053 - 0.065	5.7 - 6.5
2	3	0 - 0	0.053 - 0.065	22.7 - 28.0
3	1	2.0 - 2.5	0.063 - 0.077	6.8 - 8.6
3	3	2.0 - 2.5	0.063 - 0.077	22.0 - 28.9
4	1	3.8 - 4.7	0.066 - 0.081	7.1 - 8.7
4	3	3.8 - 4.7	0.066 - 0.081	21.3- 26.7

Figure 5.13



The decay width  $\Gamma(Z \rightarrow hhh)$  as a function of the hypercolour scale  $\Lambda_H$  for different values of the energy cutoff  $\epsilon$ .  $C$  is taken to be  $(g_S/\Lambda_H)^2$ ,  $\alpha_H = 0.5$  and  $N_H = 3$ .

Figure 5.14



The decay width  $\Gamma(Z \rightarrow hp\bar{p})$  as a function of the hypercolour scale  $\Lambda_H$  for different values of the energy cutoff  $\epsilon$ .  $C$  is taken to be  $(g_S/\Lambda_H)^2$ ,  $\alpha_H = 0.5$  and  $N_C = N_H = 3$ .

where the scale of the hypercolour force  $\Lambda_H$  is of the order of  $M_Z$ . In particular the decays into  $ggg$  and  $q\bar{q}g$  are enhanced and could provide one of the first signals of compositeness. However, in models of this kind, decays of the  $Z$  into hypergluons have such large widths that it seems likely that they can already be ruled out from the experimental bounds on the total  $Z$  width.

## CHAPTER 6 CONCLUSIONS

The Standard Weinberg-Salam Model described in Chapter 1 was used to successfully account for low energy ( $\ll 100$  GeV) electroweak interactions of particle physics. With the advent of the CERN  $p\bar{p}$  collider, the model has been tested at higher energies and its correct prediction of the masses of the W and Z bosons has been verified. The only events which do not appear to fit this Standard Model are the so called "monojet" and "isolated like-sign dilepton" events detected by UA1 although explanations within the Standard Theory have been postulated and in any case the status of these events is uncertain. The initial excess of  $Z \rightarrow e^+e^-\gamma$  events which encouraged physicists to explore beyond the Standard Model has not been confirmed.

Compositeness of quarks, leptons and weak bosons is one possible way of going beyond the Weinberg-Salam Model both to account for observations and to answer questions which it cannot explain. These questions include the pattern of charge and colour exhibited by the fermions, the relationship between their masses and the reason for the occurrence of three or more generations. However, as yet there is no experimental evidence in favour of compositeness and as was shown in Chapter 2 the bound on the scale  $\Lambda_H$  of any such substructure is at least 100 GeV.

The composite models proposed so far fall into two classes - those with purely fermionic constituents and those including both fermions and bosons. In such models the quarks and leptons are composite whilst gauge bosons i.e. the photon and the gluons remain elementary. In many schemes the weak bosons are composite too. In

Chapter 3 it was demonstrated that by using the ideas of  $W$ - $\gamma$  mixing and  $W$ -dominance of the weak current, one could reproduce the Weinberg mass relations and the observed structure of the weak neutral current in agreement with the Standard Model. In addition, the universal couplings of  $W$ 's to fermions could arise from the weak isospin current algebra.

In Chapter 4 some of the consequences of assuming composite  $W$ 's and  $Z$ 's are examined. Many additional particles are predicted including excited  $W$  and  $Z$  bosons and their pseudoscalar partners, and the dominant decay modes of these states are studied. One cannot rule out compositeness merely because these particles have not yet been seen. However, spin 0 isovector partners of  $W$ ,  $Z$  ought, if they exist, to be discovered in  $e^+e^-$  annihilation experiments in the energy range which will become available at SLC and LEP within the next few years. If the boson constituents are coloured there should be colour octet partners of  $W$  and  $Z$ , colour octet leptons and possibly colour sextet quarks too. There is at present no experimental evidence to suggest the existence of any of these particles.

In Chapter 5 the decays of a composite  $Z$  boson are examined in detail. It is found that the width is likely to be significantly different from that of the Standard Model elementary  $Z$ . In particular the decays  $Z \rightarrow q\bar{q}g$  and  $Z \rightarrow ggg$  are likely to affect the total  $Z$  width by an appreciable amount. However, the  $Z$  may also decay into hypergluons ( $h$ ) which are the gauge bosons of the hypercolour force binding the constituent preons ( $p$ ). Although there is much uncertainty in estimating the hypercolour coupling  $\alpha_H$ , potential models and an effective Lagrangian approach both give very large

widths for  $Z \rightarrow h p \bar{p}$  and  $Z \rightarrow h h h$ . For this reason, composite models where the scale  $\Lambda_H$  is of the order of  $M_Z$  are in conflict with experiment unless the dynamics of the hypercolour force is completely different from that of the hadronic QCD bound states.

Given that hadronic masses are of order  $\Lambda_C$  (the scale of the QCD colour force) it is difficult to see why  $M_Z$  should be very much less than  $\Lambda_H$ . It is of course possible that only the quarks and leptons are composite but the weak gauge bosons are elementary despite their finite mass. In this case there are fewer difficulties for theories with  $\Lambda_H$  greater than or equal to 1 TeV because the fermions can be light as a result of chiral symmetry.

The conclusion of this analysis is that it seems more likely that the W and Z bosons discovered at the CERN  $p \bar{p}$  collider are elementary and that the Standard Model unification of electromagnetic and weak interactions is correct. It has been shown that a wide variety of composite models for the W and Z bosons are incompatible with current experimental knowledge.

## References Chapter 1

- 1.1 C. Itzykson and J. Zuber, Quantum Field Theory, McGraw-Hill (1978)
- 1.2 H.D. Politzer, Phys. Rep. 14C (1974) 129
- 1.3 M.R. Pennington, Rep. on Prog. in Phys. 46 (1983) 393
- 1.4 R.M. Barnett and D. Schlatter, Phys. Lett. 112B (1982) 475
- 1.5 R.M. Barnett, Phys. Rev. Lett. 48 (1982) 1657
- 1.6 S.L. Glashow, Nucl. Phys. 22 (1961) 579
- 1.7 S. Weinberg, Phys. Rev. Lett. 19 (1967) 1264
- 1.8 A. Salam, Proc. 8th Nobel Symp. Almqvist and Wiskell, Stockholm (1968) p.367
- 1.9 P. Higgs, Phys. Rev. Lett. 12 (1964) 132; 13 (1964) 508
- 1.10 G. t'Hooft, Nucl. Phys. B33 (1971) 173; B35 (1971) 167
- 1.11 J. Panman, CERN preprint EP/85-35 (1985)
- 1.12 C.H.Llewellyn-Smith and J.F.Wheater, Phys.Lett. 105B (1981) 486
- 1.13 G. Arnison et al. UA1 Collab., Phys. Lett. 129B (1983) 273
- 1.14 M. Banner et al. UA2 Collab., Phys. Lett. 122B (1983) 476
- 1.15 L. Mapelli, talk 5th Topical Workshop on  $p\bar{p}$  Collider Physics Aosta Valley (1985)
- 1.16 J. Kim, P. Langacker, M. Levine and H. Williams, Rev. Mod. Phys. 53 (1980) 211
- 1.17 W.J. Marciano and A. Sirlin, Phys. Rev. D29 (1984) 945
- 1.18 W.J. Marciano, Proc. 4th Topical Workshop on  $p\bar{p}$  Collider Physics, Berne (1984)

## References Chapter 2

- 2.1 J.C. Pati and A. Salam, Phys. Rev. Lett. 31 (1973) 661
- 2.2 P. Langacker, Phys. Rep. 72C (1981) 185
- 2.3 L. Susskind, Phys. Rev. D20 (1979) 2619
- 2.4 P. Fayet and S. Ferrara, Phys. Rep. 32C (1977) 249
- 2.5 L. Lyons, Prog. Part. Nucl. Phys. 10 (1983) 227
- 2.6 M. Kobayashi and T. Maskawa, Prog. Theor. Phys. 49 (1973) 652
- 2.7 G. t'Hooft, "Recent Developments in Gauge Theories", Cargese Lectures (1979) (Plenum Press, New York 1980) p.135
- 2.8 S. Adler, Phys. Rev. 177 (1969) 2426
- 2.9 J.S. Bell and R. Jackiw, Nuov. Cim., 60A (1969) 47
- 2.10 S. Coleman and B. Grossman, Nucl. Phys. B203 (1982) 205
- 2.11 Y. Frishman, A. Schwimmer, T. Banks and S. Yankielowicz, Nucl. Phys. B177 (1981) 157
- 2.12 J. Calmet et al., Rev. Mod. Phys. 49 (1977) 21
- 2.13 T. Konoshita and W. Lindquist, Phys. Rev. Lett. 47 (1981) 1573
- 2.14 R. Barbieri, L. Maiani and R. Petronzio, Phys. Lett. 96B (1980) 63
- 2.15 S. Brodsky and S. Drell, Phys. Rev. D22 (1980) 2236
- 2.16 E. Eichten, K. Lane and M. Peskin, Phys. Rev. Lett. 50 (1983) 811
- 2.17 M. Abolins et al., Proc. 1982 DPF Summer Study (Snowmass 1982), Donaldson, Gustafson, Paige eds.
- 2.18 R.M. Bionta et al., Phys. Rev. Lett. 51 (1983) 27
- 2.19 R. Ruckl, CERN preprint TH3897 (1984)
- 2.20 D.H. Saxon, Rutherford preprint RL-82-096 (1982)
- 2.21 G. Arnison et al. UA1 Collab., Phys. Lett. 126B (1983) 398
- 2.22 P. Bagnaia et al. UA2 Collab., Phys. Lett. 129B (1983) 130
- 2.23 K.E. Enqvist and J. Maalampi, Phys. Lett. 135B (1984) 329

- 2.24 N. Cabibbo, L. Maiani and Y. Srivastava, Phys. Lett. 139B (1984) 459
- 2.25 C. Rubbia, talk Annual Theory Meeting, Rutherford Appleton Lab. (1984)
- 2.26 L. Mapelli, talk 5th Topical Workshop on pp Collider Physics, Aosta Valley (1985)
- 2.27 A. De Rujula, L. Maiani and R. Petronzio, Phys. Lett. 140B (1984) 253
- 2.28 H. Fritzsch and G. Mandelbaum, Phys. Lett. 102B (1981) 319
- 2.29 O. Greenberg and J. Sucher, Phys. Lett. 99B (1981) 339
- 2.30 R. Barbieri, A. Masiero and R.N. Mohapatra, Phys. Lett. 105B (1981) 369
- 2.31 L. Abbott and E. Farhi, Phys. Lett. 101B (1981) 69
- 2.32 B. Schrepf and F. Schrepf, Nucl. Phys. B231 (1984) 109; B242 (1984) 203
- 2.33 H. Harari and N. Seiberg, Phys. Lett. 98B (1981) 269; 102B (1981) 263
- 2.34 J. Pati and A. Salam, Phys. Rev. D10 (1974) 275
- 2.35 J. Pati, A. Salam and J. Strathdee, Phys. Lett. 59B (1975) 265
- 2.36 H. Terazawa, Y. Chikashige and K. Adama, Phys. Rev. D15 (1977) 480
- 2.37 H. Terazawa, Phys. Rev. D22 (1980) 184

### References Chapter 3

- 3.1 J.J. Sakurai, Ann. Phys. N.Y. 11 (1960) 1
- 3.2 M. Gell-Mann and F. Zachariasen, Phys. Rev. 124 (1961) 963
- 3.3 Particle Data Group, Rev. Mod. Phys. 56 (1984) 51
- 3.4 J.D. Bjorken, Phys. Rev. D19 (1979) 335
- 3.5 E.H. de Groot and D. Schildknecht, Z. Phys. C10 (1981) 55
- 3.6 P.Q. Hung and J.J. Sakurai, Nucl. Phys. B143 (1978) 81
- 3.7 H. Fritzsche and G. Mandelbaum, Phys. Lett. 109B (1982) 224
- 3.8 H. Fritzsche, D. Schildknecht and R. Kogerler, Phys. Lett. 114B (1982) 157
- 3.9 R. Kogerler and D. Schildknecht, CERN preprint TH-3231 (1982)
- 3.10 I.Yu. Kobzarev, L.B. Okun and I.Ya. Pomeranchuk, JETP(Sov.Phys.) 14 (1962) 355
- 3.11 G. Feldman and P.T. Matthews, Phys. Rev. 132 (1963) 823
- 3.12 S. Coleman and H.J. Schnitzer, Phys. Rev. 134B (1964) 863
- 3.13 K. Kuroda and D. Schildknecht, Phys. Lett. 121B (1983) 173
- 3.14 G. Gounaris, R. Kogerler and D. Schildknecht, Phys. Lett. 133B (1983) 118
- 3.15 J.S. Bell and J. Pasupathy, Phys. Lett. 83B (1979) 389
- 3.16 P. Chen and J.J. Sakurai, Phys. Lett. 110B (1982) 481
- 3.17 P.D.B. Collins and N.A. Speirs, Durham preprint DTP/85/4 (1985)

#### References Chapter 4

- 4.1 A. De Rujula, H. Georgi and S.L. Glashow, Phys. Rev. D12 (1975) 147
- 4.2 S. Ono and F. Schoberl, Phys. Lett. 118B (1982) 419
- 4.3 P.D.B. Collins and N.A. Speirs, J. Phys. G 11 (1985) L5
- 4.4 M. Althoff et al., DESY preprint 82-069 (1982)
- 4.5 J.L. Richardson, Phys. Lett. 82B (1979) 272
- 4.6 V. Visnjic, Phys. Lett. 143B (1984) 158
- 4.7 F.M. Renard, Phys. Lett. 144B (1984) 119
- 4.8 U. Baur, H. Fritzsche and H. Faissner, Phys. Lett. 135B (1984) 313
- 4.9 R.D. Peccei, Phys. Lett. 136B (1984) 121
- 4.10 W.J. Marciano, Phys. Rev. Lett. 53 (1984) 975
- 4.11 M. Althoff et al. TASSO Collab., Phys. Lett. 154B (1985) 236
- 4.12 D. Gromes, Nucl. Phys. B131 (1977) 80
- 4.13 M.G. Olsson, Private Communication
- 4.14 W. Buchmuller, CERN preprint TH-3938/84 (1984)
- 4.15 D. Grosser, P. Falkensteiner and F. Schoberl, Phys. Lett. 153B (1985) 179
- 4.16 B. Guberina, J.H. Kuhn, R.D. Peccei and R. Ruckl, Nucl. Phys. B174 (1980) 317
- 4.17 R. Barbieri, M. Caffo and E. Remiddi, Nucl. Phys. B162 (1980) 220
- 4.18 V.A. Novikov et al., Phys. Rep. 41C (1978) 1
- 4.19 G. Arnison et al. UA1 Collab., Phys. Lett. 139B (1984) 115
- 4.20 G.J. Gounaris and A. Nicolaidis, Phys. Lett. 148B (1984) 239
- 4.21 U. Baur and K.H. Streng, Munich preprint MPI-PAE/PTh 50/84 (1984)
- 4.22 P. Bagnaia et al. UA2 Collab., Phys. Lett. 139B (1984) 105

- 4.23 E.W.N. Glover and A.D. Martin, Durham preprint DTP 85/10 (1985)
- 4.24 S.D. Ellis, R. Kleiss and W.J. Stirling, CERN preprint TH 4096/85 (1985)
- 4.25 H. Fritzsche and G. Mandelbaum, Phys. Lett. 150B (1985) 395

## References Chapter 5

- 5.1 D. Albert, W.J. Marciano, D. Wyler and Z. Parsa, Nucl. Phys. B166 (1980) 460
- 5.2 T.R. Grose and K.O. Mikaelian, Phys. Rev. D23 (1981) 123
- 5.3 M.L. Laursen, K.O. Mikaelian and M.A. Samuel, Phys. Rev. D23 (1981) 2795
- 5.4 F.M. Renard, Phys. Lett. 116B (1982) 269
- 5.5 F.M. Renard, Phys. Lett. 132B (1983) 450
- 5.6 M. Leurer, H. Harari and R. Barbieri, Phys. Lett. 141B (1984) 455
- 5.7 C.N. Yang, Phys. Rev. 77 (1950) 242
- 5.8 P.D.B. Collins and N.A. Speirs, Phys. Lett. 144B (1984) 275
- 5.9 R. Barbieri, R. Gatto and E. Remiddi, Phys. Lett. 61B (1976) 465
- 5.10 G. Feldman, T. Fulton and A. Devoto, Nucl. Phys. B154 (1979) 441
- 5.11 C. Quigg and J.L. Rosner, Phys. Rep. 56C (1979) 167
- 5.12 D.P. Stoker et al., Phys. Rev. Lett. 54 (1985) 1887
- 5.13 D.H. Perkins, Introduction to High Energy Physics (2nd edition) Addison-Wesley (1982)
- 5.14 F.M. Renard, Phys. Lett. 139B (1984) 449
- 5.15 E.W.N. Glover, A.D. Martin and M.R. Pennington, Phys. Lett. 153B (1985) 330
- 5.16 M.E. Peskin, Proc. of the 1981 Int. Symp. on Lepton and Photon Interactions at High Energies, W. Pfeil ed. Bonn (1981)
- 5.17 I.J.R. Aitchison and J.G. Hey, Gauge Theories in Particle Physics, Adam Hilger (1982)

